DEVELOPMENT OF METAL CHELATING MATERIALS FOR ANTIOXIDANT ACTIVE PACKAGING

A Dissertation

Presented to the Faculty of the Graduate School

of Cornell University

In Partial Fulfillment of the Requirements for the Degree of

Doctor of Philosophy

by

Zhuangsheng Lin

August 2018

DEVELOPMENT OF METAL CHELATING MATERIALS FOR ANTIOXIDANT ACTIVE PACKAGING

Zhuangsheng Lin, Ph. D.

Cornell University 2018

Synthetic metal chelators (e.g. ethylenediaminetetraacetic acid, EDTA) are widely used as additives to control trace transition metal induced oxidation in consumer products. To enable removal of synthetic chelators in response to increasing consumer demand for clean label products, metal-chelating active food packaging technologies have been developed with demonstrated antioxidant efficacy in simulated food systems. However, fabrication of metal-chelating materials in the proof of concept research leveraged batch processes (e.g. degassing, and long reaction in solution) to immobilize metal-chelating ligands, and had limited industrial translatability for large-scale fabrication. In this dissertation work, various synthesis techniques were investigated to the scalability of the material preparation processes. A scalable laminated photografting technique successfully replaced batch degassing process originally required to prepare functional surfaces. Finally, a photocurable metal chelating copolymer coating was developed to enable potential simple coat/cure preparation of materials. Iminodiacetic acid (IDA) was investigated as a primary metal chelating ligand and was immobilized onto food packaging materials using the above techniques. The surface chemistry, chemical chelating performance and antioxidant performance against oxidative spoilage (lipid oxidation and ascorbic acid degradation as model systems) of the resulting IDA functionalized materials were demonstrated.

BIOGRAPHICAL SKETCH

Zhuangsheng (Jason) Lin was born and raised in Wenzhou, Zhejiang, China. After graduating from Wenzhou Middle School in 2008, he came to the States to study food science. He got a B.S. degree in food science from the Iowa State University (2012) and a M.S. degree in food science from the University of Georgia (2014). He joined the Goddard Research Group at University of Massachusetts-Amherst in 2014 to pursue a Ph.D. degree in food science. In 2016, he transferred to Cornell University with the research group to continue pursuing the degree.

I’d like to dedicate it to my wife and my parents.

ACKNOWLEDGMENTS

Special thanks to Dr. Julie Goddard for giving me the opportunity to receive such a high quality Ph.D. training. I deeply appreciate your mentorship and entrustment and I enjoyed every single minute of the training.

Many thanks to Dr. Christopher Ober and Dr. Carmen Moraru for their mentorship.

Many thanks to all colleagues who worked on the metal chelating projects: Dr. Eric Decker, Dr. Fang Tian, Dr. Maxine Roman, Dr. David Johnson, Yoshiko Ogiwara, Paul Castrale, Joshua Herskovitz, and Pei Zhu.

The dissertation materials are based on work supported by Agriculture and Food Research Initiative grant no. 2012-67017-30157 and no. 2015-67017-23119 from the USDA National Institute of Food and Agriculture, Improved Processing Technologies (A1351). Thanks to Cornell Graduate *ad hoc* Fellowship and Dr. John Kinsella Memorial Fellowship for partially supporting me financially during my Ph.D. training.

TABLE OF CONTENTS

CHAPTER 1

INTRODUCTION

Active food packaging provides additional functional properties beyond containment, protection and communication of the packaged goods, with the major purposes being maintaining product quality (and in turn reducing food waste) and improving product safety.[1] According to a recent market forecast, the global revenue for active and intelligent packaging is projected to be $31.1 billion in 2016 and is expected to grow steadily worldwide, surged by increasing consumer demand for smarter packaging solutions.[2] Emerging forms of active packaging technology such as ferulic acid imprinted antioxidant hydrogel,[3] selenium incorporated free radical scavenging material,[4] and natural antimicrobials incorporated antimicrobial materials,[5-6] have been successfully developed in laboratory scale. In order for the new active packaging technologies to be realized commercially, many obstacles will need to be addressed, such as industrial translatability, cost of production, effectiveness after storage, and heat sealing property.

The Goddard research group has developed a non-migratory metal chelating antioxidant active packaging technology[7-11] to enhance shelf-life of packaged foods without the addition of synthetic additives (Figure 1.1). By immobilizing metal-chelating ligands onto traditional food packaging materials, the resulting active packaging materials were able to scavenge transition metals from the product to control transition-metal-induced oxidation. Trace transition metals in foods (mostly known as iron) are responsible for oxidative degradation of many food components, such as lipid[12] and ascorbic acid,[13] and cause changes in quality attributes, such as texture, flavor, color

and nutritive value. The industrial gold standard to control transition-metal-induced oxidation is to add synthetic metal chelators (e.g. ethylenediamine tetraacetic acid (EDTA)). The overall hypothesis of our research is that the non-migratory metal-chelating antioxidant active packaging technology can serve as an effective alternative for EDTA in liquid and semi-liquid products, and can potentially address the increasing consumer demand for additive-free and clean label food products. Such antioxidant active packaging technology works by scavenging pro-oxidant (i.e. transition metal) from products, therefore, does not require migration of active compounds to be effective. In the United States, such non-migratory metal-chelating antioxidant active packaging technology will potentially be regulated as food contact substance (FCS) by the FDA,[14] a potential regulatory benefit.

An early concept of the metal-chelating active packaging materials was developed by grafting poly(acrylic acid) (PAA) and poly(hydroxamic acid) (PHA) onto polypropylene films.[15-17] PP-g-PAA films were made by a two-step process by functionalizing polypropylene (PP) film with benzophenone (BP) followed by UV induced polymerization of acrylic acids (Figure 1.2).[15, 17] PP-g-PAA films had carboxylic acid density of around 70 nmol/cm^2 film, which was responsible for ferrous chelating activity of around 70 nmol ferrous ion/cm^2 [15]. In a half gallon package with around 960 cm^2 surface area, the ferrous ion chelating capacity of PP-g-PAA film correlates to equivalent of 21 ppm EDTA, below FDA maximum of 33 ppm.[18] Biomimetic iron chelating chemical group with strong iron binding capacity, hydroxamic acid (HA) was grafted to PP films through graft polymerization of methyl acrylate (MA) from photo initiated PP film, followed by chemical transformation of

methoxyl group into HA in hydroxamine solution.[16] PP-g-PHA films showed ferrous ion chelating capacity of around 80 nmol/cm^2 film.[16] Both PP-g-PAA and PP-g-PHA films inhibited lipid oxidation in food emulsion. PP-g-PAA extended the lag phase of lipid oxidation in soybean oil-in-water emulsion from 2 days to 9 days,[15] and is the most effective in inhibiting lipid oxidation at pH 7.0,[17] while PP-g-PHA inhibited lipid oxidation at pH 3.0.[16]

While effective in inhibiting lipid oxidation, the previously reported metal chelating active packaging materials were synthesized in a batch process which used nitrogen inerting steps, limiting commercial translatability. In Chapter 2, we report on a laminated photografting technique to introduce metal-chelating grafts on the surface of polypropylene films with similar chemistry and chelating functionality as the previously reported PP-*g*-PAA and PP-*g*-PHA (Figure 1.3). Laminated photografting was conducted by laminating the solution of monomer and photoinitiator between UV-ozone functionalized PP film (PP-UVO) and a glass slide, followed by UV irradiation. The resulting PP-*g*-PAA and PP-*g*-PHA films were characterized using Fourier transform infrared spectroscopy, scanning electron microscopy (SEM), water contact angle analysis, dye assay, and iron chelating assay. Both PP-*g*-PAA and PP-*g*-PHA films prepared by laminated photografting had similar surface chemistry and iron chelating activity compared to materials prepared using the degassing process. The laminated photografting may be adapted for roll-to-roll continuous preparation of surface modified films such as metal chelating active packaging on an industrial scale. In addition to eliminating nitrogen inerting steps, the laminated photografting requires reduced UV dose and can be performed without a solvent and may utilize less acrylate

monomer. The laminated photografting consumed 12 times less acrylic acid monomer and 48 times less methyl acrylate monomer to modify an equivalent surface area of film. The laminated photografting technique may serve as an efficient, economical and environmentally friendly surface modification technique for preparation of active packaging materials for consumer products.

To design a metal chelating interface for food packaging application, it was critical to have metal chelating ligands that were highly selective for transition metals, so that the ligands could overcome proton interference in a broad pH range, especially in food systems with low pH values. High acid condition was challenging for grafted ligands to effectively scavenge metal ions from the food system because of the increased degree of proton interference and increased solubility of transition metal ions. Meanwhile, oxidative spoilage tended to be more of a concern in high acid food (pH<3.6) than low acid food (pH>3.6), because in the latter condition, microbial spoilage tended to take place ahead of oxidative spoilage. Our groups demonstrated that carboxylic acid surface grafts lost antioxidant efficacy as the pH value was below 5.0, while iron specific hydroxamate metal chelating ligand had application in broader pH range. In this study, iminodiacetate (IDA) was immobilized onto PP. Iminodiacetate (IDA) was a tridentate polyaminocarboxylate ligand with half the chemical structure of EDTA and had high stability constant for major transition metal ions in food. The stability constant values were 10.72 and 10.57 for IDA-Fe^{3+} and IDA-Cu^{2+} complex, respectively.[19] IDA ligand was often used in metal chelating resins [20-23] and ion exchange membranes [24-26] to remove heavy metals from water, due to the high ligand specificity to heavy metals. Furthermore, IDA had low stability constant for multivalent

macro minerals in food, such as calcium and magnesium (reported stability constant of 2.59 and 2.98, respectively),[19] therefore, when applied in food system, the macro minerals may have less competition for the ligand.

In Chapter 3, a metal chelating polypropylene material with surface grafted IDA (PP-*g*-IDA) was developed for antioxidant active packaging application. The PP-*g*-IDA film was prepared by a two-step surface modification process on native PP film (Figure 1.4). In the first step, a chlorinated vinyl monomer, 3-chloro-2-hydroxypropyl methacrylate was graft-polymerized from polypropylene surface via laminated photografting. The resulting PP-*graft*-CHPM (PP-*g*-CHPM) film contained grafted polymer chains bearing reactive chlorine groups. In the second step, IDA ligands were immobilized on grafted polymer chains on PP-*g*-CHPM via nucleophilic substitution of the chlorine groups, to give PP-*g*-IDA. The PP-*g*-IDA surface was characterized using microscopic analysis, water contact angle, and spectrometric analysis including Fourier transform infrared spectroscopy (FTIR) and X-ray photoelectron spectroscopy (XPS). Metal chelation and antioxidant activity studies were conducted in high acid stress condition of pH 3 as the ligands experienced high proton interference. The metal chelation towards ferric and cupric ion was quantified and the ligand chemistry after metal chelation was analyzed spectrometrically. The antioxidant activities of PP-*g*-IDA film against lipid oxidation and ascorbic acid degradation in simulated food models were also analyzed. The resulting PP-*g*-IDA films effectively chelated Fe^{3+} and Cu^{2+} in acidic conditions (pH 3.0), with relative affinity constants on the order of common soluble chelators of citric acid, IDA and NTA. It is likely that carboxylates and tertiary amine on grafted IDA ligand coordinated with the metal ions to form colorless PP-*g*-

IDA metal chelates, which potentially led to a formation of tridentate chelating coordination. The PP-*g*-IDA film demonstrated antioxidant efficacy in emulsified oil system at pH 3.0, and was as effective as EDTA in controlling lipid oxidation. PP-*g*-IDA film also demonstrated potential to control ascorbic acid degradation. Surface grafts exhibited stability against delamination after exposure to food simulants under accelerated storage conditions. This work supports the potential application of metal chelating IDA functionalized polypropylene films as antioxidant active packaging materials in neutral to acidic emulsified foods and beverages.

Despite the promise of IDA functionalized metal chelating materials prepared via laminated photografting, a significant hurdle exists in the translation of bench-scale synthesis routes to high-throughput, continuous coating or production operations. Indeed, traditional techniques for immobilization of metal-chelating ligands required organic chemical reactions to tether the ligands, with long-time, batch style reactions. Such batch chemical reactions have been reported for preparation of a range of metal-chelating materials, such as nanoparticles,[27] resins,[23, 28] membranes [24, 29] and fabrics.[25] In our previous studies, metal-chelating active packaging materials were also fabricated via batch reactions in ligand solutions to tether metal-chelating ligands.[7-8, 30] For example, the IDA functionalized materials were prepared via a 10-hour chemical reaction in a concentrated IDA solution to tether IDA ligands to reactive surfaces bearing chlorine groups [8]. Therefore, despite the promising laboratory results of metal-chelating active packaging technologies, the industrial translatability of the technology remains limited. The overall goal of the work described in the following chapters was to design a new synthesis route to improve the throughput of introducing IDA metal

chelating ligands onto polymer films.

Photo-curing is a low energy, high speed industrial coating process in which liquid coatings are cured onto solid supports by exposure to ultraviolet radiation and has potential for solvent-free roll-to-roll processing.[31 32] Photo-curing can be used to photo-graft vinyl monomers onto material surfaces to introduce added functionalities.[33-34] In our previous study, a laminated photo-grafting technique was investigated in order to graft acrylic acids from PP surface, resulting in carboxylic acid functionalized materials [30]. In Chapter 4, a high-throughput fabrication method was designed to prepare IDA coated PP materials with metal-chelating properties, without the need for batch solution reaction (Figure 1.5). IDA functionalized monomers (GMA-IDA) were synthesized, which were then grafted onto food packaging materials via a two-step photo-grafting process. The two-step photo-grafting process eliminated the solution reaction step to tether ligands onto materials, and could potentially enable high-throughput roll-to-roll fabrication of metal-chelating materials. The material's ability to chelate trace transition metals (iron, copper) responsible for metal promoted oxidative degradation in foods and beverages, and its antioxidant efficacy against ascorbic acid degradation were also investigated. The IDA based coatings were prepared by a two-step photo-grafting process using an IDA functionalized vinyl monomer. The two-step photo-grafting process eliminated the need for lengthy batch chemical reactions. This material fabrication technique can potentially be adopted as a high-throughput roll-to-roll photo-curing process for large-scale fabrication of the metal-chelating active packaging materials. The photo-grafting technique may also be applied to large-scale surface immobilization of other bio-active compounds, such as antimicrobial and catalytic

agents. The IDA functionalized materials exhibited pH dependent metal chelating capacity and antioxidant efficacy against ascorbic acid degradation. Metal-chelating active packaging technology can potentially be used to control transition metal induced oxidative degradation of ascorbic acids in aqueous products (e.g. beverages and salad dressings). The technology may also be used synergistically with natural antioxidants such as ascorbic acids to control oxidative degradations in consumer products.

In Chapter 5, we described a simple coat/cure preparation of metal chelating materials using a photocurable metal chelating copolymer coating technology.[35] We prepared a poly(*n*-butyl acrylate) based copolymer coating with IDA and benzophenone moieties to impart metal-chelating and photocrosslinking, respectively, via emulsion copolymerization (Figure 1.6). The copolymer coating was applied onto polypropylene surface as a latex paint, followed by photocuring to attach the coating to the surface of the substrate. The resulting coatings were characterized for surface chemistry, thickness, chelating capacity, and surface energy. The IDA chelating moieties were capable of chelating transition metal ions, with chelating capacity tunable by coating thickness. The benzophenone moieties enabled rapid photocuring, resulting in a robust, uniformly applied coating. The integration of poly(*n*-butyl acrylate) permitted a final coating with surface energy values sufficiently low to be considered low fouling and suitable for product release, an important parameter in active packaging applications. Despite the low surface energy and the high hydrophobicity, the high contact angle hysteresis suggested sufficient interaction of IDA ligands, which was supported by the efficacy of the materials in both chelating ferric ions and inhibiting transition metal induced ascorbic acid degradation. The photocured coating on polypropylene was stable both

chemically and physically after exposure to fatty, alcoholic, acidic, and aqueous product simulants, supporting its stability in active packaging applications. Their antioxidant efficacy against transition metal-induced ascorbic acid degradation and stability in food simulants were also tested. The photocurable polymer coatings enables scalable production of active materials with metal chelating functionality. The copolymer coating can potentially be applied onto plastic films and bottles via industrially scalable coat/cure processes for the manufacture of metal chelating active packaging.

In total, this dissertation work describes the advances of metal chelating active packaging from proof of concept work to readily commercially translatable process. In the concluding chapter, key thought processes during the development process and potential future research further to advance the technology are described. Notable trials and fails are mentioned in Appendix.

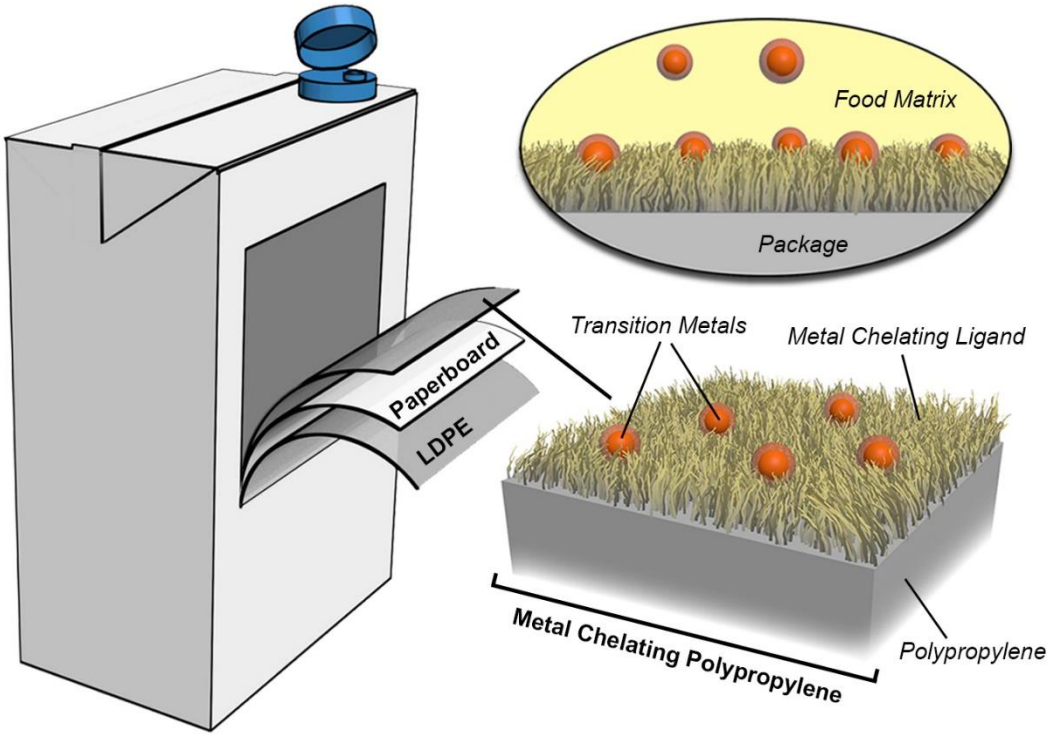

Figure 1.1. Conceptual illustration of metal chelating active packaging.

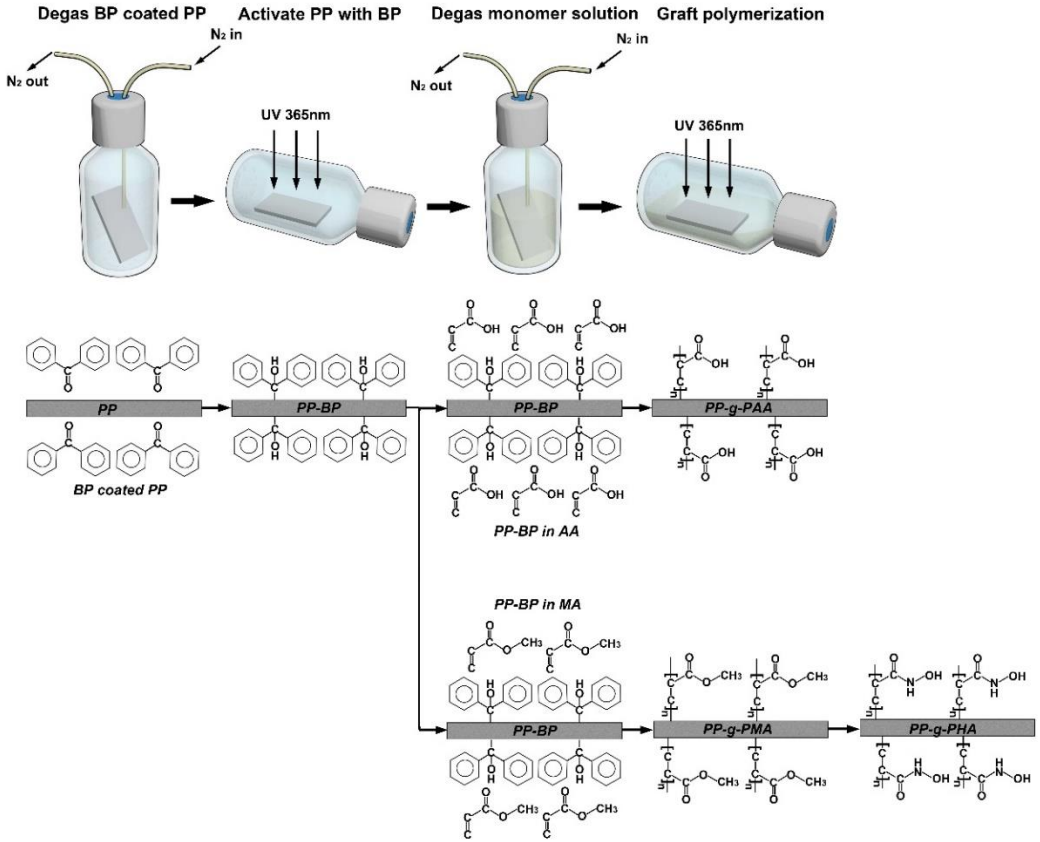

Figure 1.2. Schematic procedure of the methods to prepare polypropylene-graft-poly(acrylic acid) (PP-g-PAA) and polypropylene-graft-poly(hydroxamic acid) (PP-g-PHA) using batch degassing and photocuring process.

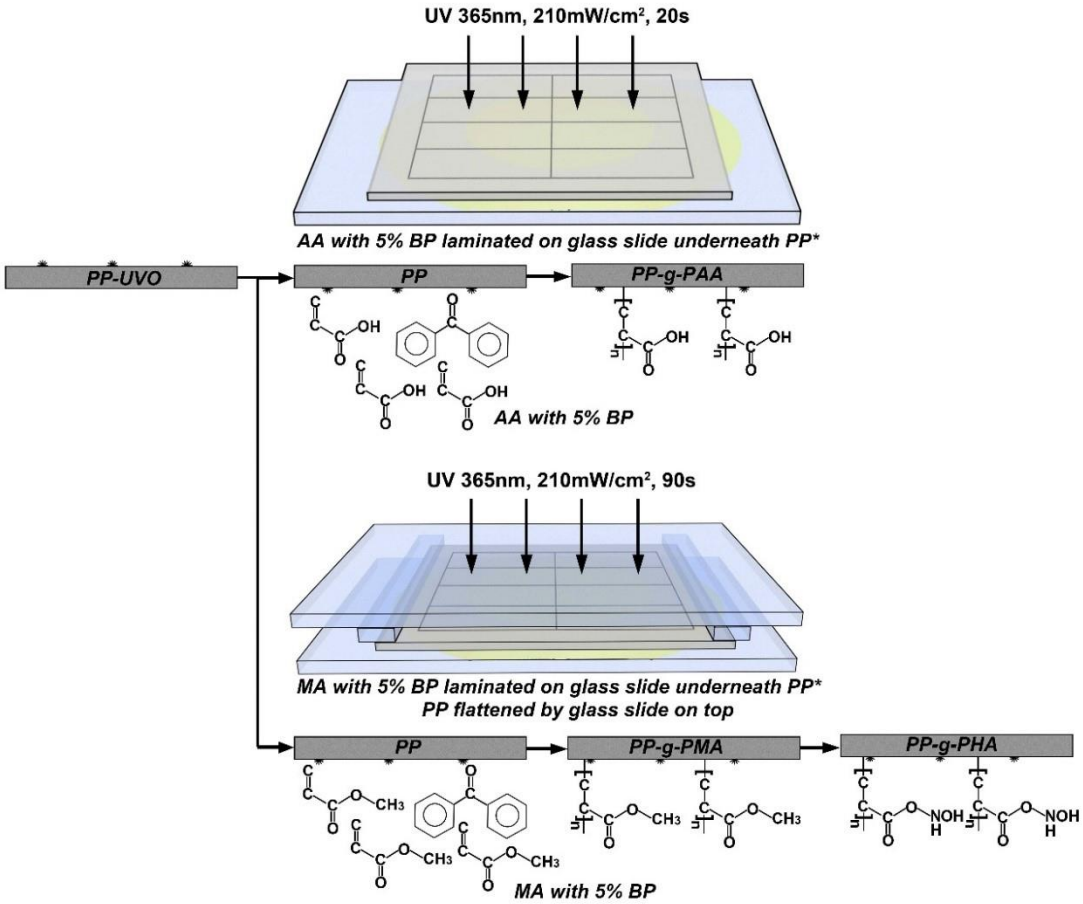

Figure 1.3. Schematic procedure of the method to prepare polypropylene-graft-poly(acrylic acid) (PP-g-PAA) and polypropylene-graft-poly(hydroxamic acid) (PP-g-PHA) using laminated photografting.

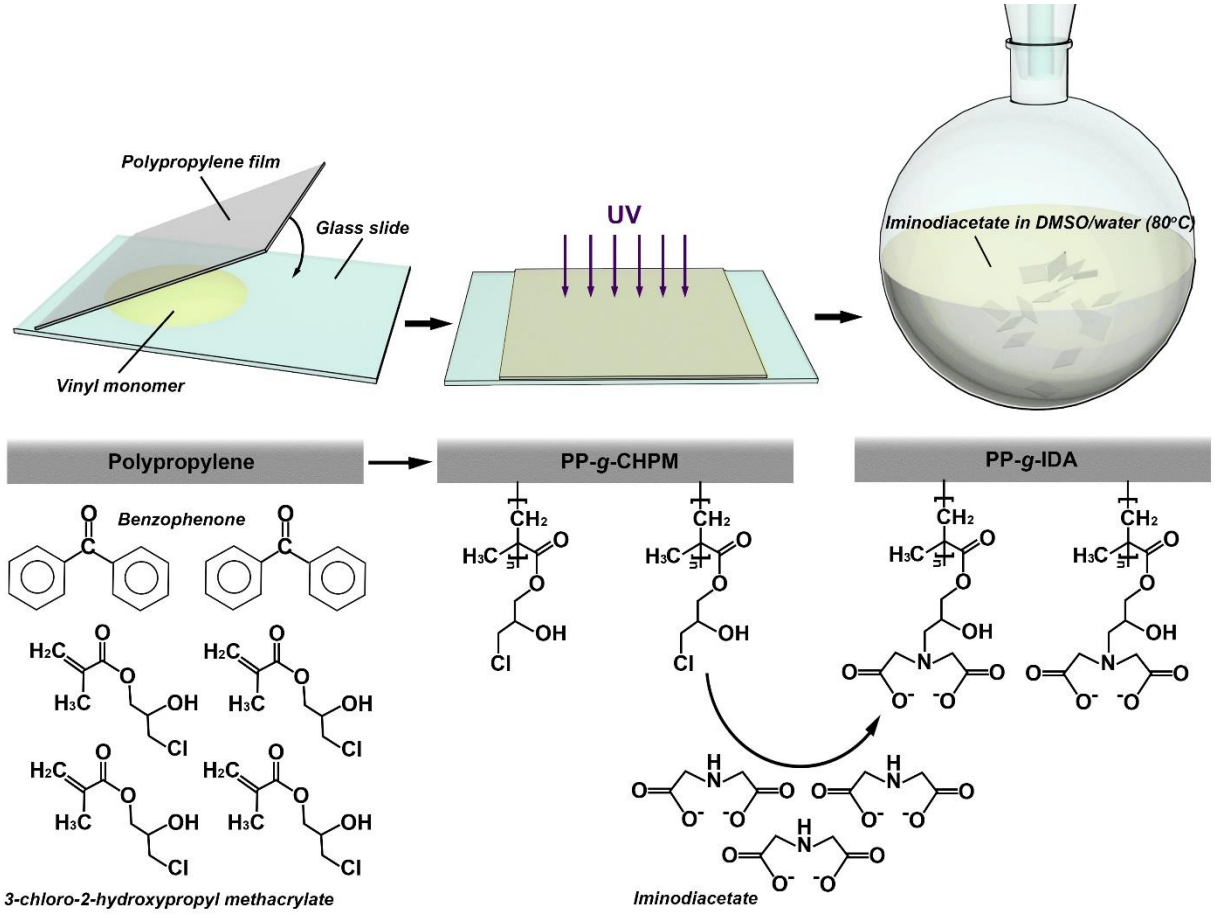

Figure 1.4. Schematic depicting method (top) and proposed synthesis chemistry (bottom) of PP-*g*-IDA.

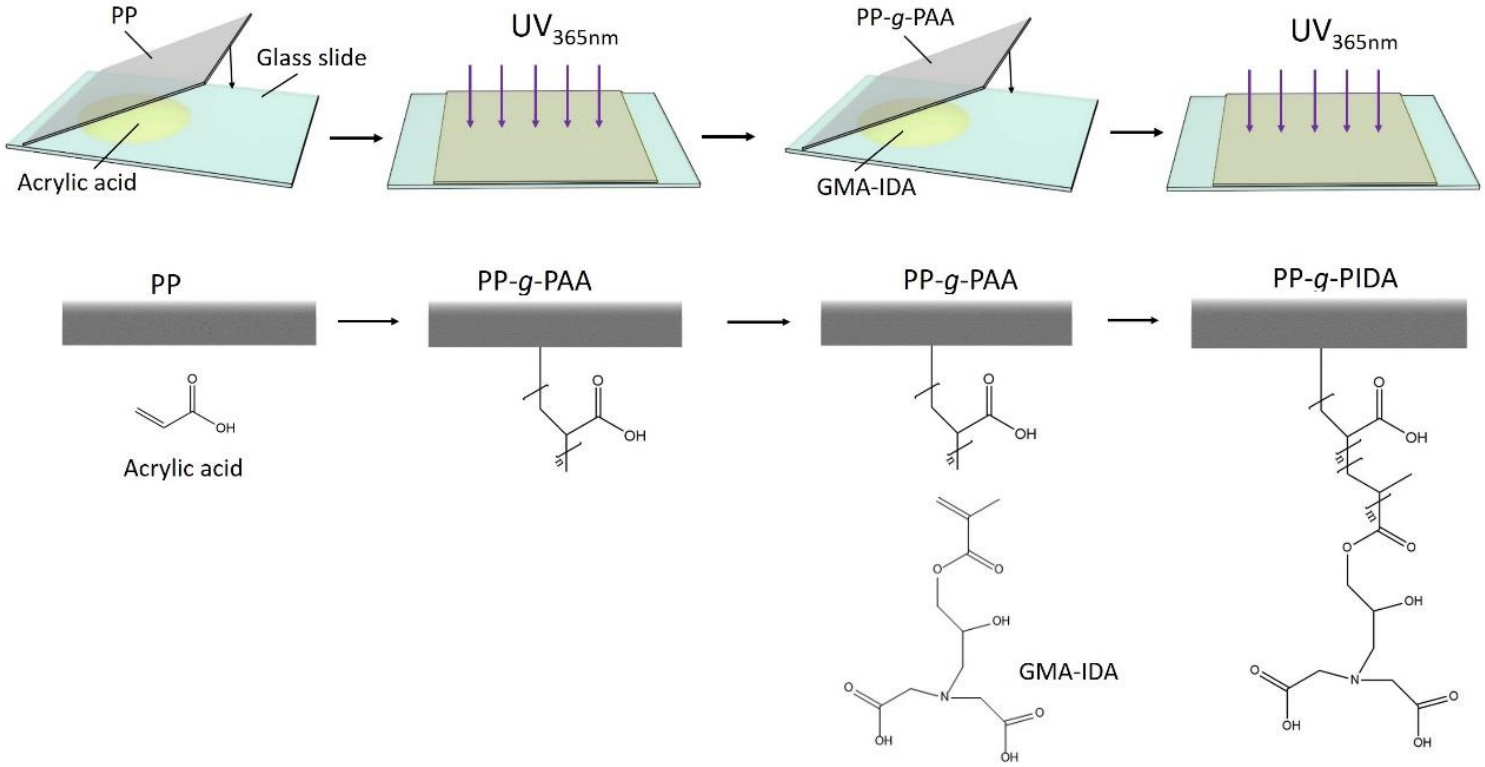

Figure 1.5. Synthesis scheme of metal-chelating PP-*g*-PIDA materials via a two-step laminated photo-grafting process.

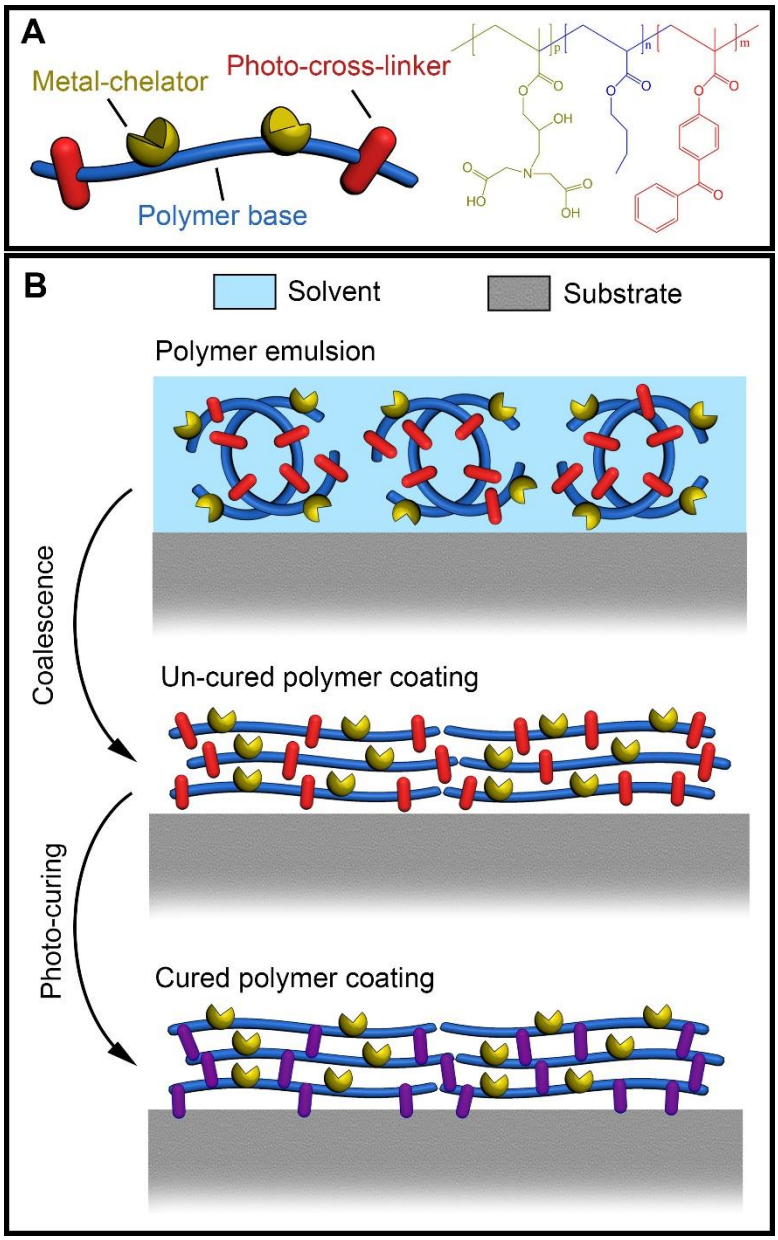

Figure 1.6. Conceptual illustration of the photocurable metal chelating polymer (A) and the process of preparing metal chelating films using the photocurable metal chelating coating (B).

REFERENCES

1. Brody, A. L.; Bugusu, B.; Han, J. H.; Sand, C. K.; McHugh, T. H., Innovative food packaging solutions. *Journal of food science* **2008,** *73* (8), R107-R116.

2. Anonymous *Smart Packaging Market Report 2016-2026*; Visiongain: 2016.

3. Benito-Pena, E.; Gonzalez-Vallejo, V.; Rico-Yuste, A.; Barbosa-Pereira, L.; Cruz, J. M.; Bilbao, A.; Alvarez-Lorenzo, C.; Moreno-Bondi, M. C., Molecularly imprinted hydrogels as functional active packaging materials. *Food Chem* **2016,** *190*, 487-94.

4. Vera, P.; Echegoyen, Y.; Canellas, E.; Nerín, C.; Palomo, M.; Madrid, Y.; Cámara, C., Nano selenium as antioxidant agent in a multilayer food packaging material. *Analytical and Bioanalytical Chemistry* **2016,** *408* (24), 6659-6670.

5. Moshe, I.; Weizman, O.; Natan, M.; Jacobi, G.; Banin, E.; Dotan, A.; Ophir, A., Multiphase thermoplastic hybrid for controlled release of antimicrobial essential oils in active packaging film. *Polymers for Advanced Technologies* **2016,** *27* (11), 1476-1483.

6. Duran, M.; Aday, M. S.; Zorba, N. N. D.; Temizkan, R.; Büyükcan, M. B.; Caner, C., Potential of antimicrobial active packaging 'containing natamycin, nisin, pomegranate and grape seed extract in chitosan coating' to extend shelf life of fresh strawberry. *Food and Bioproducts Processing* **2016,** *98*, 354-363.

7. Roman, M. J.; Decker, E. A.; Goddard, J. M., Retaining Oxidative Stability of Emulsified Foods by Novel Nonmigratory Polyphenol Coated Active Packaging. *J Agric Food Chem* **2016,** *64* (27), 5574-82.

8. Lin, Z.; Roman, M. J.; Decker, E. A.; Goddard, J. M., Synthesis of Iminodiacetate Functionalized Polypropylene Films and Their Efficacy as Antioxidant Active-Packaging Materials. *J. Agric. Food. Chem.* **2016,** *64* (22), 4606-4617.

9. Tian, F.; Decker, E. A.; Goddard, J. M., Controlling lipid oxidation via a biomimetic iron chelating active packaging material. *J. Agric. Food. Chem.* **2013,** *61* (50), 12397-12404.

10. Tian, F.; Decker, E. A.; Goddard, J. M., Control of lipid oxidation by nonmigratory active packaging films prepared by photoinitiated graft polymerization. *J. Agric. Food. Chem.* **2012,** *60* (31), 7710-7718.

11. Tian, F.; Decker, E. A.; McClements, D. J.; Goddard, J. M., Influence of non-migratory metal-chelating active packaging film on food quality: impact on physical and chemical stability of emulsions. *Food Chem.* **2014,** *151*, 257-265.

12. McClements, D. J.; Decker, E. A., Lipid Oxidation in Oil-in-Water Emulsions: Impact of Molecular Environment on Chemical Reactions in Heterogeneous Food Systems. *Journal of food science* **2000,** *65* (8), 1270-1282.

13. Lee, Y. C.; Kirk, J. R.; Bedford, C. L.; Heldman, D. R., Kinetcs and computer simulation of ascorbic acid stability of tomato juice as functions of temperature, pH and metal catalyst. *Journal of food science* **1977,** *42* (3), 640-643.

14. Anonymous, TITLE 21--FOOD AND DRUGS. In *CITE: 21CFR172.120*, Regulations, C. o. F., Ed. 2017.

15. Tian, F.; Decker, E. A.; Goddard, J. M., Control of lipid oxidation by nonmigratory active packaging films prepared by photoinitiated graft polymerization. *Journal of agricultural and food chemistry* **2012,** *60* (31), 7710-8.

16. Tian, F.; Decker, E. A.; Goddard, J. M., Controlling lipid oxidation via a biomimetic iron chelating active packaging material. *Journal of agricultural and food chemistry* **2013,** *61* (50), 12397-404.

17. Tian, F.; Decker, E. A.; McClements, D. J.; Goddard, J. M., Influence of non-migratory metal-chelating active packaging film on food quality: impact on physical and chemical stability of emulsions. *Food chemistry* **2014,** *151*, 257-65.

18. Goddard, J. M.; McClements, D. J.; Decker, E. A., Innovative technologies in the control of lipid oxidation. *Lipid Technology* **2012,** *24* (12), 275-277.

19. Martell, A. E.; Robert, M. S., *Critical stability constants*. Plenum Press: New York, 1974; Vol. 1.

20. Noureddine, C.; Lekhmici, A.; Mubarak, M. S., Sorption properties of the iminodiacetate ion exchange resin, amberlite IRC-718, toward divalent metal ions. *J. Appl. Polym. Sci.* **2008,** *107* (2), 1316-1319.

21. Malla, M. E.; Alvarez, M. B.; Batistoni, D. A., Evaluation of sorption and desorption characteristics of cadmium, lead and zinc on Amberlite IRC-718 iminodiacetate chelating ion exchanger. *Talanta* **2002,** *57* (2), 277-287.

22. Ling, C.; Liu, F. Q.; Xu, C.; Chen, T. P.; Li, A. M., An integrative technique based on synergistic coremoval and sequential recovery of copper and tetracycline with dual-functional chelating resin: roles of amine and carboxyl groups. *ACS applied materials & interfaces* **2013,** *5* (22), 11808-17.

23. Atzei, D.; Ferri, T.; Sadun, C.; Sangiorgio, P.; Caminiti, R., Structural Characterization of Complexes between Iminodiacetate Blocked on Styrene−Divinylbenzene Matrix (Chelex 100 Resin) and Fe(III), Cr(III), and Zn(II) in

Solid Phase by Energy-Dispersive X-ray Diffraction. *Journal of the American Chemical Society* **2001,** *123* (11), 2552-2558.

24. Yamada, K.; Nagano, R.; Hirata, M., Adsorption and desorption properties of the chelating membranes prepared from the PE films. *J. Appl. Polym. Sci.* **2006,** *99* (4), 1895-1902.

25. Kavaklı, P. A.; Kavaklı, C.; Güven, O., Preparation and characterization of Fe(III)-loaded iminodiacetic acid modified GMA grafted nonwoven fabric adsorbent for anion adsorption. *Radiation Physics and Chemistry* **2014,** *94*, 105-110.

26. Choi, S.-H.; Nho, Y. C.; Kim, G.-T., Adsorption of Pb2+ and Pd2+ on polyethylene membrane with amino group modified by radiation-induced graft copolymerization. *J. Appl. Polym. Sci.* **1999,** *71* (4), 643-650.

27. Goon, I. Y.; Zhang, C.; Lim, M.; Gooding, J. J.; Amal, R., Controlled fabrication of polyethylenimine-functionalized magnetic nanoparticles for the sequestration and quantification of free Cu2+. *Langmuir* **2010,** *26* (14), 12247-52.

28. El-Nahhal, I.; Zaggout, F.; Nassar, M.; El-Ashgar, N.; Maquet, J.; Babonneau, F.; Chehimi, M., Synthesis, Characterization and Applications of Immobilized Iminodiacetic Acid-Modified Silica. *Journal of Sol-Gel Science and Technology* **2003,** *28* (2), 255-265.

29. Zhu, J.; Sun, G., Facile fabrication of hydrophilic nanofibrous membranes with an immobilized metal-chelate affinity complex for selective protein separation. *ACS applied materials & interfaces* **2014,** *6* (2), 925-32.

30. Lin, Z.; Decker, E. A.; Goddard, J. M., Preparation of metal chelating active packaging materials by laminated photografting. *Journal of Coatings Technology and Research* **2016,** *13* (2), 395-404.

31. Ligon, S. C.; Husár, B.; Wutzel, H.; Holman, R.; Liska, R., Strategies to Reduce Oxygen Inhibition in Photoinduced Polymerization. *Chem. Rev.* **2013,** *114* (1), 557-589.

32. Ahn, S. H.; Guo, L. J., High-Speed Roll-to-Roll Nanoimprint Lithography on Flexible Plastic Substrates. *Advanced Materials* **2008,** *20* (11), 2044-2049.

33. Decker, C.; Zahouily, K., Surface modification of polyolefins by photografting of acrylic monomers. *Macromol. Symp.* **1998,** *129* (1), 99-108.

34. Yang, W.; Rånby, B., Radical Living Graft Polymerization on the Surface of Polymeric Materials. *Macromolecules* **1996,** *29* (9), 3308-3310.

35. Lin, Z.; Goddard, J., Photocurable coatings prepared by emulsion polymerization present chelating properties. *Colloids and Surfaces B: Biointerfaces* **2018,** *Submitted*.

CHAPTER 2

PREPARATION OF METAL CHELATING ACTIVE PACKAGING MATERIALS BY LAMINATED PHOTOGRAFTING*

Abstract

Active packaging materials with surface immobilized metal chelating ligands were prepared by laminated photografting technique. The resulting materials presented transition metal scavenging properties with potential application in non-migratory antioxidant active packaging materials. Photografting of functional polymer ligands is typically performed in an oxygen-free environment, requiring a nitrogen inerting step, which limits potential industrial scale-up. Laminated photografting eliminates the need for nitrogen inerting by sandwiching the monomer solution between base material and an oxygen barrier layer. In this study, we demonstrated the ability to synthesize metal chelating active packaging materials, previously prepared by standard batch photografting, using a laminated photografting technique. The polypropylene-*graft*-poly(acrylic acid) (PP-*g*-PAA) and polypropylene-*graft*-poly(hydroxamic acid) (PP-*g*-PHA) chelating films prepared by laminated photografting presented similar surface chemistry as those reported previously, as characterized by infrared spectroscopy, and presented ferric ion chelating capacity of 182 ± 29 nmol/cm^2 and 89 ± 10 nmol/cm^2, respectively, at pH 5.0. The reported laminated photografting represents a coating technology with potential for adaptation to roll-to-roll manufacture of metal chelating films on an industrial scale.

*Zhuangsheng Lin, Eric A. Decker, Julie M. Goddard.

Published in Journal of Coatings Technology and Research. 13, 395-404.

Introduction

Ultraviolet (UV) light initiated surface graft polymerization of vinyl monomers (i.e. photografting) enables surface modification of inert polymeric materials to achieve improved functional properties such as wettability, printability, and adhesiveness.[1-3] Surface grafted polymer chains bearing reactive groups can undergo post-graft modifications such as conjugation of bioactive compounds[4-10] to prepare biomaterials with applications such as water treatment[11], membrane filtration[12], microfluidic device[13], and active packaging materials.[14,15] Active packaging materials are those which provide some function beyond containment and basic protection of the packaged goods, for example antioxidant or antimicrobial character.[16,17] Active packaging materials are typically prepared by coating (e.g. nisin, rosemary extract, and green tea extract) or co-extrusion/multilayer lamination (butylated hydroxytoluene), ferrous oxide, and ascorbic acid).[16,18,19] Such active packaging technologies may be subject to uncontrolled migration of active agents or impaired bulk thermomechanical properties of the packaging materials. In contrast, active packaging materials prepared by covalent immobilization of active agents onto material surfaces enables retention of desirable bulk thermomechanical properties and potential regulatory benefits owing to the non-migratory nature of the active agent. Surface photografting has been reported for use in preparing non-migratory active packaging materials.[14,15,20,21] However, because oxygen inhibits free radical polymerization[22], standard photografting techniques require an oxygen-free environment, typically achieved by nitrogen inerting.[1,23-25] Surface photografting is therefore typically achieved as a *batch* process, which limits its commercial translatability in active packaging applications both in terms of throughput

and cost effectiveness. Indeed, it is estimated that 15 % of the total variable cost of producing packaged foods is spent on packaging materials,[19] making the profit margin low for industries to adopt active packaging materials of higher cost. Laminated surface photografting, during which monomers are laminated between the base material and an oxygen barrier (glass slide or polymer film),[5,8,26-28] does not require oxygen-free environment, and represents a *continuous* alternative to traditional batch surface photografting. Yang and Rånby have reported photografting of acrylic acid and methacrylic acid onto low density polyethylene (LDPE) by sandwiching monomer and benzophenone (BP) mixtures between laminated LDPE films.[29] Decker and Zahouily also prepared poly(acrylic acid) and poly(hydroxypropyl acrylate) grafted polypropylene (PP) and polyethylene (PE) film using the same photografting technique.[5]

We have previously reported a batch photografting technique to prepare non-migratory active packaging materials capable of removing trace metal ions from packaged goods and demonstrated their ability to reduce transition metal induced lipid oxidation in consumer products[15,29,30] (Figure 2.1). These reported metal chelating active packaging materials address the increasing consumer demand for 'clean label' food products,[31] by enabling removal of synthetic metal chelators (e.g. EDTA) from product formulations. The metal chelating films were synthesized by photografting acrylate monomers from PP films to introduce metal chelating ligands of carboxylic acids (PP-*g*-PAA)[20,30] and hydroxamic acids (PP-*g*-PHA).[15,32] The metal chelating films had up to approximately 80 nmol/cm^2 iron chelating capacity and reduced lipid oxidation in emulsified oil systems by delaying formation of lipid hydroperoxides and

hexanal.[15,20,30] While effective in inhibiting lipid oxidation, the previously reported metal chelating active packaging materials were synthesized in a batch process which used nitrogen inerting steps, limiting commercial translatability[15,20,30] (Figure 2.2A). In this work we report on a laminated photografting technique to introduce metal-chelating grafts on the surface of polypropylene films with similar chemistry and chelating functionality as the previously reported PP-*g*-PAA and PP-*g*-PHA, prepared using a batch process. Laminated photografting was conducted by laminating the solution of monomer and photoinitiator between UV-ozone functionalized PP film (PP-UVO) and a glass slide, followed by UV irradiation (Figure 2.2B). The resulting PP-*g*-PAA and PP-*g*-PHA films were characterized using Fourier transform infrared spectroscopy, scanning electron microscopy (SEM), water contact angle analysis, dye assay, and iron chelating assay.

Experimental Methods and Materials

Materials

HPLC grade water, isopropanol, acetone, methanol, sodium hydroxide, hydrochloric acid, sodium acetate trihydrate, ferric chloride (anhydrous), hydrochloric acid, trichloroacetic acid (TCA), 4-(2-hydroxyethyl)-1-piperazineethanesulfonic acid (HEPES) and glacial acetic acid were purchased from Fisher Scientific (Fair Lawn, NJ). Hydroxylamine hydrochloride, toluidine blue O (TBO), imidazole (99%), 3-(2-pyridyl)-5,6-diphenyl-1,2,4-triazine-*p,p'*-disulfonic acid disodium salt hydrate (ferrozine, 98%+) were purchased from Acros Organics (Morris Plains, NJ). Acrylic acid (anhydrous), methyl acrylate (99%), and benzophenone (99%) were purchased from

Sigma-Aldrich (St. Louis, MO). All the chemicals were used without further purification.

Surface Modification

Polypropylene (PP) pellets (isotactic, Scientific Polymer Products, Ontario, NY) were cleaned by sonication separately in isopropanol, acetone, and deionized water, followed by drying over anhydrous calcium sulfate in a desiccator (25 ^{o}C, 15 % relative humidity). Cleaned PP pellets were hot pressed (Carver Laboratory Press, Model B, Fred S. Carver, NJ) with 9000 lbs press force at 170 ^{o}C into films of 390 ± 40 µm thickness. PP films were cut into 5×5 cm^2 pieces and were cleaned and dried in the same way as PP pellets. PP films were subjected to 15 min UV-ozone treatment (PP-UVO) at 185 nm and approximately 5.6 mW/cm^2 (Jelight Co. model 42, Irvine, CA) for initial functionalization to improve wettability,[33] which subsequently improves monomer grafting. Laminated photografting was then performed by sandwiching a thin layer of monomer solution (0.5 mL acrylic acid or 0.35 mL methyl acrylate) containing 5 wt % BP between a glass slide and the PP-UVO film as illustrated in Figure 2.2B. The monomer and BP mixture laminated with PP-UVO was exposed to 365 nm UV irradiation at approximately 210 mW/cm^2 fluence (Dymax 5000-EC Series, Torrington, CT) for 20 s (acrylic acid) or 90 s (methyl acrylate) in a fume hood (Figure 2.3). To prevent film deformation during longer exposure times, a glass slide was placed on top of the PP-UVO for photografting methyl acrylate. The perimeter of the film may be prone to oxygen inhibition as oxygen can diffuse into monomer from the sides; therefore, only the center 4×4 cm^2 portion of the resulting films were utilized as 1×2 cm^2 coupons. Poly(acrylic acid) and poly(methyl acrylate) grafted polypropylene (PP-

g-PAA and PP-*g*-PMA, respectively) were subjected to rigorous washing steps to remove adsorbed monomer and homopolymers as follows. PP-*g*-PAA coupons were washed in deionized water sequentially at room temperature (30 min), at 60 ^{o}C (60 min) and at room temperature (30 min). PP-*g*-PMA coupons were washed in acetone by Soxhlet extraction (16 h) followed by conversion to PP-*g*-PHA by reaction in basic hydroxylamine in methanol/water (4:1) for 4 h at 73 ^{o}C. The resulting PP-*g*-PHA coupons were acidified in 0.2 M hydrochloric acid in methanol/water (5:1), and washed in deionized water three times (30 min each). Coupons were stored in a desiccator (25 ^{o}C, 15 % relative humidity) until further analysis.

Surface Characterization

Attenuated total reflectance Fourier transform infrared spectroscopy (ATR-FTIR) was performed to characterize surface chemistry of films using an IRTracer-100 FTIR spectrometer (Shimadzu Scientific Instruments, Kyoto, Japan) equipped with a diamond ATR crystal. Each spectrum was collected using Happ-Genzel apodization at a resolution of 4 cm^{-1} with 32 scans, using air for background spectra. Advancing and receding water contact angles were measured to quantify film surface hydrophobicity using a Kruss DSA100 (Hamburg, Germany) equipped with a DO3210 direct dosing system (Hamburg, Germany) under ambient conditions. Advancing and receding contact angles were measured by adding (or withdrawing in the case of receding angles) 5 µL water on the surface at a rate of 25 µL/min and calculated every 0.1 s using tangent-2 method. Contact angle hysteresis was then calculated by difference between advancing and receding contact angles. Scanning electron microscopy (SEM) was performed to characterize surface morphology of the films. Coupons were sputter coated

(Cressington 108, Cressington Scientific, Watford, UK) with gold and imaged at 10 kV (JEOL 6000 FXV, Japan). The carboxylic acid density of PP-*g*-PAA was quantified by TBO dye assay.[29,34] Briefly, each coupon was submerged in 0.5 mM TBO in deionized water at pH 10 for 2 h, and then desorbed in 50% acetic acid in water. The absorbance of the desorbed TBO was measured at 633 nm and compared against TBO standards to determine the amount of TBO absorbed from each coupon. The number of surface grafted carboxylic acids per unit area was calculated assuming a one to one ratio of carboxylic acids to bound TBO.[34]

Iron Chelating Capacity

Iron chelating capacity was analyzed for both PP-*g*-PAA and PP-*g*-PHA films as described previously,[15,30] using an adaptation of the colorimetric ferrozine assay[35] with PP and PP-UVO films serving as controls. Briefly, each coupon was submerged in a solution of 0.08 mM ferric chloride in 50 mM sodium acetate/imidazole buffer, pH 5.0, for 24 h. Ferric ion concentration in the buffered iron solution after exposure to the coupon was quantified by addition of a reducing agent containing 5 wt % hydroxylamine chloride and 10 wt % TCA, and 18 mM ferrozine in 50 mM HEPES (pH 7). The absorbance of the mixture was measured at 562 nm and iron concentration was calculated by comparison to a standard curve prepared using ferric chloride. Ferric ion chelation by each coupon was then quantified by determining the reduction in iron concentration of the buffered iron solution after exposure to the films.

Statistics

Each surface modification was prepared independently four times. Reported ATR-FTIR spectra are representative of eight total spectra collected on duplicate

coupons, from four independent preparations. SEM micrographs are representative of a total of at least sixteen images acquired at random locations on quadruplicate coupons, from four independent preparations. Water contact angle, carboxylic acid density and iron chelating capacity measurements were acquired in quadruplicates, from four independent preparations. Means of advancing and receding water contact angles were analyzed using ANOVA and compared using Fischer's least significant difference ($P<0.05$) with SAS 9.3 (SAS Institute Inc., Cary, NC).

Results and Discussion

Surface characterization

Surface chemistry of clean and photografted PP films was characterized by ATR-FTIR at each stage of the surface modification (Figure 2.4). All film variants exhibited signature absorbance bands of PP at 3000-2800 cm^{-1} from alkane C-H stretching vibrations and absorbance bands at 1450 and 1370 cm^{-1}, from C-H bending vibrations. PP-UVO films had a small absorbance band at 1710 cm^{-1}, attributed to carbonyl bond stretching vibration from carboxylic acids introduced during UV-ozone treatment.[29,33] PP-*g*-PAA films exhibited a strong absorbance band at 1710 cm^{-1}, indicating stretching vibration of carbonyl bond, a broad absorbance band at 3600-2400 cm^{-1}, indicating stretching vibration of O-H bond, and absorbance bands at 1260-1160 cm^{-1}, indicating C-O related stretching vibration. These absorbance bands are all supportive of successful grafting of poly(acrylic acid) from the PP surface. PP-*g*-PMA films presented spectral bands characteristic of ester bonds present in poly(methyl acrylate), including a strong absorbance band at 1730 cm^{-1}, indicating carbonyl bond stretching vibration, and absorbance bands at 1260-1160 cm^{-1}, indicating C-O related

stretching vibration. After conversion of methyl acrylate groups to hydroxamic acids by exposure to hydroxylamine, PP-*g*-PHA films exhibited overlapping absorbance bands at 1560 and 1650 cm^{-1}, indicating stretching vibration of carbonyl bonds and bending vibration of N-H bonds, respectively. The PP-*g*-PHA film exhibited absorbance spectra typical of hydroxamic acid groups, including a weak absorbance band at 3200 cm^{-1}, indicative of N-H stretching vibration, and was superimposed with a broad absorbance band at 3600-2400 cm^{-1}, indicating O-H stretching vibration. The ATR-FTIR spectra of the PP-*g*-PAA, PP-*g*-PMA and PP-*g*-PHA films reported here using the laminated photografting technique had the same major absorbance bands as the corresponding films made with the previously reported batch photografting method.[32,36] These results suggest that laminated photografting can produce PP-*g*-PAA and PP-*g*-PHA metal chelating films with similar surface chemistry as that introduced using the batch method.

Surface hydrophobicity of films at each stage in the surface modification was quantified using water contact angle (Table 2.1). Cleaned PP films were hydrophobic with advancing and receding contact angle values of 102.0^{o} and 81.7^{o}, respectively. It has been reported that due to the hydrophobic nature of polyolefin films, acrylate monomers have higher affinity to semipinacol radical and tend to result in homopolymerization,[1] thus reducing graft efficiency and increasing the likelihood of homopolymers that may migrate from the material surface.[26-28] Introducing an initial UV-ozone treatment step created trace amount of carboxylic acids on the PP surface as suggested in ATR-FTIR analysis, and was effective in increasing the wettability of the PP film prior to photografting (advancing and receding angles of 82.6° and 49.2°, respectively, for PP-UVO films). The initial UV-ozone treatment of PP film resulted in

more uniform coating of the initiator and monomer. The decrease in surface hydrophobicity enhanced the affinity of acrylate monomer to the surface radical during photografting, thus improving grafting efficiency. Based on our preliminary studies, photografting conducted on native PP resulted in high degree of homopolymerization and low grafting efficiency. This is in agreement with other reports, for example Castell at el. reported a laminated photografting protocol with initial grafting of BP on LDPE, which increased surface energy of inert LDPE surface thus improving photografting efficiency.[26]

PP-*g*-PAA films presented an advancing contact angle of 96.7^{o}, and a receding contact angle of 38.6^{o}. The PP-g-PAA films were more hydrophilic than native PP films as a result of hydrophilic carboxylic acid surface grafts. These values are higher than those previously reported on PP-*g*-PAA materials prepared using batch photografting technique,[20] yet the hysteresis value (difference between advancing and receding angles) was similar. Hysteresis can reflect the interaction between probe fluid and the surface and is an indicator of surface roughness/heterogeneity;[37] therefore, the similar hysteresis values may suggest the surfaces of PP-*g*-PAA films synthesized by both methods exhibited similar surface roughness, and similar water wetting properties when water droplet was dispersed onto and withdrawn from the surface. As expected after introduction of the polar ester groups, PP-*g*-PMA films were more hydrophilic than PP, with advancing and receding water contact angles of 79.2 ^{o} and 47.0 ^{o}, respectively. The PP-*g*-PHA film presented low advancing and receding contact angles of 16.3^{o} and 10.0^{o}, respectively, as expected after grafting highly hydrophilic hydroxamic acid moieties. PP-*g*-PMA and PP-*g*-PHA films prepared using the laminated photografting technique

presented equivalent advancing and receding contact angles as the corresponding films prepared using the batch technique as reported previously.[32] Surface morphology and uniformity were characterized using SEM micrographs presented in Figure 5 are representative of a total of at least sixteen images acquired at random locations on quadruplicate coupons, from four independent preparations. SEM revealed uniform, smooth surface topography, with evidence of a surface coating on PP-*g*-PAA, PP-*g*-PMA and PP-*g*-PHA films.

The density of grafted carboxylic acid groups on PP-*g*-PAA film surfaces was quantified using TBO dye assay, with PP and PP-UVO as controls (Figure 2.6). PP-*g*-PAA films presented 206 ± 43 nmol/cm^2 of carboxylic acids, while both PP and PP-UVO controls presented no carboxylic acids. As mentioned in ATR-FTIR analysis, PP-UVO had small carbonyl absorbance band at 1710 cm^{-1}, suggesting the presence of trace amount of carboxylic acid after UV-ozone functionalization. However, the trace amount of carboxylic acid was not quantifiable using TBO dye assay due to the limit of detection. It is worth noting that the average carboxylic acid density of PP-*g*-PAA films prepared by laminated photografting was about 3 times higher than that of PP-*g*-PAA prepared by the batch process.[30] The difference in graft density was due to the completely different photografting conditions, especially differences in monomer solution used in the two methods (25 wt % acrylic acid in ethanol in batch photografting,[30] no dilution of monomer in laminated photografting technique). The graft density of acrylic acid monomer can be controlled by manipulating monomer concentration and UV dose.[1,36] Ma at el. reported kinetic equation of acrylic acid graft polymerization indicating the reaction rate was positively proportional to monomer

concentration.[1] In the case of laminated photografting, the increased monomer concentration resulted in increase in polymerization rate and reduction of UV dose (from 360 s at approximately 210 mW/cm^2 in batch photografting,[30] to 20 s at approximately 210 mW/cm^2 in laminated photografting), along with increase in graft density. Yet Yang and Rånby had controlled graft density of acrylic acid monomer by manipulating UV dose using laminated photografting technique;[29] therefore, it is possible to control graft density on PP-g-PAA by controlling the UV irradiation time. The absence of carboxylic acid groups (and corresponding lack of chelating capacity as described below) in PP-UVO films suggests that while UV-ozone pretreatment was effective in improving wettability of the film, the chelating capacity of the PP-*g*-PAA and PP-*g*-PHA films is due to the photografted chelating ligands.

Iron Chelating Capacity

The iron chelating capacities of PP-*g*-PAA and PP-*g*-PHA were determined at pH 5.0 (pH value at which optimum iron chelation was achieved in previous reports),[30,32] with PP, PP-UVO and PP-*g*-PMA as controls (Figure 2.7). The controls had negligible iron chelating activity, again supporting the conclusion that the observed iron chelation by the PP-*g*-PAA and PP-*g*-PHA films was a result of specific ligand: ion interactions and not a result of precipitation or non-specific adsorption. PP-*g*-PAA films exhibited a ferric ion chelating capacity of 182 ± 29 nmol/cm^2, about three times higher than that of PP-*g*-PAA films prepared by batch photografting as previously reported,[30] which was consistent with the increment in carboxylic acid density suggested above. In contrast, PP-*g*-PHA films exhibited a ferric ion chelating capacity of 89 ± 10 nmol/cm^2, similar to that of PP-*g*-PHA films prepared by batch photografting.[15,32] It suggested that

the photografting condition applied in this study synthesized PP-*g*-PHA film with similar graft density as the one reported previously, while the UV dose required to achieve similar graft density was reduced (from 180 s at approximately 210 mW/cm^2 in batch photografting,[15,32] to 90 s at approximately 210 mW/cm^2 in laminated photografting). The increase in MA monomer concentration (from 70 wt % in acetone in batch photografting,[15,32] to no dilution of monomer in laminated photografting) enabled increased rate of polymerization, therefore, reduced UV dose. Yet it is possible to prepare PP-*g*-PHA film with higher graft density and subsequent higher iron chelating capacity using laminated photografting, by increasing UV irradiation time at the photografting stage to give PP-*g*-PMA film with higher graft density of PMA.

Conclusions

We have previously reported on the preparation of polymer films surface modified with chelating ligands, and demonstrated their ability to inhibit oxidative degradation reactions such as lipid oxidation. In this work we have reported on a laminated photografting technique capable of preparing metal chelating PP films similar to those previously prepared by a standard batch photografting technique, but without the need for a nitrogen inerting step. Surface chemistry and ability to chelate iron ions were similar for films prepared by both photografting techniques. Such laminated photografting may be adapted for roll-to-roll continuous preparation of surface modified films such as metal chelating active packaging on an industrial scale. In addition to eliminating nitrogen inerting steps, the laminated photografting requires reduced UV dose and can be performed without a solvent and may utilize less acrylate monomer. In this work, laminated photografting consumed 12 times less acrylic acid monomer and

48 times less methyl acrylate monomer to modify an equivalent surface area of film. The laminated photografting technique may serve as an efficient, economical and environmentally friendly surface modification technique for preparation of active packaging materials for consumer products.

Table 2.1. The surface water contact angles of polypropylene (PP), UV-ozone functionalized polypropylene (PP-UVO), polypropylene-*graft*-poly(acrylic acid) (PP-*g*-PAA), polypropylene-*graft*-poly(methyl acrylate) (PP-*g*-PMA) and polypropylene-*graft*-poly(hydroxamic acid) (PP-*g*-PHA).

Contact angle	Advancing (θ)	Receding ((θ)	Hysteresis (θ)
PP	102.0 [a] ± 1.9	81.7 [a] ± 2.8	20.3 ± 3.4
PP-UVO	82.6 [c] ± 2.1	49.2 [b] ± 0.7	33.3 ± 2.2
PP-*g*-PAA	96.7 [b] ± 3.3	38.6 [c] ± 2.3	58.1 ± 4.0
PP-*g*-PMA	79.2 [c] ± 1.7	47.0 [b] ± 1.1	32.2 ± 2.0
PP-*g*-PHA	16.3 [d] ± 1.9	10.0 [d] ± 0.5	6.3 ± 2.0

Means of contact angles are significantly different (Fisher's least significant difference, $P<0.05$) if they share different superscripts in the same column.

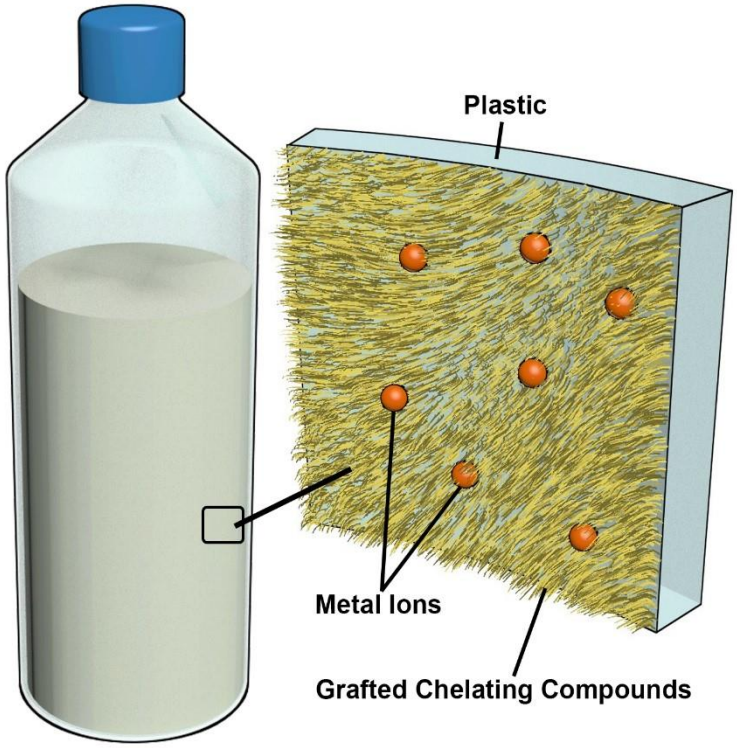

Figure 2.1. Concept of metal chelating active package materials.

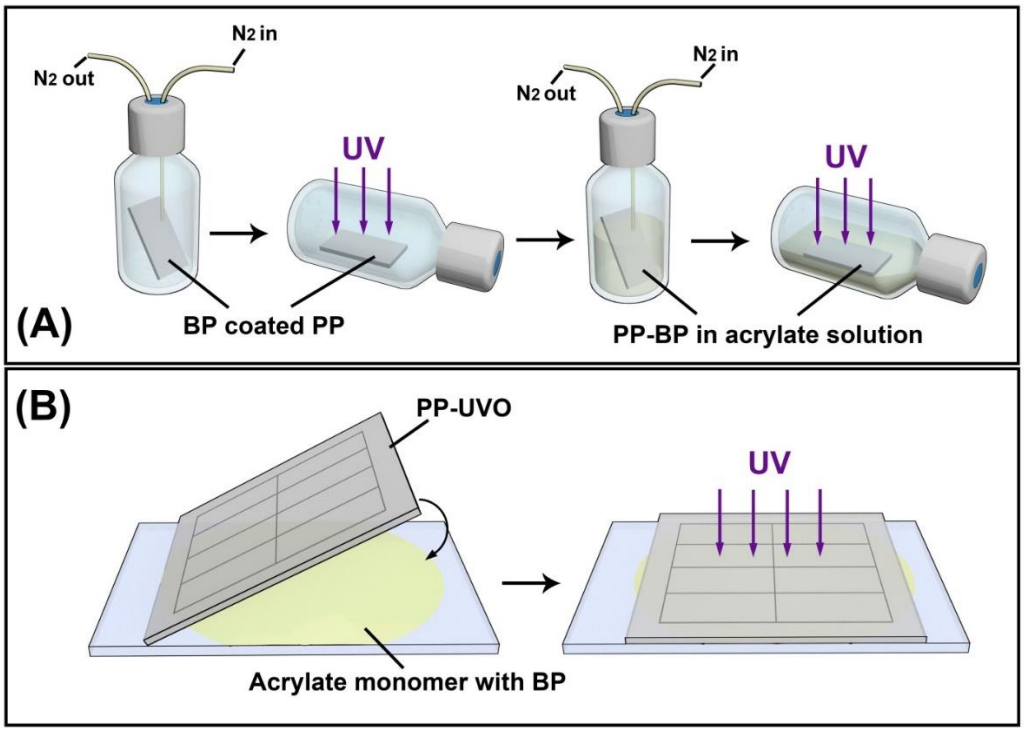

Figure 2.2. (A) Schematic of batch photografting method with nitrogen inerting. (B) Schematic of laminated photografting technique reported in this work. Abbreviations: benzophenone (BP), polypropylene (PP), benzophenone activated polypropylene (PP-BP), UV-ozone functionalized polypropylene (PP-UVO).

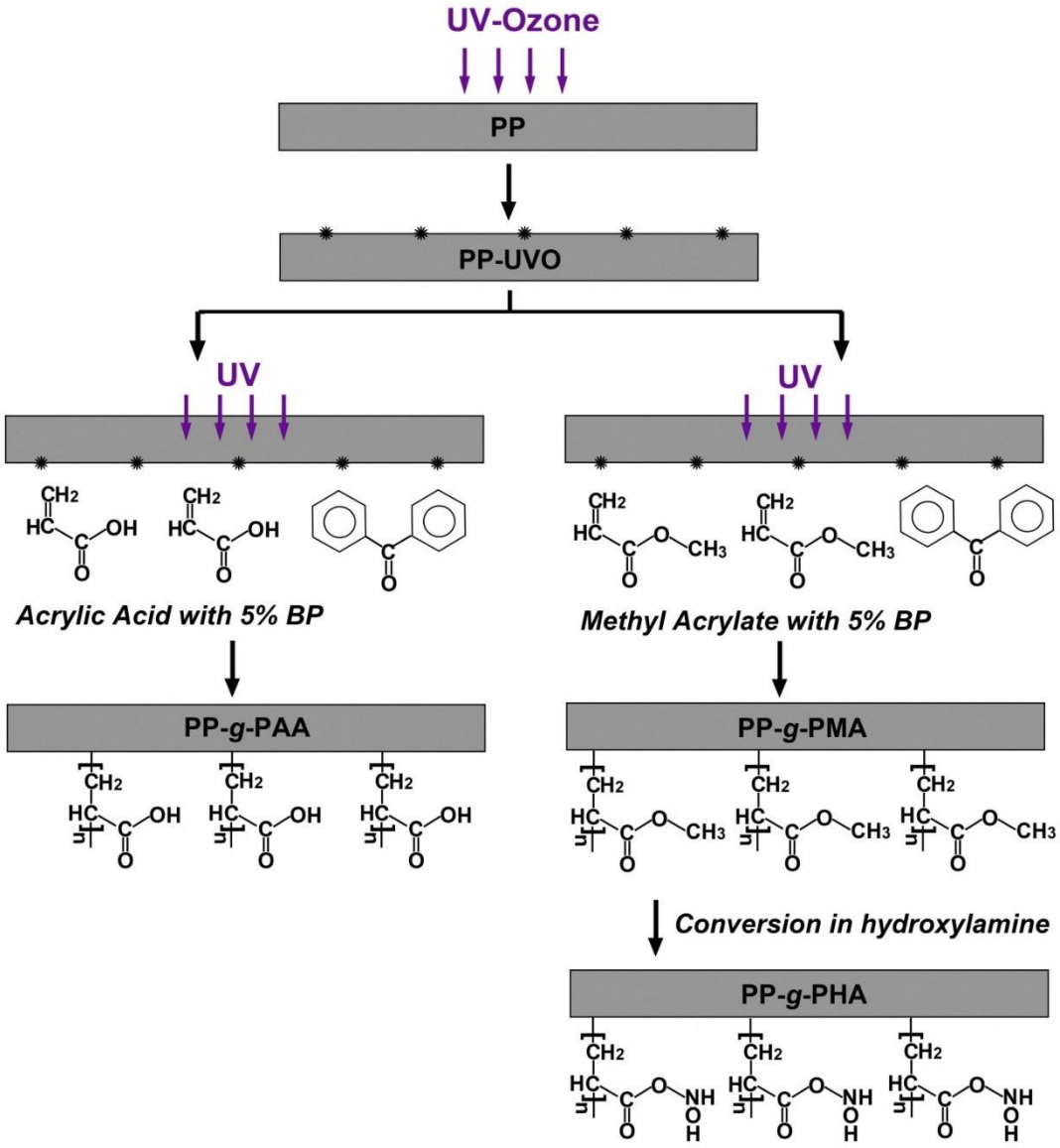

Figure 2.3. Synthesis of metal chelating films, polypropylene-*graft*-poly(acrylic acid) (PP-*g*-PAA) and polypropylene-*graft*-poly(hydroxamic acid) (PP-*g*-PHA).

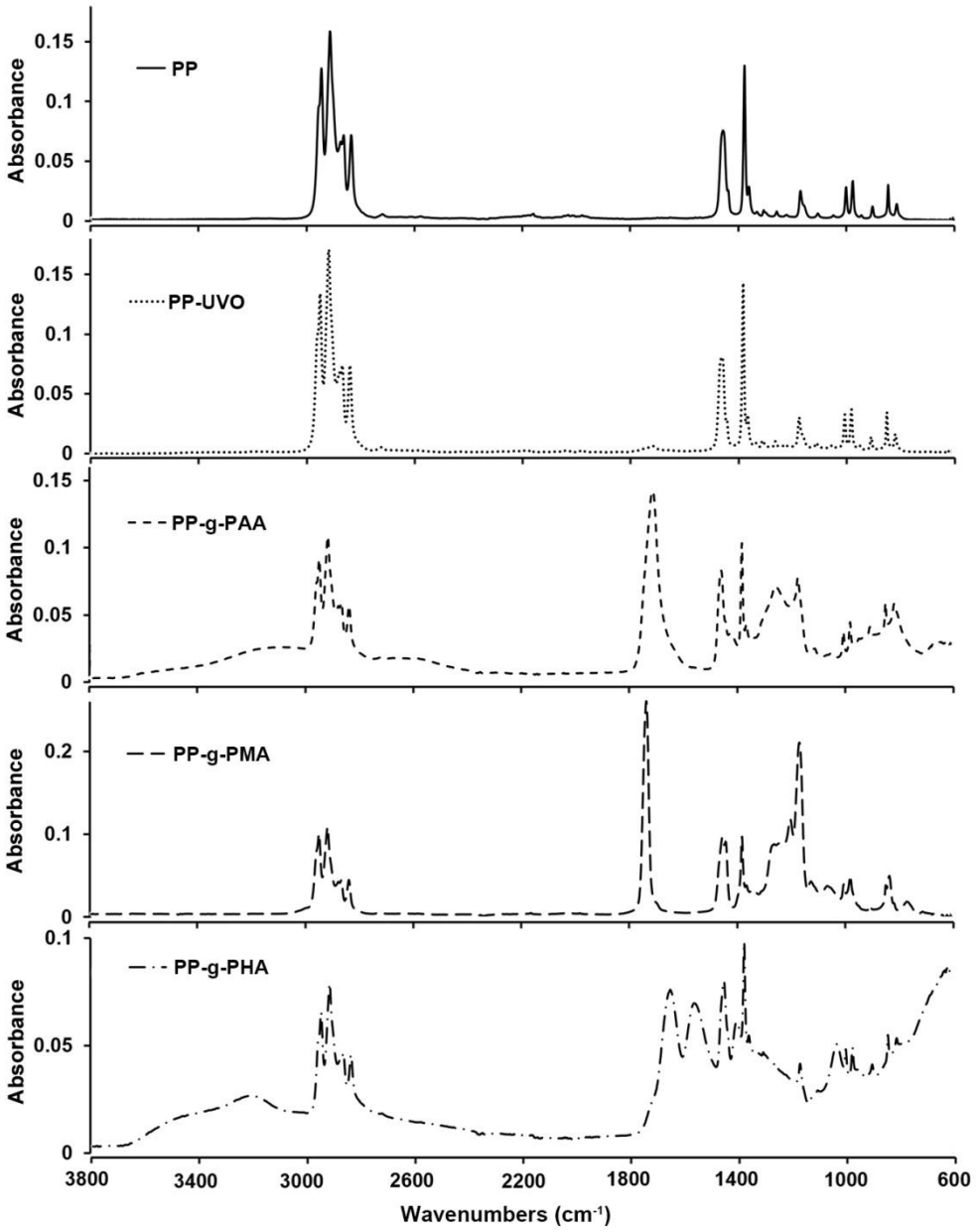

Figure 2.4. Representative Attenuated total reflectance Fourier transform infrared spectroscopy (ATR-FTIR) spectra of the polypropylene (PP), UV-ozone functionalized polypropylene (PP-UVO), polypropylene-*graft*-poly(acrylic acid) (PP-*g*-PAA), polypropylene-*graft*-poly(methyl acrylate) (PP-*g*-PMA) and polypropylene-*graft*-poly(hydroxamic acid) (PP-*g*-PHA).

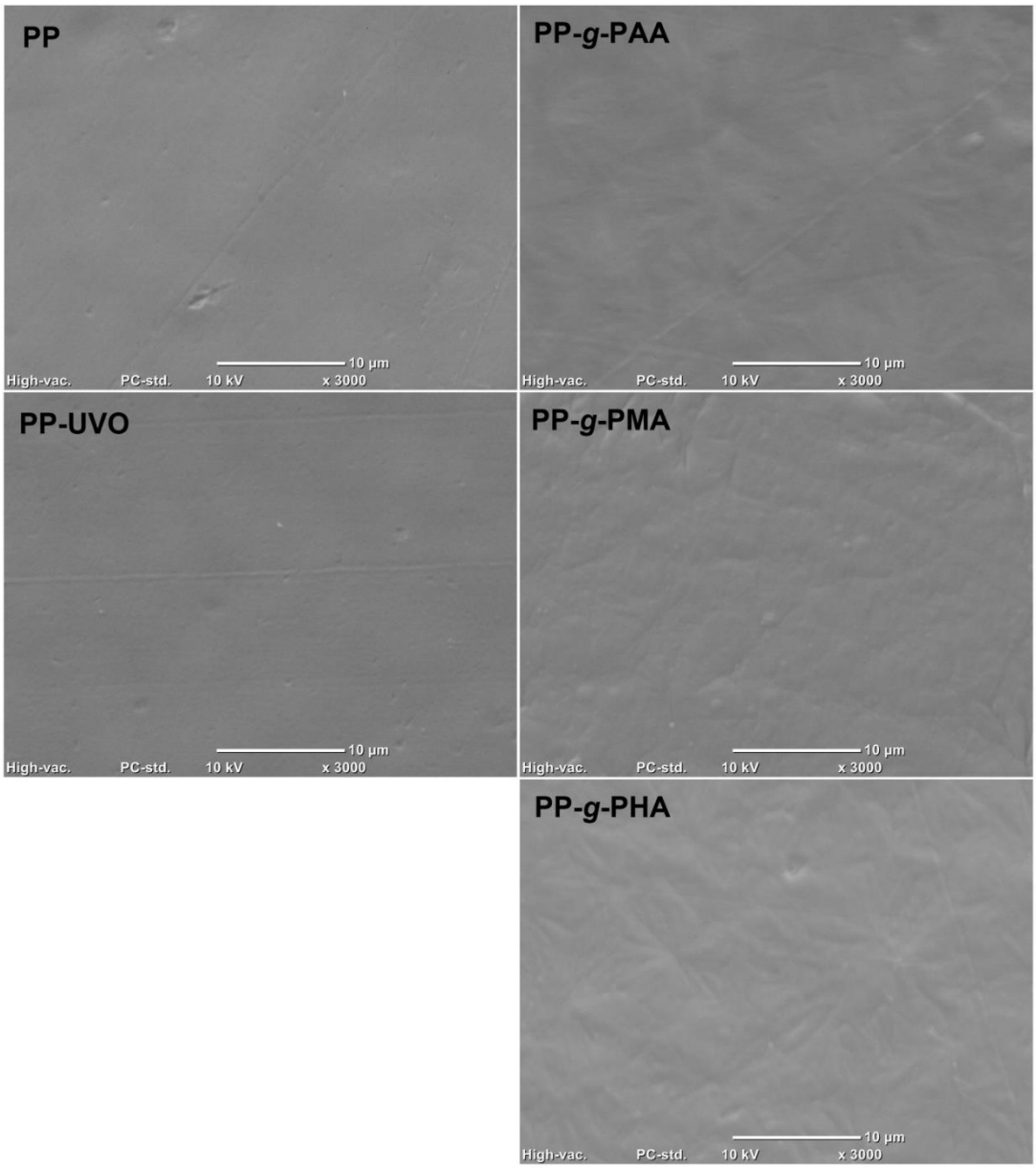

Figure 2.5. Representative scanning electron microscopy (SEM) images of the surfaces of polypropylene (PP), UV-ozone functionalized polypropylene (PP-UVO), polypropylene-*graft*-poly(acrylic acid) (PP-*g*-PAA), polypropylene-*graft*-poly(methyl acrylate) (PP-*g*-PMA) and polypropylene-graft-poly(hydroxamic acid) (PP-*g*-PHA).

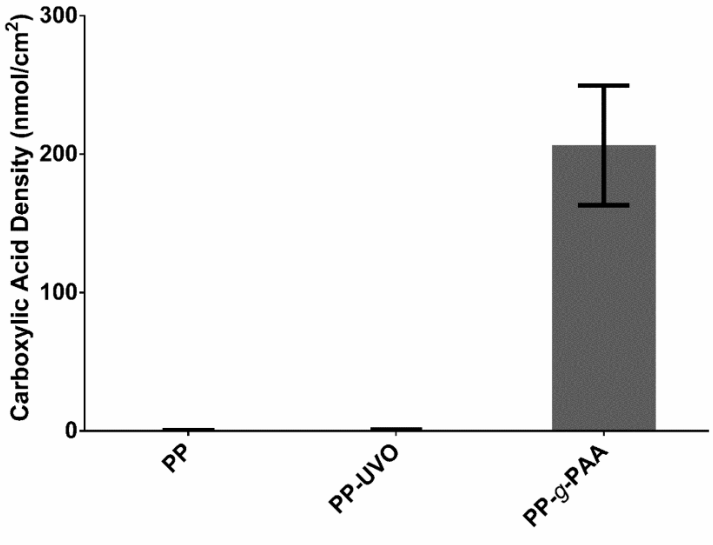

Figure 2.6. Carboxylic acid density of polypropylene (PP), UV-ozone functionalized polypropylene (PP-UVO) and polypropylene-*graft*-poly(acrylic acid) (PP-*g*-PAA).

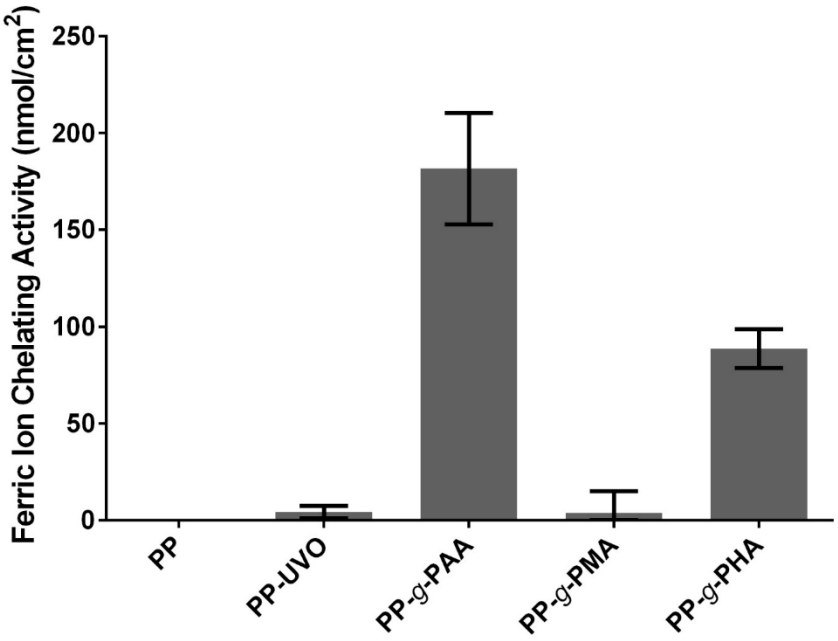

Figure 2.7. Ferric ion chelating capacity at pH 5 of polypropylene (PP), UV-ozone functionalized polypropylene (PP-UVO), polypropylene-*graft*-poly(acrylic acid) (PP-*g*-PAA), polypropylene-*graft*-poly(methyl acrylate) (PP-*g*-PMA) and polypropylene-*graft*-poly(hydroxamic acid) (PP-*g*-PHA).

REFERENCES

1. Ma, H.; Davis, R. H.; Bowman, C. N., A Novel Sequential Photoinduced Living Graft Polymerization. *Macromolecules* **2000,** *33* (2), 331-335.

2. Dyer, D., Photoinitiated Synthesis of Grafted Polymers. In *Surface-Initiated Polymerization I*, Jordan, R., Ed. Springer: Berlin, 2006; Vol. 197, pp 47-65.

3. Ulbricht, M.; Yang, H., Porous Polypropylene Membranes with Different Carboxyl Polymer Brush Layers for Reversible Protein Binding via Surface-Initiated Graft Copolymerization. *Chemistry of Materials* **2005,** *17* (10), 2622-2631.

4. Lee, K.-P.; Kang, H.-J.; Joo, D.-L.; Choi, S.-H., Adsorption behavior of Urokinase by the polypropylene film with amine, hydroxylamine and polyol groups. *Radiation Physics and Chemistry* **2001,** *60* (4–5), 473-482.

5. Decker, C.; Zahouily, K., Surface modification of polyolefins by photografting of acrylic monomers. *Macromol. Symp.* **1998,** *129* (1), 99-108.

6. Yamada, K.; Nagano, R.; Hirata, M., Adsorption and desorption properties of the chelating membranes prepared from the PE films. *J. Appl. Polym. Sci.* **2006,** *99* (4), 1895-1902.

7. Uchida, E.; Uyama, Y.; Ikada, Y., Grafting of Water-Soluble Chains onto a Polymer Surface. *Langmuir* **1994,** *10* (2), 481-485.

8. El Kholdi, O.; Lecamp, L.; Lebaudy, P.; Bunel, C.; Alexandre, S., Modification of adhesive properties of a polyethylene film by photografting. *J. Appl. Polym. Sci.* **2004,** *92* (5), 2803-2811.

9. Yong Wen, S. S.; Rahman, M. L.; Arshad, S. E.; Surugau, N. L.; Musta, B., Synthesis and characterization of poly(hydroxamic acid)–poly(amidoxime) chelating

ligands from polymer-grafted acacia cellulose. *J. Appl. Polym. Sci.* **2012,** *124* (6), 4443-4451.

10. Yamagishi, H.; Saito, K.; Furusaki, S.; Sugo, T.; Ishigaki, I., Introduction of a high-density chelating group into a porous membrane without lowering the flux. *Ind. Eng. Chem. Res.* **1991,** *30* (9), 2234-2237.

11. Kavaklı, P. A.; Kavaklı, C.; Güven, O., Preparation and characterization of Fe(III)-loaded iminodiacetic acid modified GMA grafted nonwoven fabric adsorbent for anion adsorption. *Radiation Physics and Chemistry* **2014,** *94*, 105-110.

12. Yamada, K.; Taki, T.; Sato, K.; Hirata, M., Electrotransport of organic electrolytes through 2-(dimethylamino)ethyl methacrylate–grafted polyethylene films and their separation and concentration. *J. Appl. Polym. Sci.* **2003,** *89* (9), 2535-2544.

13. Rohr, T.; Ogletree, D. F.; Svec, F.; Fréchet, J. M. J., Surface Functionalization of Thermoplastic Polymers for the Fabrication of Microfluidic Devices by Photoinitiated Grafting. *Adv. Funct. Mater.* **2003,** *13* (4), 264-270.

14. Arrua, D.; Strumia, M. C.; Nazareno, M. A., Immobilization of Caffeic Acid on a Polypropylene Film: Synthesis and Antioxidant Properties. *J. Agric. Food. Chem.* **2010,** *58* (16), 9228-9234.

15. Tian, F.; Decker, E. A.; Goddard, J. M., Controlling lipid oxidation via a biomimetic iron chelating active packaging material. *J. Agric. Food. Chem.* **2013,** *61* (50), 12397-12404.

16. Gómez-Estaca, J.; López-de-Dicastillo, C.; Hernández-Muñoz, P.; Catalá, R.; Gavara, R., Advances in antioxidant active food packaging. *Trends Food Sci. Technol.* **2014,** *35* (1), 42-51.

17. Suppakul, P.; Miltz, J.; Sonneveld, K.; Bigger, S. W., Active Packaging Technologies with an Emphasis on Antimicrobial Packaging and its Applications. *Journal of food science* **2003,** *68* (2), 408-420.

18. Tian, F.; Decker, E. A.; Goddard, J. M., Controlling lipid oxidation of food by active packaging technologies. *Food Funct.* **2013,** *4* (5), 669-680.

19. Brody, A. L.; Bugusu, B.; Han, J. H.; Sand, C. K.; McHugh, T. H., Innovative food packaging solutions. *Journal of food science* **2008,** *73* (8), R107-R116.

20. Tian, F.; Decker, E. A.; Goddard, J. M., Control of lipid oxidation by nonmigratory active packaging films prepared by photoinitiated graft polymerization. *J. Agric. Food. Chem.* **2012,** *60* (31), 7710-7718.

21. Johnson, D. R.; Tian, F.; Roman, M. J.; Decker, E. A.; Goddard, J. M., Development of Iron-Chelating Poly(ethylene terephthalate) Packaging for Inhibiting Lipid Oxidation in Oil-in-Water Emulsions. *J. Agric. Food. Chem.* **2015,** *63* (20), 5055-5060.

22. Ligon, S. C.; Husár, B.; Wutzel, H.; Holman, R.; Liska, R., Strategies to Reduce Oxygen Inhibition in Photoinduced Polymerization. *Chem. Rev.* **2013,** *114* (1), 557-589.

23. Janorkar, A. V.; Metters, A. T.; Hirt, D. E., Modification of Poly(lactic acid) Films: Enhanced Wettability from Surface-Confined Photografting and Increased Degradation Rate Due to an Artifact of the Photografting Process. *Macromolecules* **2004,** *37* (24), 9151-9159.

24. Konradi, R.; Rühe, J., Interaction of Poly(methacrylic acid) Brushes with Metal Ions: Swelling Properties. *Macromolecules* **2005,** *38* (10), 4345-4354.

25. Yamada, K.; Kimura, T.; Tsutaya, H.; Hirata, M., Hydrophilic and adhesive properties of methacrylic acid-grafted polyethylene plates. *J. Appl. Polym. Sci.* **1992,** *44* (6), 993-1001.

26. Castell, P.; Wouters, M.; de With, G.; Fischer, H.; Huijs, F., Surface modification of poly(propylene) by photoinitiators: Improvement of adhesion and wettability. *Journal of Applied Polymer Science* **2004,** *92* (4), 2341-2350.

27. Rånby, B., Surface modification and lamination of polymers by photografting. *Int. J. Adhes. Adhes.* **1999,** *19* (5), 337-343.

28. Yang, W.; Rånby, B., Radical Living Graft Polymerization on the Surface of Polymeric Materials. *Macromolecules* **1996,** *29* (9), 3308-3310.

29. Tian, F.; Decker, E. A.; Goddard, J. M., Development of an iron chelating polyethylene film for active packaging applications. *J. Agric. Food. Chem.* **2012,** *60* (8), 2046-2052.

30. Tian, F.; Decker, E. A.; McClements, D. J.; Goddard, J. M., Influence of non-migratory metal-chelating active packaging film on food quality: impact on physical and chemical stability of emulsions. *Food Chem.* **2014,** *151*, 257-265.

31. Goddard, J. M.; McClements, D. J.; Decker, E. A., Innovative technologies in the control of lipid oxidation. *Lipid Technology* **2012,** *24* (12), 275-277.

32. Tian, F.; Roman, M. J.; Decker, E. A.; Goddard, J. M., Biomimetic design of chelating interfaces. *J. Appl. Polym. Sci.* **2015,** *132* (1), 41231.

33. Bastarrachea, L. J.; McLandsborough, L. A.; Peleg, M.; Goddard, J. M., Antimicrobial N-halamine Modified Polyethylene: Characterization, Biocidal Efficacy, Regeneration, and Stability. *Journal of food science* **2014,** *79* (5), E887-E897.

34. Kang, E. T.; Tan, K. L.; Kato, K.; Uyama, Y.; Ikada, Y., Surface Modification and Functionalization of Polytetrafluoroethylene Films. *Macromolecules* **1996,** *29* (21), 6872-6879.

35. Dawson, M. V.; Lyle, S. J., Spectrophotometric determination of iron and cobalt with Ferrozine and dithizone. *Talanta* **1990,** *37* (12), 1189-1191.

36. Roman, M. J.; Tian, F.; Decker, E. A.; Goddard, J. M., Iron chelating polypropylene films: Manipulating photoinitiated graft polymerization to tailor chelating activity. *Journal of Applied Polymer Science* **2014,** *131* (4), 39948.

37. Gao, L.; McCarthy, T. J., Wetting 101°†. *Langmuir* **2009,** *25* (24), 14105-14115.

CHAPTER 3

SYNTHESIS OF IMINODIACETATE FUNCTIONALIZED POLYPROPYLENE FILMS AND THEIR EFFICACY AS ANTIOXIDANT ACTIVE PACKAGING MATERIALS*

Abstract

Introduction of metal chelating ligands to the surface of food packaging materials is a strategy for antioxidant active packaging, enabling removal of synthetic antioxidants from food products. In this study, the metal chelating ligand iminodiacetate (IDA) was covalently grafted onto polypropylene surfaces to produce metal chelating PP-*g*-IDA film. The metal chelating capacity of PP-*g*-IDA was demonstrated under acidic conditions (pH 3.0) with metal chelating capacity of 138.1 ± 26 nmol/cm^2 and 210.0 ± 28 nmol/cm^2 for Fe^{3+} and Cu^{2+}, respectively. Infrared and X-ray photoelectron spectroscopy analysis of the grafted ligand suggested potential formation of tridentate metal chelate complex. The produced PP-*g*-IDA demonstrated antioxidant efficacy both by controlling lipid oxidation as effectively as EDTA in an emulsified oil system, and by inhibition of ascorbic acid degradation. This work demonstrates the potential application of surfaces with grafted IDA ligands as effective antioxidant active food packaging materials.

*Zhuangsheng Lin, Maxine J. Roman, Eric A. Decker, Julie M. Goddard

Published in Journal of Agricultural and Food Chemistry. 64, 4606-4617.

Introduction

Immobilization of metal chelating ligands onto solid support materials has application in water treatment,[1-3] protein separation,[4-5] catalysis,[6-7] antimicrobial applications,[8] and active food packaging.[9-13] In active food packaging applications, metal chelating ligands grafted to the food contact surface of packaging materials can scavenge trace transition metal ions (i.e. iron, copper),[14] inhibiting them from promoting oxidative degradation of food components such as lipids,[15] ascorbic acid,[16] β-carotene[17] and lycopene.[18] Such non-migratory metal chelating active packaging technologies address recent consumer demands for removing synthetic additives such as metal chelators (e.g. ethylenediamine tetraacetic acid, EDTA) from food products.[19-20] For a metal chelating interface to effectively inhibit oxidative degradation of food components, the selected metal chelating ligand must be specific to the prooxidant transition metals and perform at acidic pH values (typical of many foods and beverages). The work by Tian *et al.* first demonstrated the antioxidant efficacy of metal chelating active packaging materials, yet using carboxylate chelating ligands had limited performance at pH values below 5.0.[9] Further work in which the more iron specific hydroxamate ligand was grafted onto polypropylene resulted in a material with retained antioxidant activity at pH 3.0[10] and ability to selectively chelate iron over calcium, magnesium, and sodium.[21] However, upon chelation the hydroxamate groups turned a characteristic orange color, a potential limitation to commercial adaptation.

Iminodiacetate (IDA) is a common transition metal chelating ligand that has been utilized in commercial chelating resins for heavy metal removal from water,[22-25] and immobilized onto a variety of materials for ion and protein separation applications.[2-

[4, 26-28] IDA is a tridentate metal chelator with a total of three metal chelating sites, two carboxylates and a tertiary amine. Its high affinity for iron (log K=10.72 for Fe^{3+}) and copper (log K=10.57 for Cu^{2+}), and low stability constant for other multivalent ions common in food, such as calcium (log K=2.59 for Ca^{2+}) and magnesium (log K=2.98 Mg^{2+}),[29] support its specificity towards transition metals responsible for oxidative degradation in foods. Despite the potential for IDA to be utilized as the ligand in metal chelating active packaging, its transition metal chelating capacity and potential antioxidant efficacy have not been investigated.

In this study, we aimed to characterize the surface chemistry, metal chelating activity and antioxidant efficacy of surface immobilized IDA ligand in acidic environments (pH 3.0). IDA was grafted onto the surface of polypropylene films by photografting of a vinyl monomer and subsequent immobilization of IDA to yield metal chelating PP-*g*-IDA film. The surface modification was quantified by contact angle, electron microscopy, and spectroscopy. The dissociation behavior and estimated bulk pKa value of carboxylate group were determined using FTIR titration. Relative stability constants for Fe^{3+} and Cu^{2+} were estimated using a competitive chelation assay. The metal chelating activity and the resulting antioxidant activity against lipid and ascorbic acid degradation were tested in high acid condition of pH 3.0.

Materials and Methods

Materials

Benzophenone (99%), 3-chloro-2-hydroxypropyl methacrylate, sodium iminodiacetate dibasic monohydrate (≥95%), dimethyl sulfoxide (≥99.5%), barium chloride dihydrate, ammonium thiocyanate, cumene hydroperoxide (80%), hexanal

(98%), zincon monosodium salt, nitric acid, D-penicillamine, nitrilotriacetic acid (98%), and 3-(2-pyridyl)-5,6-diphenyl-1,2,4-triazine-*p,p'*-disulfonic acid disodium salt hydrate (ferrozine, 98%+) were purchased from Sigma-Aldrich (St. Louis, MO). HPLC grade water, isopropanol, acetone, methanol, iso-propanol, iso-octane, 1-butanol, sodium hydroxide, glacial acetic acid, hydrochloric acid (trace metal grade), trichloroacetic acid (TCA), oxalic acid dihydrate, sodium acetate trihydrate, 4-(2-hydroxyethyl)-1-piperazineethanesulfonic acid (HEPES), sodium phosphate monobasic monohydrate, sodium carbonate anhydrous, sodium bicarbonate, ferric chloride hexahydrate, Tween 20, ethylenediamine tetraacetic acid (EDTA) (disodium salt dehydrate), and 2,6-dichloroindophenol were purchased from Fisher Scientific (Fair Lawn, NJ). Imidazole (99%), citric acid monohydrate (99.5%), iminodiacetatic acid (98+%), ferrous sulfate heptahydrate (99+%), cupric sulfate pentahydrate (99+%), and L-ascorbic acid were purchased from Acros Organics (Morris Plains, NJ). Absolute ethanol was purchased from Pharmco-Aaper (Brookfield, CT). Commercial soybean oil (Wesson 100% natural vegetable oil) was purchased from a local grocer. All chemicals and reagents were used as received without further purification.

Metal Chelating Film Synthesis

To prepare polypropylene films, polypropylene pellets (isostatic, Scientific Polymer Products, Ontario, NY) were washed by sonicating sequentially in isopropanol, acetone and deionized (DI) water, and dried in a desiccator (25^{o}C, 15 % relative humidity). Dried polypropylene pellets were hot pressed (Carver Laboratory Press, Model B, Fred S. Carver, NJ) into polypropylene films with 9000 lbs press force at 180^{o}C. Polypropylene films were cut into 5x5 cm^2 pieces, cleaned by sonicating

sequentially in isopropanol, acetone and water, and then dried in a desiccator. Iminodiacetate grafted polypropylene (PP-*g*-IDA) films were prepared by a two-step method, as illustrated in Figure 3.1. Polypropylene films underwent initial surface functionalization by laminated photografting of a vinyl monomer described in Lin *et al.* with modifications.[30] 3-Chloro-2-hydroxypropyl methacrylate (CHPM) monomer containing 5 wt % benzophenone was sandwiched between a polypropylene film and a glass slide (5x7 cm^2, Ted Pella, Inc. Redding, CA) followed by 60 seconds exposure to UV irradiation (365 nm, approximately 210 mW/cm^2 fluence, Dymax 5000-EC Series, Torrington, CT). The resulting 3-chloro-2-hydroxypropyl methacrylate grafted polypropylene (PP-*g*-CHPM) films were cut into 1x1 cm^2 coupons and washed in acetone at 70^{o}C for 16 hours to remove residual monomers and homopolymers, followed by submersion in 0.425 M IDA in DMSO/water (1:1 v/v) solution according to method described in Yamada et al.[2] for 10 hours at 80^{o}C with vigorous stirring under reflux, to covalently immobilize IDA ligands. The resulting PP-*g*-IDA films were washed in DI water for 30 min three times, and stored in a desiccator until further analysis.

Surface Characterization

Surface morphology and wettability

Surface morphology was characterized using scanning electron microscopy (SEM). Samples were sputter coated with gold (Cressington 108, Cressington Scientific, Watford, UK) and imaged at 10 kV (JEOL 6000 FXV, Japan). Graft thickness was determined by optical profilometry (Zeta-20, Zeta Instruments, San Jose, CA) on films for which a small portion was left ungrafted. The average of three measurements was

recorded for the graft thickness for each sample. Surface wettability was characterized using water contact angle analysis, using a Kruss DSA100 (Hamburg, Germany) equipped with a DO3210 direct dosing system (Hamburg, Germany). Advancing and receding water contact angles were measured every 0.1 s using tangent-2 method when 5 µL water was added (or withdrawn in the case of receding angles) to the sample surface at a rate of 25 µL/min.

Surface chemistry

The surface chemistry of native and modified polypropylene films was analyzed using attenuated total reflectance Fourier transform infrared spectroscopy (ATR-FTIR) on an IRTracer-100 FTIR spectrometer (Shimadzu Scientific Instruments, Kyoto, Japan) equipped with a diamond ATR crystal. Each absorbance spectrum was collected from each piece of film at a resolution of 4 cm^{-1} (32 scans) using Happ-Genzel apodization, with air as background spectrum. Surface chemistry of PP-*g*-CHPM and PP-*g*-IDA was further analyzed using X-ray photoelectron spectroscopy (XPS). The instrument (Physical Electronics Quantum 2000, Chanhassen, MN) had an Al Kα excitation spot size of 100 µm at 25 W. Each spectrum was collected from each piece of film at an angle of 45º. Survey scan spectra were collected at a pass energy of 187.85 eV with a step size of 1.6 eV, and high resolution spectra were collected at a pass energy of 46.95 eV with a step size of 0.2 eV.

Ligand dissociation

Dissociation behavior of the carboxylates on the grafted IDA ligand was analyzed using an adaptation of the FTIR titration method according to Dong et al.[31] and Roman et al.,[32] which monitor changes in absorbance wavenumbers and intensities

of key functional groups according to their protonation state. PP-*g*-IDA films were stored in solutions with pH values ranging from 2.0 to 12.0 (prepared in 0.01 M sodium phosphate buffer, adjusted using hydrochloric acid or sodium hydroxide) for 24 hours to modulate the ionic exchange between the grafted ligands and solutions. After storage in pH adjusted solutions, PP-*g*-IDA films were rinsed with absolute ethanol, dried in a desiccator, and analyzed by ATR-FTIR. The degree of dissociation (α) of the carboxylate group can be calculated by dividing the molar concentration of deprotonated carboxylate by the sum of molar concentration of both protonated and deprotonated carboxylate, as follows:

$$\alpha = \frac{c(COO-)}{c(COOH)+c(COO-)} \quad (0 \leq \alpha \leq 1) \qquad (1)$$

where α is the degree of dissociation of carboxylate group, c(COOH) is the molar concentration of protonated carboxylate, and c(COO-) is the molar concentration of deprotonated carboxylate. Molar concentration for each species can be determined by Beer-Lambert law:

$$A = c*D*\varepsilon \qquad (2)$$

Where A is the integrated area of the absorption band on FTIR spectrum dedicated to the stretching vibration each carbonyl species, c is the molar concentration of each carbonyl species, D is the penetration depth of ATR-FTIR radiation, and ε is the extinction coefficient of each carbonyl species. Integrated areas were determined using curving fitting analysis of FTIR spectra with absorbance maxima of 1720 cm^{-1} and 1620-1580 cm^{-1} (variable depending on protonation or chelation) for protonated and deprotonated carboxylates, respectively. As PP-*g*-IDA films contain acetate ester groups, which also absorb at 1720 cm^{-1}, determination of degree of dissociation of

carboxylate group required introduction of the following two parameters:

a) the integrated area percentage of the absorption band at 1720 cm^{-1}, denoted R:

$$R = \frac{A(O-C=O)+A(COOH)}{A(O-C=O)+A(COOH)+A(COO-)} \qquad (3)$$

in which A(O-C=O) is the integrated area of the acetate ester carbonyl absorption, A(COOH) is the integrated area of the protonated carboxylate absorption, and A(COO-) is the integrated area of the deprotonated carboxylate absorption, and

b) the ratio between the molar concentration of acetate ester and the sum of protonated and deprotonated carboxylates, denoted λ ($0<\lambda\leq0.5$):

$$c(O-C=O) = \lambda*(c(COOH)+c(COO-)) \qquad (4)$$

in which c(O-C=O) is the molar concentration of acetate ester groups.

By combining Equations 1-4, and substituting the value of 0.556 reported by Konradi and Rühe[33] for ε(COOH)/ε(COO-), we derived:

$$\alpha \ \frac{\varepsilon(COO-)}{\lambda*\varepsilon(O-C=O)+\varepsilon(COOH)} = \frac{1}{\frac{R}{1-R}+0.556} \qquad (5)$$

As $\frac{\varepsilon(COO-)}{\lambda*\varepsilon(O-C=O)+\varepsilon(COOH)}$ is a fixed value, the function $\frac{1}{\frac{R}{1-R}+0.556}$ is positively proportional to the degree of dissociation of carboxylate group, and was plotted against the corresponding pH values at which R was acquired. The resulting plot was fit to a sigmoidal model to describe the dissociation behavior of the carboxylates and derive the equation for the degree of dissociation of carboxylates, as follows:

$$\alpha = \frac{1}{0.685*((\frac{R}{1-R})+0.556)} - 0.921 \qquad (6)$$

A titration curve was obtained by plotting the degree of dissociation (α) against corresponding pH values, followed by fitting with a sigmoidal model. Finally, the bulk pKa value of carboxylate was estimated as the solution pH value when degree of dissociation was 0.50.

Metal Chelation

Metal chelating capacity

Fe^{3+} and Cu^{2+} chelating capacities of PP-*g*-IDA films were analyzed using the colorimetric ferrozine[10, 34] and zincon[35] assays, respectively. Briefly, films were incubated in 0.08 mM ferric chloride or cupric sulfate in 50 mM sodium acetate/imidazole buffer (pH 3.0, 24 hours, room temperature, dark). Ferric ion concentration in the buffered solution remaining after exposure to the film was quantified by adding a reducing agent (5 wt % hydroxylamine chloride and 10 wt % TCA) and ferrozine solution (18 mM ferrozine in 50 mM HEPES (pH 7.0)). The absorbance of the mixture was measured at 562 nm after 1 hour incubation period and the Fe^{3+} concentration was calculated by comparison to a standard curve prepared using ferric chloride. Cu^{2+} ion concentration in the buffered solution remaining after exposure to the film was quantified by adding 0.0625 mM zincon in 0.1 M sodium carbonate (pH 9.0). The absorbance of the mixture was measured at 600 nm after 30 min incubation and Cu^{2+} concentration was calculated by comparison to a standard curve prepared using cupric sulfate. Fe^{3+} and Cu^{2+} chelating capacities of PP-*g*-IDA films were quantified by measuring the decrease in Fe^{3+} or Cu^{2+} concentration in the buffered ion solution after exposure to the film, with polypropylene and PP-*g*-CHPM films exposed to buffered

ion solution serving as controls. A separate set of films that had been exposed to buffered metal ion solutions were rinsed with absolute ethanol and dried in a desiccator for subsequent analysis by ATR-FTIR and XPS as described above to monitor ligand metal coordination behavior.

Relative Stability Constant Determination by Competitive Binding

To estimate the relative stability constants of the PP-*g*-IDA metal chelate complexes (Fe^{3+} and Cu^{2+}), PP-*g*-IDA films were subjected to metal chelating capacity analysis as described above with the inclusion of metal chelators with known stability constants in the buffered ion solutions. The chelators citric acid, IDA, nitrilotriacetic acid (NTA), EDTA, or D-penicillamine, were included at 0.08 mM, with PP-*g*-IDA films stored in pH 3 buffer, 0.08 mM Fe^{3+} or 0.08 mM Cu^{2+} as controls. After 24 hours incubation, the PP-*g*-IDA films were rinsed with absolute ethanol and dried in a desiccator. PP-*g*-IDA films were subjected to ATR-FTIR analysis and degrees of dissociation of carboxylate groups were calculated based on Equation 6. The total metal content chelated by PP-*g*-IDA films was quantified using inductively coupled plasma mass spectrometry (ICP-MS).[36] To prepare samples for ICP-MS, each piece of PP-*g*-IDA film (approximately 20 mg) was weighed directly into microwave digestion vessels (Mars Xpress 75ml vessels, CEM, Matthews, NC). The microwave digestion was conducted in 5 mL nitric acid using the Mars Xpress (CEM, Matthews, NC) and was carried out at 210°C for 30 min. Digested samples were diluted with DI water, and held at 4°C until analysis. ICP-MS analysis was conducted on a Perkin Elmer Elan 9000 equipped with an autosampler (Waltham, MA). Calibration standards were prepared with iron and copper solutions (1,000 ppm ICP-MS Standard, Ricca Chemical

Company, Arlington, TX) and clean polypropylene films. Relative stability constants were determined based on the retention of metal chelation and change in the degree of dissociation of the carboxylate group.

Food Applications: Inhibiting Oxidative Degradation Reactions

Lipid oxidation

PP-*g*-IDA films were characterized for their ability to control transition metal promoted lipid oxidation in emulsified oil systems using an accelerated lipid oxidation study,[11] with some modifications. Briefly, 1 wt % soybean oil was mixed with 50 mM sodium acetate/imidazole (pH 3) buffer, with 0.1 wt % Tween 20 as emulsifier. The mixture was emulsified by homogenizing using a hand-held homogenizer (Biospec Products, Inc., Bartlesville, OK), followed by passing through a microfluidizer (Microfluidics, Newton, MA) three times at 9000 bar. Each piece of PP-*g*-IDA film was stored with 1 mL emulsion at 55^{o}C in a sealed 10 mL gas chromatography (GC) vial, with blank emulsion (no film), emulsion with clean polypropylene film, and 0.08 mM EDTA as controls. The emulsions were sampled every two days to analyze lipid hydroperoxide (a primary oxidation product) and hexanal (a secondary oxidation product) contents.

Lipid hydroperoxides were quantified using a modification of the method of Shantha and Decker.[37] Briefly, 0.30 mL emulsion was mixed with 1.5 mL iso-octane/iso-propanol (3:1 v/v) by vortex and then centrifuged at 3000 rpm for 3 min. An aliquot of 0.2 mL upper phase (containing the hydroperoxides) was pipetted into 2.8 mL methanol/butanol (2:1 v/v) and mixed with 30 µL thiocyanate/ferrous solution, which was made by mixing an equal volume of 3.94 M thiocyanate and 0.072 M ferrous

chloride. The mixture was incubated at room temperature for 20 min and then absorbances were read at 510 nm. The lipid hydroperoxide concentration was calculated by comparison to standards prepared using cumene hydroperoxide.

Hexanal content was determined by head space analysis using gas chromatography (GC-2014, Shimadzu, Tokyo, Japan) with a flame ionization detector (FID) and a fused-silica capillary column (30 m x 0.32 mm x 1 µm) with poly(dimethylsiloxane) coating (Equity 1, Supelco, Bellefonte, PA). Samples were pre-incubated at 55^{o}C for 10 min to release volatile compounds to the headspace, which were then extracted using a divinylbenzene/carboxen/polydimethylsiloxane solid-phase microextract (SPME) fiber (50/30 µm, Supelco, Bellefonte, PA) for 2 min. The SPME fiber was desorbed in the GC injector at 250^{o}C for 3 min at a split ratio of 1:7, to release the absorbed volatile compounds. The injector, oven and detector temperatures were set at 250^{o}C, 65^{o}C and 250^{o}C, respectively. The integrated area of the hexanal peak was calculated and the hexanal concentration was determined by comparison to hexanal standards prepared by addition of hexanal in ethanol solution into 50 mM sodium acetate/imidazole buffer (pH 3.0).

Ascorbic acid degradation

PP-*g*-IDA film was analyzed for the ability to control oxidative degradation of bioactive nutrients using a model ascorbic acid solution. PP-*g*-IDA films were incubated in 1 mL ascorbic acid solution (20 mM ascorbic acid in 10 mM sodium acetate/imidazole buffer, pH 3) at 37^{o}C for 18 days in 10 mL sealed GC vials. At each time point during the study, ascorbic acid content of solutions incubated with PP-*g*-IDA films was determined using modified dichloroindophenol assay based on Association

of Official Analytical Chemists (AOAC) official method 967.21.[38] Briefly, 0.2 mL aliquot of ascorbic acid solution was mixed with 4.8 mL 0.04 wt % oxalic acid, and 0.3 mL aliquot of mixture was added to 4.7 mL 0.2 mM dichloroindophenol solution to yield a colored reaction product. The absorbance was measured immediately at 520 nm and ascorbic acid content was calculated by comparing to ascorbic acid standards, with blank ascorbic acid solution (no film), ascorbic acid solutions incubated with clean polypropylene films, and ascorbic acid solutions with 0.08 mM EDTA as controls. Data were fitted to a first order degradation rate equation to determine half-life and rate coefficients of ascorbic acid degradation.

Graft Stability

PP-*g*-IDA films were subjected to a stability study to assess possible migration or delamination of the surface grafts by incubating films in food simulants recommended by the Food and Drug Administration (FDA)'s guideline for '*Preparation Of Premarket Submissions For Food Contact Substances'.*[39] Swatches of PP-*g*-IDA films (1x1 cm^2) were stored in 1.55 mL of DI water, 3 wt % acetic acid, 10 v/v % ethanol or 10 v/v % corn oil, representing aqueous, acidic, alcoholic or fatty foods, respectively, for 10 days at 40^oC. After storage, films were rinsed with absolute ethanol, washed in DI water for 30 min and then dried in a desiccator. The surface chemistry and surface morphology of the PP-*g*-IDA films after incubation with the food simulants were analyzed using ATR-FTIR and SEM.

Statistics

Preparation of PP-*g*-CHPM and PP-*g*-IDA films was conducted in duplicate batches. All analyses on PP-*g*-CHPM and PP-*g*-IDA films were conducted on

quadruplicate samples (duplicate samples from duplicate batches). ATR-FTIR and XPS spectra are representative of a total of four spectra collected on quadruplicate films. SEM micrographs are representative of a total of eight images on quadruplicate films (two images collected at random locations on each film). Curve fitting analysis for ATR-FTIR spectra and XPS was conducted using Gaussian models in OriginPro 9.0 (OriginLab Corporation, Northampton, MA) and MultiPak 9.3 (Physical Electronics, Chanhaseen, MN), respectively. Means from analysis of variance (ANOVA) analysis were compared using Fischer's least significant difference ($P<0.05$) in GraphPad Prism 6.0 (La Jolla, CA) or in OriginPro 9.0. Sigmoidal fitting for the titration curve was conducted in OrginPro 9.0, and non-linear fitting for ascorbic acid degradation was conducted in GraphPad Prism 6.0.

Results and Discussions

Surface Modification

Surface morphology and wettability

The surface morphologies of the native and modified polypropylene films were imaged under SEM (Figure 3.2). PP-*g*-CHPM and PP-*g*-IDA exhibited uniformly dispersed surface grafts, with similar surface morphology between the two. The surface grafts gave apparent increase in surface roughness comparing to the surface of native polypropylene. PP-*g*-IDA film had some noticeable surface cracks, likely caused by surface dehydration prior to imaging. The surface grafts on PP-*g*-CHPM and PP-*g*-IDA films had an equivalent estimated thickness of 2-3 μm (Table 3.1), determined using optical profilometry. The similarities in surface morphology and graft thickness of PP-*g*-CHPM and PP-*g*-IDA suggested that IDA may be immobilized to only the very

surface of the PP-*g*-CHPM. Water contact angle analysis was conducted to characterize wettability of the native and modified polypropylene films (Table 3.1). Native polypropylene exhibited a hydrophobic surface with an advancing water contact angle of 106.6°. After photografting of 3-chloro-2-hydroxypropyl methacrylate, PP-*g*-CHPM films retained hydrophobicity (91.7° advancing contact angle). PP-*g*-CHPM had increased degree of hysteresis (difference between advancing and receding angles) compared to polypropylene film, as expected by introduction of grafted chains with increased molecular mobility and roughness.[40] After immobilization of the aminodicarboxylate metal chelating ligand IDA, PP-*g*-IDA became hydrophilic as expected, with low water contact angles of 14.1° and 8.7°, for advancing and receding angles, respectively.

Surface chemistry

The surface chemistry of PP-*g*-CHPM and PP-*g*-IDA films was characterized by ATR-FTIR spectroscopy, with native polypropylene as control (Figure 3.3). Native polypropylene exhibited characteristic absorption bands at 3000-2800 cm^{-1} and 1450-1370 cm^{-1}, which were ascribed to alkane C-H stretching and bending vibrations, respectively. PP-*g*-CHPM films presented a broad absorption band at around 3400 cm^{-1}, indicating O-H stretching vibration from the alcohol group, and strong absorption bands at 1720 cm^{-1} and 1200 cm^{-1}, indicating C=O and C-O stretching vibrations, respectively, from the acetate ester group on the grafted polymer. After chemical conversion to immobilize the IDA chelating ligand, the PP-*g*-IDA film presented a weaker, but still strong, absorption band at 1720 cm^{-1}, characteristic of both the acetate ester group of the grafted polymer and the introduction of carboxylic acids from the

IDA. Introduction of a strong absorption band at 1620 cm^{-1}, characteristic of deprotonated carboxylates, further supports successful introduction of IDA chelating ligands. The double bands at 1720 cm^{-1} and 1620 cm^{-1}, as well as the absorption band at 1400 cm^{-1}, are characteristic of protonated and deprotonated carboxylates immobilized on solid support.[32-33] The broad absorption band at around 3300 cm^{-1} was from O-H bond from both alcohol group on CHPM and protonated carboxylates of IDA, as well as water swelled into the graft due to its high hydrophilicity. Since the amine group in IDA was a tertiary amine, no N-H stretching or bending vibration was observed, as expected.[41] The specific absorption band for amine C-N stretching vibration in the 1250-1020 cm^{-1} region[41] could not be identified due to overlapping bands.

The surface chemistry was further characterized using XPS analysis. Survey scans indicated successful nucleophilic substitution of the alkyl halide on CHPM by the secondary amine during IDA immobilization, by the apparent loss in Cl2p band and introduction of N1s band in the PP-*g*-IDA spectra (Figures 3.4A and 3.4C). High resolution C1s spectra of PP-*g*-CHPM and PP-*g*-IDA films (Figures 3.4B and 3.4D) support this conclusion, with an apparent loss in the deconvolution band characteristic of the C-Cl bond at 284.3 eV.[42] Comparison of the integrated area percentages of the deconvolution bands corresponding to C=O, C-O, C-Cl, and C-C from the high resolution C1s spectra (reported in a table inset to Figures 3.4B and 3.4D) further supports the reaction scheme proposed in Figure 3.1. The stoichiometric ratio of C=O: C-O: C-Cl: C-C in the proposed surface chemistry of PP-*g*-CHPM was 1:3:1:5, which was close to the corresponding area percentages of C=O, C-O, C-Cl and C-C (10.30 %,

34.04 %, 11.76 % and 43.90 %, respectively). The stoichiometric ratio of C=O: C-O/C-N: C-C in the proposed surface chemistry of PP-*g*-IDA film was 3:8:7, which was again close to the corresponding area percentages calculated from the high resolution C1s scan (18.83 %, 41.21 % and 39.96 %, respectively). These results, along with those of the FTIR spectral interpretation, support the proposed reaction scheme in Figure 3.1, as well as apparent complete nucleophilic substitution of chlorine groups by IDA on the surface.

Ligand dissociation

The dissociation behavior of the carboxylates was analyzed using an adaptation of an FTIR titration method previously reported for surface grafted polymers.[31-32, 43] The portion of ATR-FTIR spectra ascribed to carbonyl stretching vibrations (1780 cm^{-1} to 1520 cm^{-1}) were acquired from PP-*g*-IDA films after incubation in solutions at different pH values (Figure 3.5A). The 1780 to 1520 cm^{-1} spectra region contained an absorption band centered at 1720 cm^{-1} (corresponding to protonated carboxylates as well as acetate ester groups) and one at 1620-1580 cm^{-1} (corresponding to deprotonated carboxylates, which shifts with change in pH value). As pH value increased, carboxylates deprotonated, resulting in a decrease in the integrated area of the absorption band at 1720 cm^{-1}. Similar down shift of carbonyl absorption band intensity as a result of deprotonation has been reported for poly(acrylate) and poly(methacrylate) surface grafts.[31-32] At alkaline pH values (pH 8.0 to pH 12.0), the absorption band at 1620 cm^{-1} shifted to 1580 cm^{-1}. The pH range where the shift occurred was close to the reported pKa value of 9.89[29] for the amine group on IDA. Since the absorption band at 1620-1580 cm^{-1} was ascribed to deprotonated carboxylates, the down shift of the frequency was most likely a result of deprotonation of tertiary amine. The frequency of the

absorption band for C=O stretching vibration can be affected by adjacent chemical bonds.[41] Chen et al.[44] and Kaliyappan et al.[45] reported similar down shift of C=O band on IDA caused by deprotonation of tertiary amine induced by metal chelation.

Curve fitting analysis was conducted to calculate the integrated area percentage of the two absorption bands in the 1780 -1520 cm^{-1} region, and finally the degree of dissociation (α) of the carboxylate. A titration curve was obtained by plotting the degree of dissociation against the corresponding pH value and fit to a sigmoidal model (Figure 3.5B). The bulk pKa value (the solution pH value at which degree of dissociation of ligand equals 0.5) of the iminodiacetic acid ligand grafted onto polypropylene films was estimated to be 4.85. This estimated bulk pKa value was higher than the reported pKa values for each individual carboxylate on free IDA, which were 1.82 and 2.61, respectively,[29] and was also higher than the pKa value of 3.81 reported by Chen et al.[44] for IDA ligand on soluble polymer. Comparing to free IDA and IDA in soluble polymer, the carboxylate groups in the surface grafted IDA ligand have higher proximity, which may impede proton removal from the surface grafted ligands.[31] The steric hindrance may also explain the observation of a single pKa value rather than distinct pKa values for each carboxylate, and is in agreement with other reports.[44] A bulk pKa of 4.85 suggests that the carboxylate group would be protonated at very low pH values (pH 2.0-3.0), and deprotonated at neutral to alkaline conditions (pH 7.0-12.0). This dissociation behavior suggests that at acidic conditions (e.g. pH 3.0), the metal chelating groups on grafted IDA ligand are protonated, therefore, are less likely to have ionic interaction with charged substances such as food proteins.

Metal chelating capacity

Carboxylate based chelating grafts have been reported to lose efficacy at pH values below 5.0 due to protonation and loss of negative charge of the chelating ligands[9].However, performance of chelating films at low pH values is industrially important as many foods and beverages have pH values less than 4.0 to enhance microbial stability. The metal chelating capacity of PP-*g*-IDA measured at pH 3.0 was 138.1 ± 26 nmol/cm^2 for Fe^{3+} and 210.0 ± 28 nmol/cm^2 for Cu^{2+}. The metal chelating capacity of PP-*g*-IDA film for Fe^{3+} was about three times higher than previously reported metal chelating film with surface grafted poly(hydroxamate) ligand determined at pH 3.0,[46] and was about two times higher than metal chelating polypropylene film with grafted poly(carboxylic acid) ligand, measured at pH 5.0.[9] In addition, unlike poly(hydroxamate):iron chelate complexes, the grafted IDA ligand does not change color upon Fe^{3+} or Cu^{2+} chelation.

Deprotonation of carboxylate ligands (at the same pH value) can indicate formation of metal chelate complexes; therefore, ATR-FTIR spectra were further interpreted at the C=O stretching vibration region for PP-*g*-IDA films after incubation in buffered solution (pH 3.0), buffered solution containing Fe^{3+}, and buffered solution containing Cu^{2+} (Figure 3.6A, B, and C). The integrated area of the deconvoluted band at 1720 cm^{-1} reduced from 42.00 ± 0.9 % to 18.05 ± 2.2 % and 18.70 ± 0.4 % after exposure to Fe^{3+} and Cu^{2+} ions, respectively, suggesting formation of metal chelate complexes on the grafted IDA. The observed shift in absorbance frequency of the band ascribed to deprotonated carboxylate after exposure to Fe^{3+} and Cu^{2+} ions further supports the formation of metal chelate complexes (rather than simple absorption) and

is in agreement with prior reports.[44-45]

The ligand chemistry of the tertiary amine on PP-*g*-IDA after metal chelation was analyzed using XPS of the N1s region, (PP-*g*-IDA stored in blank buffered solution served as control) (Figure 3.6D, E, F). For PP-*g*-IDA film in buffered solution (Figure 3.6D), the XPS spectrum had two absorption bands representing amine cation (higher binding energy) and free amine (lower binding energy). The integrated area of absorption band ascribed to amine cation accounted for 68.19 ± 2.0 % for PP-*g*-IDA stored in blank buffered solution, while the corresponding integrated area reduced to 25.99 ± 6.4 % and 10.50 ± 1.0 % for PP-*g*-IDA with chelated Fe^{3+} and Cu^{2+}, respectively. The results suggested deprotonation of amine cation on grafted IDA ligand as a result of metal chelation. It was interesting to note that Cu^{2+} chelation resulted in higher reduction in the absorption band of amine cation, comparing to Fe^{3+} chelation, suggesting that Cu^{2+} had higher affinity to amine group, which may be true as polyamines are used as high affinity copper chelators.[47] The XPS results also supported the FTIR analysis, as Fe^{3+} chelation gave a lower frequency shoulder to the 1680 cm^{-1} absorption band, while Cu^{2+} shifted the absorption band, because higher degree of amine cation deprotonation was achieved in the latter case.

These results all support the conclusion that PP-*g*-IDA films form metal chelate complexes with Fe^{3+} and Cu^{2+} at pH 3.0 as a result of metal-ligand specific interactions. As suggested in the ligand dissociation analysis, at pH 3.0, the carboxylate group is highly protonated, and the tertiary amine group is also in the form of protonated amine. The chelation of both Fe^{3+} and Cu^{2+} conducted at pH 3.0 enabled deprotonation of the protonated carboxylates and tertiary amine on each grafted IDA ligand, suggesting both

groups coordinated with metal ions during metal chelation, therefore, forming a tridentate metal chelate complex with Fe^{3+} and Cu^{2+}, as was proposed in other studies.[3-4]

Relative Stability Constant Determination by Competitive binding

To estimate the relative stability constants of PP-*g*-IDA metal chelate complexes with Fe^{3+} and Cu^{2+}, films were incubated with buffered solutions (pH 3.0) of metal ions with chelators of known stability constants at a 1:1 molar ratio, with solutions of metal ion alone and buffer alone as controls. The ability of PP-*g*-IDA film to acquire metal ions from the competitor chelators was then interpreted to be indicative of the relative binding affinity of PP-*g*-IDA for the metal ions. The metal chelation was quantified using ICP-MS. PP-*g*-IDA films stored in Fe^{3+} solution (no competitive chelator) had 101.0 ± 34 nmol/cm^2 Fe^{3+} chelation (Table 3.2), consistent with the Fe^{3+} chelating capacity of 138.1 ± 26 nmol/cm^2 determined using the colorimetric ferrozine assay. PP-*g*-IDA film was able to retain metal chelating capacity with the presence of citric acid, IDA and NTA. In contrast, films had significant reduction in chelating capacity when EDTA was included in the buffered iron solution. The degree of dissociation of carboxylates after formation of iron chelate complexes was also analyzed using ATR-FTIR, and were in agreement with ICP-MS analysis. Inclusion of citric acid and IDA had no effect on the degree of dissociation. The presence of NTA slightly reduced the degree of dissociation to 0.83 ± 0.12, while the presence of EDTA reduced the degree of dissociation dramatically to 0.35 ± 0.01. The degree of dissociation and ICP-MS analyses suggest that the affinity of the PP-g-IDA films for Fe^{3+} was lower than that of EDTA, but was on the order of that of citric acid, IDA, and NTA.

PP-*g*-IDA films stored in Cu^{2+} solution (with no competitive chelator) had 201.5 ± 13 nmol/cm^2 Cu^{2+} chelation (Table 3.3), consistent with the Cu^{2+} chelating capacity of 210.0 ± 28 nmol/cm^2 determined using the colorimetric zincon assay. The presence of citric acid, IDA and NTA reduced the total Cu^{2+} chelation capacity of PP-*g*-IDA films to ~ 150 nmol/cm^2, and the presence of EDTA dramatically reduced the Cu^{2+} chelation to 41.7 ± 10 nmol/cm^2. These results suggest that PP-*g*-IDA may have similar Cu^{2+} affinity to citric acid, IDA and NTA. It was interesting to note that the presence of penicillamine, a copper chelator widely used for metal chelation therapy [48], did not affect the Cu^{2+} chelating capacity of PP-*g*-IDA. Penicillamine is known to reduce Cu^{2+} to Cu^{+} by its thiol group[49] with the penicillamine-Cu^{+} complex having high reported stability constant of 19.5.[29] It is possible that the PP-*g*-IDA:Cu^{2+} chelate complex protected Cu^{2+} from being reduced by penicillamine. The degree of dissociation after formation of copper chelate complexes was analyzed using ATR-FTIR and the results agreed with the ICP-MS analysis. PP-*g*-IDA film stored in Cu^{2+} solution had a degree of dissociation of 0.94 ± 0.01. The presence of citric acid and penicillamine had no effect on the degree of dissociation. The presence of both IDA and NTA reduced the degree of dissociation slightly to 0.89 ± 0.03 and 0.83 ± 0.02, respectively. The presence of EDTA dramatically reduced the degree of dissociation to 0.40 ± 0.01. The ICP-MS and degree of dissociation analyses suggest that the affinity of the PP-*g*-IDA films for Cu^{2+} was on the same order of citric acid, IDA and NTA, but lower than that of EDTA.

Lipid oxidation

The efficacy of the PP-g-IDA film as an antioxidant active packaging material which is capable of inhibiting oxidative degradation in packaged foods was

demonstrated in two systems: inhibiting lipid oxidation in an emulsified oil system, and inhibiting ascorbic acid in an aqueous system. In emulsified oil systems, the predominant prooxidants are transition metals, which promote lipid oxidation by decomposing lipid hydroperoxides into free radicals and fatty acid scission products such as hexanal.[15] The metal chelating PP-*g*-IDA films were stored in oil-in-water emulsions (pH 3.0) at 55ºC for up to 33 days to monitor the formation of lipid hydroperoxide in the emulsions and hexanal in the head space (Figure 3.7). Blank emulsion and emulsion with added PP film or EDTA were served as controls. The blank emulsion and emulsion with added PP film exhibited signs of lipid oxidation (increased lipid hydroperoxide and hexanal content) after 5 days of storage. Both PP-*g*-IDA and EDTA effectively extended the lag phase of lipid oxidation, delaying formation of both lipid hydroperoxide and hexanal until 25 days. These results suggest that PP-*g*-IDA had similar efficacy to EDTA in controlling lipid oxidation in oil-in-water emulsion at pH 3.0. EDTA controls lipid oxidation by reducing the redox potential of transition metal ions, due to the formation of an octahedral chelating coordination. The exact mechanism of PP-*g*-IDA antioxidant efficacy is unknown, however, is likely due to its ability to either decrease the reactivity of the transition metal ions by inhibiting their redox cycling or by physically partitioning the metals away from the emulsion droplets so their interaction with lipid hydroperoxides is decreased. These results suggest that the metal chelating PP-*g*-IDA film has potential to be used to control lipid oxidation in acidified emulsified foods, as an alternative to the synthetic additive, EDTA.

Ascorbic acid degradation

Transition metals can promote the degradation of ascorbic acid,[50] which can

contribute to loss of nutritive value and antioxidant capacity of the foods. The metal chelating PP-*g*-IDA film was tested for the ability to control ascorbic acid degradation. PP-*g*-IDA films were stored in ascorbic acid solution at pH 3.0 for up to 18 days at 37^{o}C (Figure 3.8), with blank ascorbic acid solution (no film), and ascorbic acid solution with clean polypropylene films, ascorbic acid solution with EDTA as controls. The ascorbic acid in all treatments decreased gradually during the storage period. The ascorbic acid content in the blank ascorbic acid solution and ascorbic acid solution with added polypropylene film decreased from 20 mM to 1 mM during 18 days of storage, and had a half-life of 5 days. The addition of PP-*g*-IDA slowed down the degradation of ascorbic acid during the storage period and had 9 mM ascorbic acid at the end of the storage study, with a half-life of around 14 days. While PP-*g*-IDA films inhibited ascorbic acid degradation, it was not as effective as the EDTA control, which gave 16 mM ascorbic acid retention at the day 18 and had degradation half-life of around 55 days. This again suggests that the PP-*g*-IDA complexes decreased metal reactivity by inhibiting redox activity or physical separation of the metal from the substrate. While PP-*g*-IDA films are effective in scavenging transition metal ions from solution, there likely remain unoccupied (and therefore redox active) coordination sites in the chelated metal ions. In contrast, EDTA occupies all coordination sites of the metal ions, effectively inhibiting their redox potential and therefore reactivity. This is in agreement with other reports. Kavakli et al.[3] and Zhu et al.[4] utilized immobilized IDA ligands loaded with Fe^{3+} and Cu^{2+} to achieve anionic separation of phosphates and lysozymes, respectively. In both cases, the metal ions chelated by IDA ligand had available coordination sites to enable additional binding of the anionic substances. Nevertheless, the ability to

significantly slow the rate of ascorbic acid degradation without the use of EDTA supports the potential application of chelating active packaging materials such as PP-*g*-IDA in retaining nutritive quality of packaged foods and beverages.

Graft stability study

To demonstrate the stability of the grafted metal chelating IDA ligands on the polypropylene films against migration and delamination, PP-*g*-IDA films were incubated in food simulants of water, 3% acetic acid, 10% alcohol and corn oil, to represent aqueous, acidic, alcoholic and fatty foods, respectively, for 10 days at 40^{o}C.[39] The surface chemistry and morphology were analyzed at the end of storage period to assess migration or delamination. PP-*g*-IDA stored in water, 10% alcohol and corn oil had no change in surface chemistry, with major absorption bands presenting similar absorbance intensity as freshly prepared PP-*g*-IDA. PP-*g*-IDA film stored in 3% acetic acid exhibited a change in the 1780-1520 cm^{-1} absorption region, typical of protonation of the carboxylates after storage in acidic media. SEM micrographs further supported the stability of the grafted IDA, with no signs of delamination of surface grafts after storage in each food simulant. The preliminary stability studies suggest that the surface grafts were stable in food simulants.

Conclusion

The metal chelating ligand IDA was successfully immobilized onto polypropylene by laminated photografting of 3-chloro-2-propyhydroxyl methacrylate, followed by post-graft modification to immobilize the IDA ligand. PP-*g*-IDA films effectively chelated Fe^{3+} and Cu^{2+} in acidic conditions (pH 3.0), with relative affinity constants on the order of common soluble chelators of citric acid, IDA and NTA. It is

likely that carboxylates and tertiary amine on grafted IDA ligand coordinated with the metal ions to form colorless PP-*g*-IDA metal chelates, which potentially led to a formation of tridentate chelating coordination. The PP-*g*-IDA film demonstrated antioxidant efficacy in emulsified oil system at pH 3.0, and was as effective as EDTA in controlling lipid oxidation. PP-*g*-IDA film also demonstrated potential to control ascorbic acid degradation. Surface grafts exhibited stability against delamination after exposure to food simulants under accelerated storage conditions. This work supports the potential application of metal chelating iminodiacetate functionalized polypropylene films as antioxidant active packaging materials in neutral to acidic emulsified foods and beverages.

Table 3.1. Summary of graft thickness, contact angle analysis and metal chelating capacities of polypropylene, PP-*g*-CHPM and PP-*g*-IDA.

Samples	Graft thickness (μm)	Contact angle		Metal chelating capacity (pH 3)	
		Advancing (θ)	Receding (θ)	Fe^{3+} (nmol/cm^2)	Cu^{2+} (nmol/cm^2)
Polypropylene	N/A	106.6 ± 2.2 [a]	84.2 ± 1.4 [a]	3.0 ± 4.4 [b]	4.4 ± 6.0 [b]
PP-*g*-CHPM	2.6 ± 0.8 [a]	91.7 ± 1.7 [b]	47.7 ± 1.2 [b]	5.3 ± 3.0 [b]	3.1 ± 4.5 [b]
PP-*g*-IDA	1.6 ± 0.4 [a]	14.1 ± 1.5 [c]	8.7 ± 0.3 [c]	138.1 ± 26 [a]	210.0 ± 28 [a]

Means are significantly different (Fisher's least significant difference, $P<0.05$) if they share different superscript in the same column. Each value represents mean ± standard deviation of n= 4 determinations on quadruplicate samples.

Table 3.2. Summaries of metal chelation and carboxylate dissociation of PP-*g*-IDA films stored in Fe^{3+} solutions with/without inclusion of metal chelators, and the reported stability constants of corresponding chelator-Fe^{3+} complexes.

Treatment	Metal chelation ($nmol/cm^2$)	Degree of dissociation	Stability constant[29]
Fe^{3+}	101.0 ± 33^{b}	0.96 ± 0.08^{d}	N/A
IDA-Fe^{3+}	71.7 ± 15^{b}	0.93 ± 0.08^{cd}	10.72
Citric acid-Fe^{3+}	87.7 ± 28^{b}	0.87 ± 0.10^{cd}	11.50
NTA-Fe^{3+}	69.7 ± 18^{b}	0.83 ± 0.12^{c}	15.9
EDTA-Fe^{3+}	7.7 ± 20^{a}	0.35 ± 0.01^{b}	25.0
pH 3 buffer	-10.1 ± 18.5^{a}	0.22 ± 0.02^{a}	N/A

Means are significantly different (Fisher's least significant difference, $P<0.05$) if they share different superscript in the same column.

Each value represents mean ± standard deviation of n= 4 determinations on quadruplicate samples.

Table 3.3. Summaries of metal chelation and carboxylate dissociation of PP-*g*-IDA films stored in Cu^{2+} solutions with/without inclusion of metal chelators, and the reported stability constants of corresponding chelator-Cu^{2+} complexes.

Treatment	Metal chelation ($nmol/cm^2$)	Degree of dissociation	Stability constant[29]
Cu^{2+}	201.5 ± 13^{e}	0.94 ± 0.01^{e}	N/A
Citric acid-Cu^{2+}	168.4 ± 14^{cd}	0.92 ± 0.06^{de}	5.90
IDA-Cu^{2+}	147.6 ± 21^{c}	0.89 ± 0.03^{d}	10.57
NTA-Cu^{2+}	150.4 ± 28^{c}	0.83 ± 0.02^{c}	12.94
EDTA-Cu^{2+}	41.7 ± 10^{b}	0.40 ± 0.01^{b}	18.70
Penicillamine-Cu^{2+}	193.1 ± 35^{de}	0.92 ± 0.02^{de}	19.5 *
pH 3 buffer	6.8 ± 4^{a}	0.22 ± 0.02^{a}	N/A

Means are significantly different (Fisher's least significant difference, $P<0.05$) if they share different superscript in the same column. Each value represents mean ± standard deviation of n= 4 determinations on quadruplicate samples. *stability constant for Cu^{+}

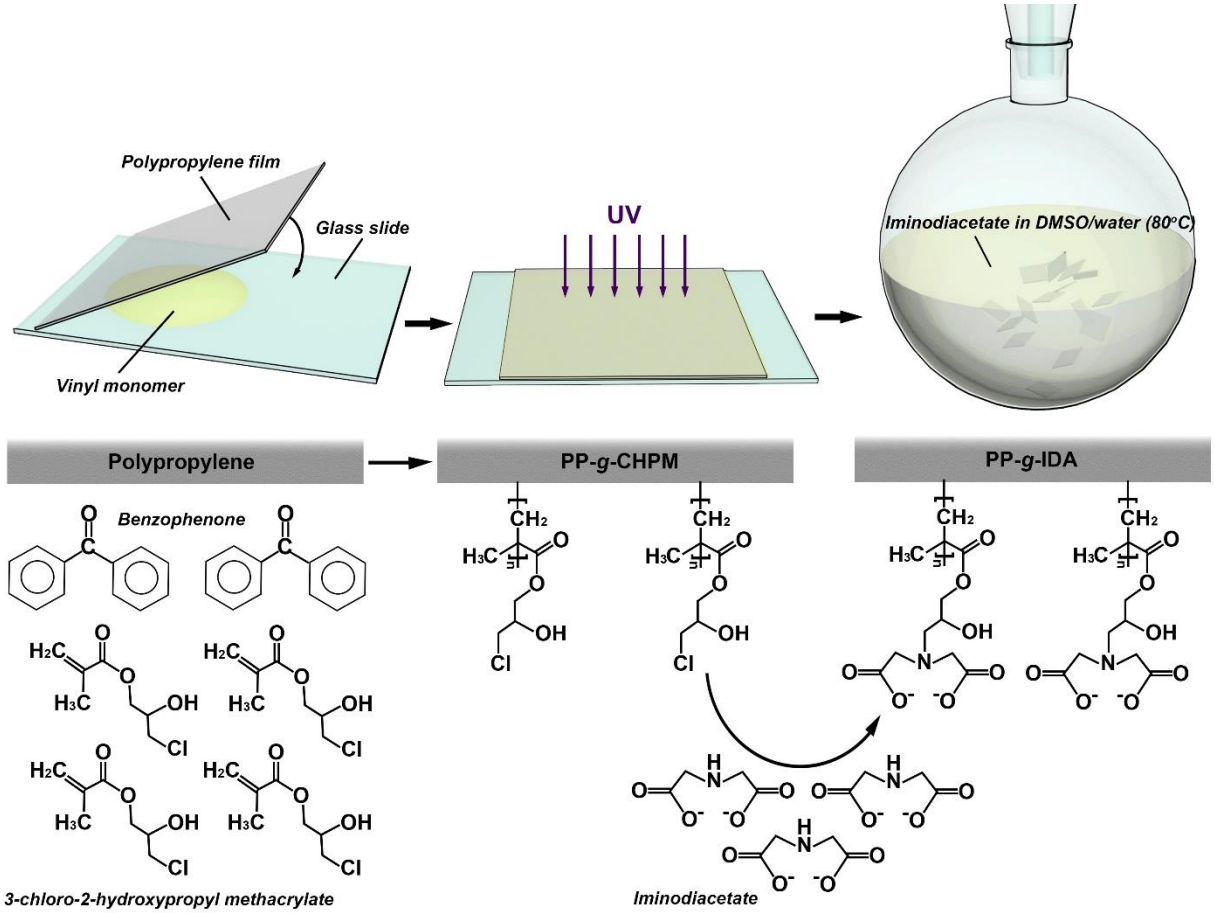

Figure 3.1. Schematic depicting method (top) and proposed synthesis chemistry (bottom) of PP-*g*-IDA.

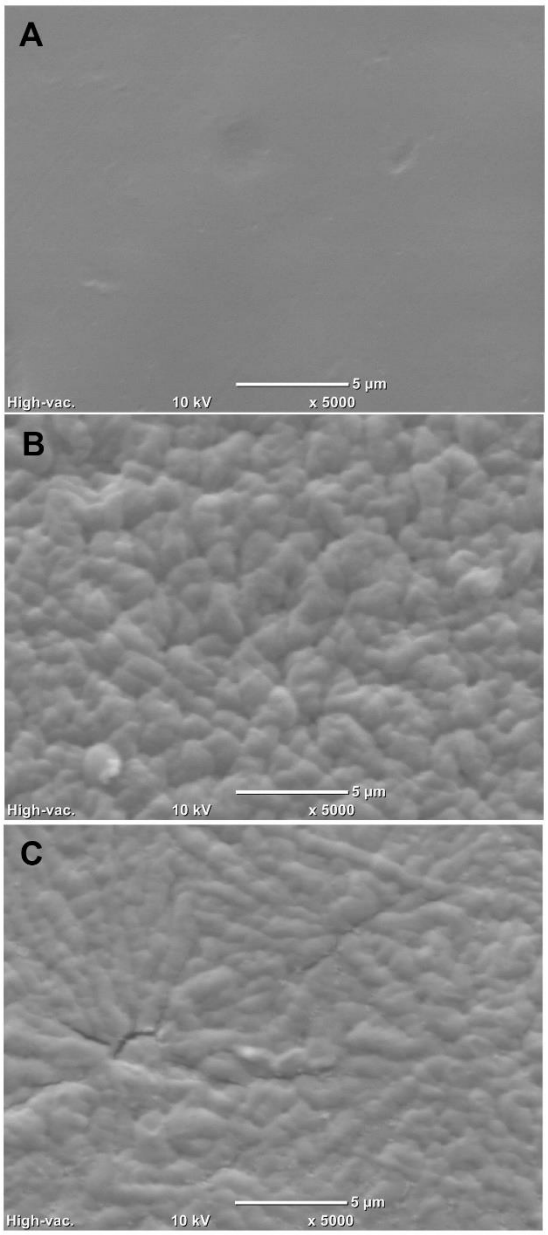

Figure 3.2. Electron micrographs of (A) polypropylene, (B) PP-*g*-CHPM, (C) PP-*g*-IDA. Each image is representative of a total of eight micrographs acquired at random locations on quadruplicate samples.

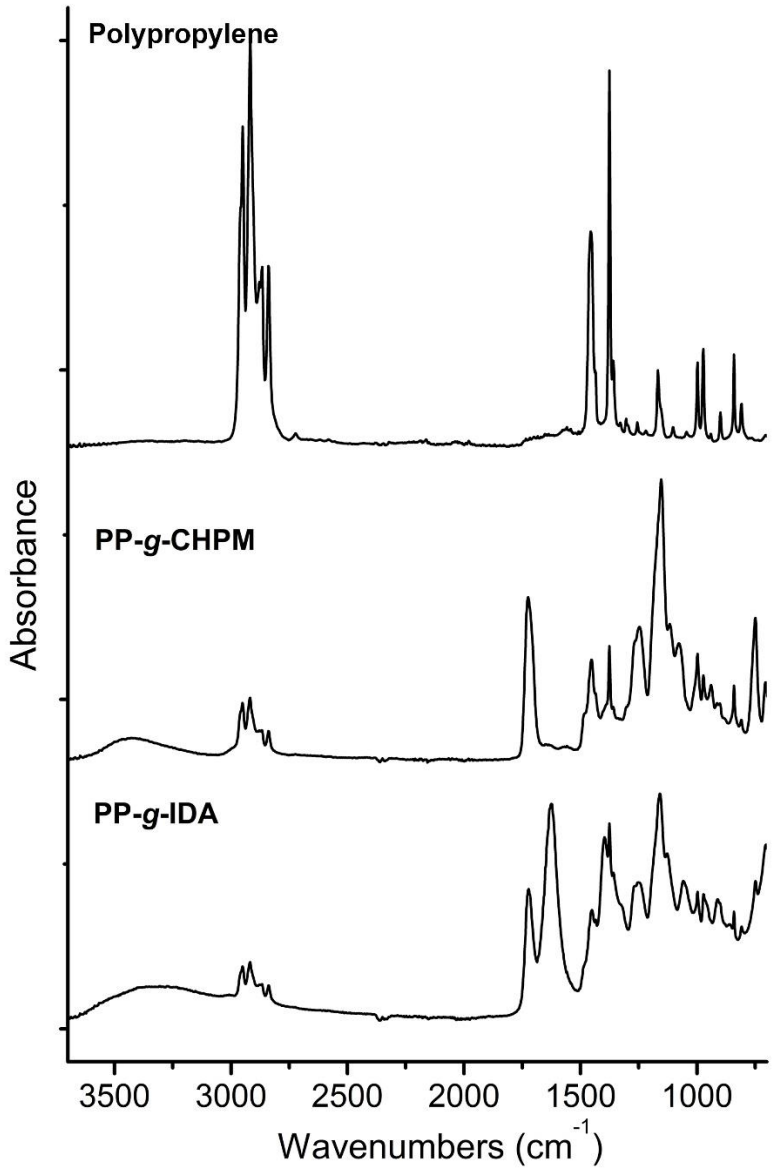

Figure 3.3. ATR-FTIR spectra of polypropylene, PP-*g*-CHPM and PP-*g*-IDA. Each spectrum is representative of a total of four spectra collected on each quadruplicate samples.

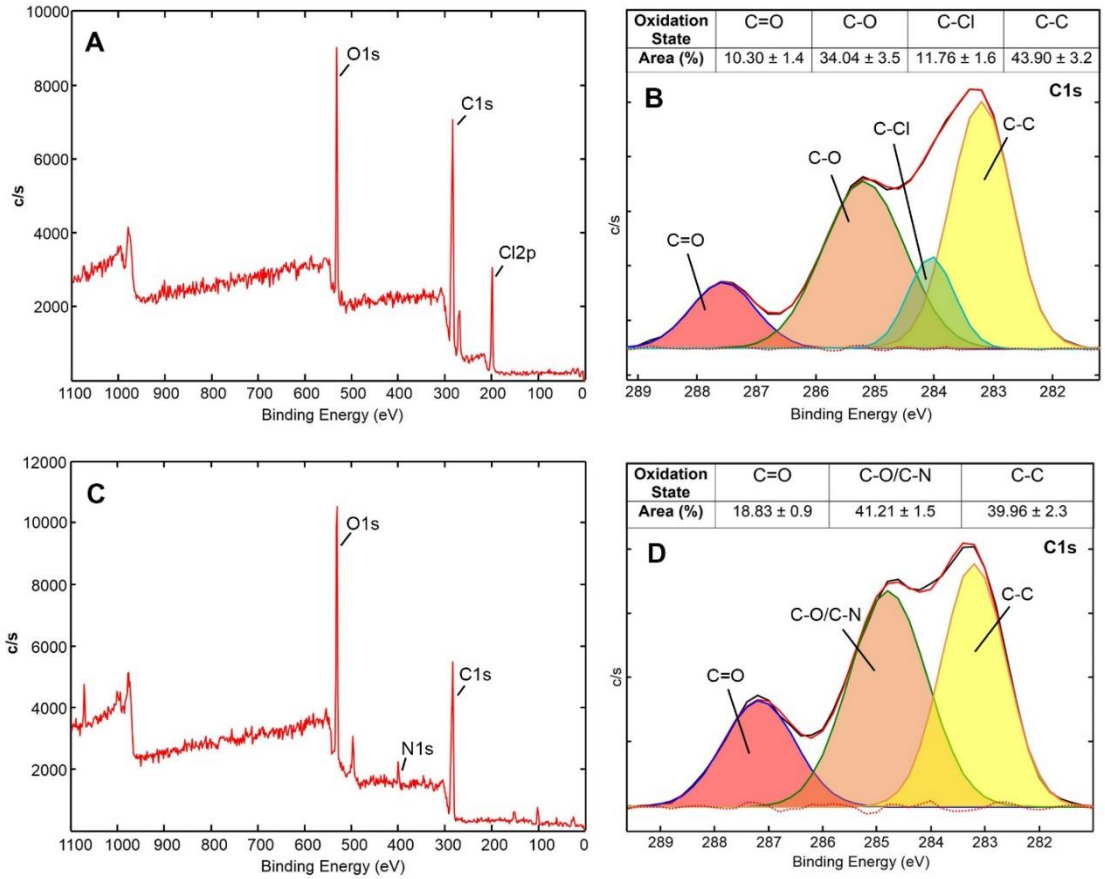

Figure 3.4. XPS spectra of survey scan (A) and high resolution scan of C1s region (B) of PP-*g*-CHPM, and survey scan (C) and high resolution scan of C1s region (D) of PP-g-IDA. Each spectrum is representative of a total of four spectra collected on quadruplicate samples.

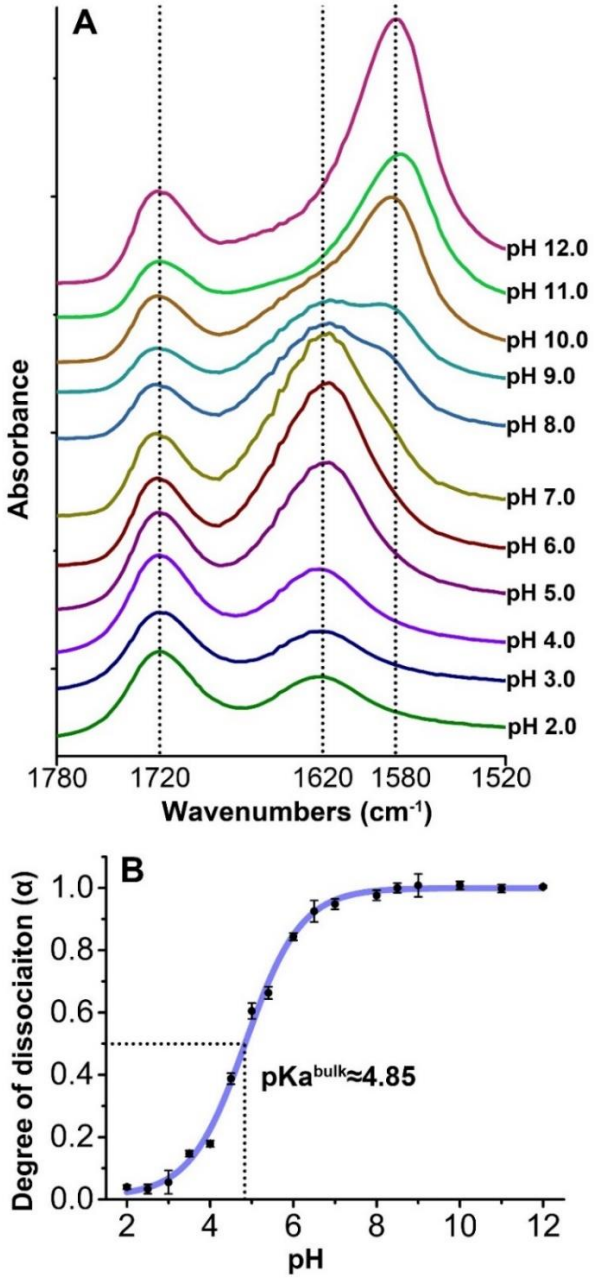

Figure 3.5. Dissociation behavior of PP-*g*-IDA, (A) Representative ATR-FTIR spectra of C=O stretching vibration region of PP-*g*-IDA film stored in solutions with different pH values. Each spectrum is representative of a total of four spectra collected on quadruplicate samples. (B) FTIR titration curve for the carboxylate group on PP-*g*-IDA.

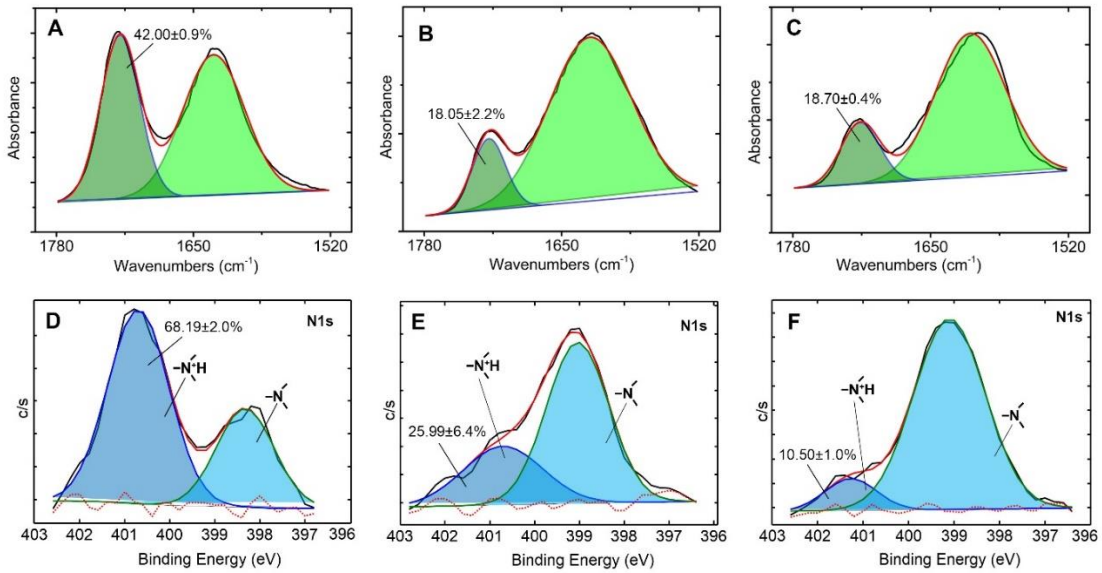

Figure 3.6. Representative ATR-FTIR spectra of C=O stretching vibration region of PP-*g*-IDA in pH 3.0 buffer (A), loaded with ferric ions (B) and loaded with cupric ions (C). Representative XPS spectra of N1s region of PP-*g*-IDA in pH 3.0 buffer (D), loaded with ferric ions (E) and loaded with cupric ions (F). Each spectrum is representative of a total of four spectra collected on quadruplicate samples.

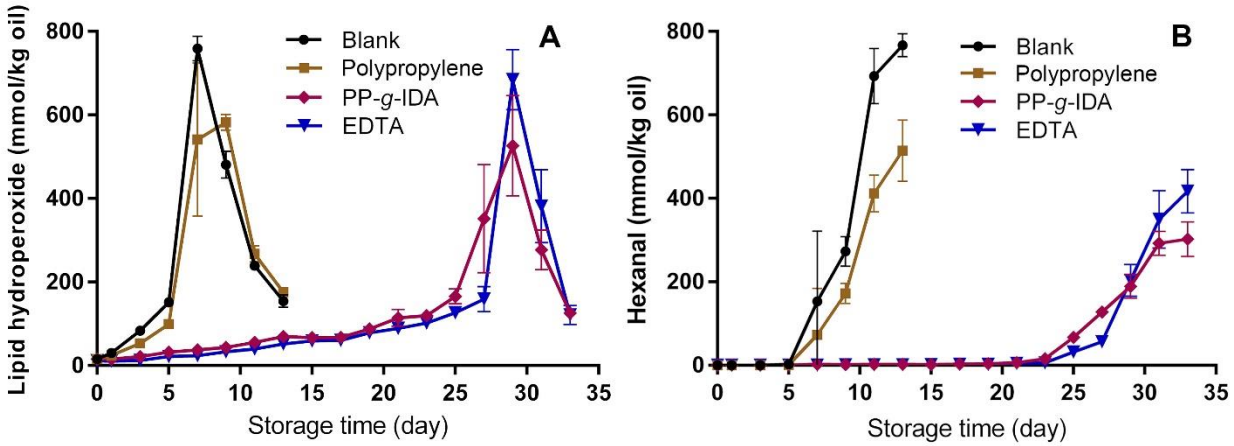

Figure 3.7. Control of lipid oxidation by PP-*g*-IDA chelating films. Lipid hydroperoxide (A) and hexanal (B) content of soybean oil-in-water emulsion (pH 3.0) stored at 55ºC over 33 days.

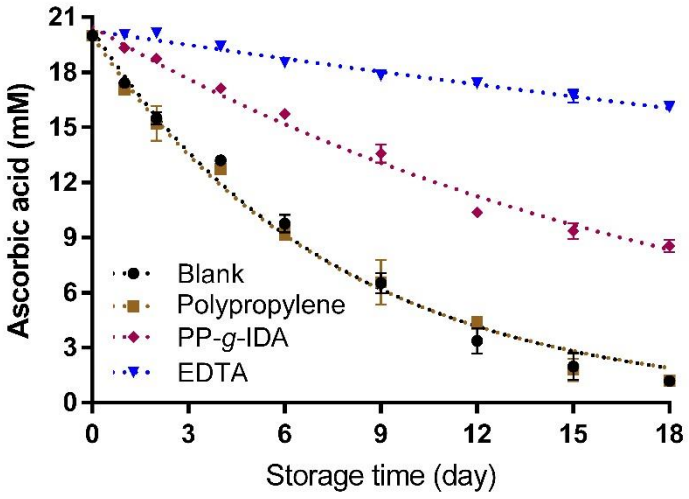

Figure 3.8. Control of ascorbic acid degradation by chelating PP-*g*-IDA films. Ascorbic acid content in pH 3.0 buffered solution stored at 37^{o}C over 18 days.

REFERENCES

1. Li, T.; Chen, S.; Li, H.; Li, Q.; Wu, L., Preparation of an ion-imprinted fiber for the selective removal of Cu2+. *Langmuir* **2011,** *27* (11), 6753-8.

2. Yamada, K.; Nagano, R.; Hirata, M., Adsorption and desorption properties of the chelating membranes prepared from the PE films. *J. Appl. Polym. Sci.* **2006,** *99* (4), 1895-1902.

3. Kavaklı, P. A.; Kavaklı, C.; Güven, O., Preparation and characterization of Fe(III)-loaded iminodiacetic acid modified GMA grafted nonwoven fabric adsorbent for anion adsorption. *Radiation Physics and Chemistry* **2014,** *94*, 105-110.

4. Zhu, J.; Sun, G., Facile fabrication of hydrophilic nanofibrous membranes with an immobilized metal-chelate affinity complex for selective protein separation. *ACS applied materials & interfaces* **2014,** *6* (2), 925-32.

5. Sun, L.; Dai, J.; Baker, G. L.; Bruening, M. L., High-Capacity, Protein-Binding Membranes Based on Polymer Brushes Grown in Porous Substrates. *Chem. Mater.* **2006,** *18* (17), 4033-4039.

6. Mentbayeva, A.; Ospanova, A.; Tashmuhambetova, Z.; Sokolova, V.; Sukhishvili, S., Polymer-metal complexes in polyelectrolyte multilayer films as catalysts for oxidation of toluene. *Langmuir* **2012,** *28* (32), 11948-55.

7. Rahim, M. A.; Islam, M. S.; Bae, T. S.; Choi, W. S.; Noh, Y.-Y.; Lee, H.-J., Metal Ion-Enriched Polyelectrolyte Complexes and Their Utilization in Multilayer Assembly and Catalytic Nanocomposite Films. *Langmuir* **2012,** *28* (22), 8486-8495.

8. de Paiva, R. G.; de Moraes, M. A.; de Godoi, F. C.; Beppu, M. M., Multilayer biopolymer membranes containing copper for antibacterial applications. *J. Appl. Polym. Sci.* **2012,** *126* (S1), E17-E24.

9. Tian, F.; Decker, E. A.; McClements, D. J.; Goddard, J. M., Influence of non-migratory metal-chelating active packaging film on food quality: impact on physical and chemical stability of emulsions. *Food Chem.* **2014,** *151*, 257-265.

10. Tian, F.; Decker, E. A.; Goddard, J. M., Controlling lipid oxidation via a biomimetic iron chelating active packaging material. *J. Agric. Food. Chem.* **2013,** *61* (50), 12397-12404.

11. Johnson, D. R.; Tian, F.; Roman, M. J.; Decker, E. A.; Goddard, J. M., Development of Iron-Chelating Poly(ethylene terephthalate) Packaging for Inhibiting Lipid Oxidation in Oil-in-Water Emulsions. *J. Agric. Food. Chem.* **2015,** *63* (20), 5055-5060.

12. Tian, F.; Decker, E. A.; Goddard, J. M., Control of lipid oxidation by nonmigratory active packaging films prepared by photoinitiated graft polymerization. *J. Agric. Food. Chem.* **2012,** *60* (31), 7710-7718.

13. Tian, F.; Decker, E. A.; Goddard, J. M., Development of an iron chelating polyethylene film for active packaging applications. *J. Agric. Food. Chem.* **2012,** *60* (8), 2046-2052.

14. Tian, F.; Decker, E. A.; Goddard, J. M., Controlling lipid oxidation of food by active packaging technologies. *Food Funct.* **2013,** *4* (5), 669-680.

15. McClements, D. J.; Decker, E. A., Lipid Oxidation in Oil-in-Water Emulsions: Impact of Molecular Environment on Chemical Reactions in Heterogeneous Food Systems. *Journal of food science* **2000,** *65* (8), 1270-1282.

16. Lee, Y. C.; Kirk, J. R.; Bedford, C. L.; Heldman, D. R., Kinetcs and computer simulation of ascorbic acid stability of tomato juice as functions of temperature, pH and metal catalyst. *Journal of food science* **1977,** *42* (3), 640-643.

17. Qian, C.; Decker, E. A.; Xiao, H.; McClements, D. J., Inhibition of beta-carotene degradation in oil-in-water nanoemulsions: influence of oil-soluble and water-soluble antioxidants. *Food Chem* **2012,** *135* (3), 1036-43.

18. Boon, C. S.; McClements, D. J.; Weiss, J.; Decker, E. A., Role of Iron and Hydroperoxides in the Degradation of Lycopene in Oil-in-Water Emulsions. *J. Agric. Food. Chem.* **2009,** *57* (7), 2993-2998.

19. Gómez-Estaca, J.; López-de-Dicastillo, C.; Hernández-Muñoz, P.; Catalá, R.; Gavara, R., Advances in antioxidant active food packaging. *Trends Food Sci. Technol.* **2014,** *35* (1), 42-51.

20. Brody, A. L.; Bugusu, B.; Han, J. H.; Sand, C. K.; McHugh, T. H., Innovative food packaging solutions. *Journal of food science* **2008,** *73* (8), R107-R116.

21. Ogiwara, Y.; Roman, M. J.; Decker, E. A.; Goddard, J. M., Iron chelating active packaging: Influence of competing ions and pH value on effectiveness of soluble and immobilized hydroxamate chelators. *Food Chem.* **2016,** *196*, 842-847.

22. Noureddine, C.; Lekhmici, A.; Mubarak, M. S., Sorption properties of the iminodiacetate ion exchange resin, amberlite IRC-718, toward divalent metal ions. *J. Appl. Polym. Sci.* **2008,** *107* (2), 1316-1319.

23. Malla, M. E.; Alvarez, M. B.; Batistoni, D. A., Evaluation of sorption and desorption characteristics of cadmium, lead and zinc on Amberlite IRC-718 iminodiacetate chelating ion exchanger. *Talanta* **2002,** *57* (2), 277-287.

24. Ling, C.; Liu, F. Q.; Xu, C.; Chen, T. P.; Li, A. M., An integrative technique based on synergistic coremoval and sequential recovery of copper and tetracycline with dual-functional chelating resin: roles of amine and carboxyl groups. *ACS applied materials & interfaces* **2013,** *5* (22), 11808-17.

25. Atzei, D.; Ferri, T.; Sadun, C.; Sangiorgio, P.; Caminiti, R., Structural Characterization of Complexes between Iminodiacetate Blocked on Styrene−Divinylbenzene Matrix (Chelex 100 Resin) and Fe(III), Cr(III), and Zn(II) in Solid Phase by Energy-Dispersive X-ray Diffraction. *Journal of the American Chemical Society* **2001,** *123* (11), 2552-2558.

26. Choi, S.-H.; Nho, Y. C.; Kim, G.-T., Adsorption of Pb2+ and Pd2+ on polyethylene membrane with amino group modified by radiation-induced graft copolymerization. *J. Appl. Polym. Sci.* **1999,** *71* (4), 643-650.

27. Wu, Y.; Tan, Y.; Wu, J.; Chen, S.; Chen, Y. Z.; Zhou, X.; Jiang, Y.; Tan, C., Fluorescence array-based sensing of metal ions using conjugated polyelectrolytes. *ACS applied materials & interfaces* **2015,** *7* (12), 6882-8.

28. Ning, W.; Wijeratne, S.; Dong, J.; Bruening, M. L., Immobilization of carboxymethylated polyethylenimine-metal-ion complexes in porous membranes to selectively capture his-tagged protein. *ACS applied materials & interfaces* **2015,** *7* (4), 2575-84.

29. Martell, A. E.; Robert, M. S., *Critical stability constants*. Plenum Press: New York, 1974.

30. Lin, Z.; Decker, E. A.; Goddard, J. M., Preparation of metal chelating active packaging materials by laminated photografting. *Journal of Coatings Technology and Research* **2016**, 1-10.

31. Dong, R.; Lindau, M.; Ober, C. K., Dissociation Behavior of Weak Polyelectrolyte Brushes on a Planar Surface. *Langmuir* **2009,** *25* (8), 4774-4779.

32. Roman, M. J.; Decker, E. A.; Goddard, J. M., Fourier transform infrared studies on the dissociation behavior of metal-chelating polyelectrolyte brushes. *ACS applied materials & interfaces* **2014,** *6* (8), 5383-7.

33. Konradi, R.; Rühe, J., Interaction of Poly(methacrylic acid) Brushes with Metal Ions: An Infrared Investigation. *Macromolecules* **2004,** *37* (18), 6954-6961.

34. Dawson, M. V.; Lyle, S. J., Spectrophotometric determination of iron and cobalt with Ferrozine and dithizone. *Talanta* **1990,** *37* (12), 1189-1191.

35. Rush, R. M.; Yoe, J. H., Colorimetric Determination of Zinc and Copper with 2-Carboxy-2-hydroxy-5-sulfoformazylbenzene. *Analytical Chemistry* **1954,** *26* (8), 1345-1347.

36. Commission, C. P. S., Test Method: CPSC-CH-E1002-08.3. In *Standard Operating Procedure for Determining Total Lead (Pb) in Nonmetal Children's Products.*, Rockville, MD, 2012.

37. Shantha, N. C.; Decker, E. A., Rapid, sensitive, iron-based spectrophotometric methods for determination of peroxide values of food lipids. *Journal of AOAC International* **1994,** (77), 421-4.

38. Horwitz, W.; Association of Official Analytical, C., Official methods of analysis of the Association of Official Analytical Chemists. *Official methods of analysis of the Association of Official Analytical Chemists.* **1970**.

39. Yassin, M. A.; Appelhans, D.; Mendes, R. G.; Rummeli, M. H.; Voit, B., pH-dependent release of doxorubicin from fast photo-cross-linkable polymersomes based on benzophenone units. *Chemistry* **2012,** *18* (39), 12227-31.

40. Gao, L.; McCarthy, T. J., Wetting 101°†. *Langmuir* **2009,** *25* (24), 14105-14115.

41. Silverstein, R. M.; Bassler, G. C.; Morrill, T. C., *Spectrometric identification of organic compounds*. Wiley: New York, 1981.

42. Papirer, E.; Lacroix, R.; Donnet, J.-B.; Nansé, G.; Fioux, P., XPS study of the halogenation of carbon black—Part 2. Chlorination. *Carbon* **1995,** *33* (1), 63-72.

43. Choi, J.; Rubner, M. F., Influence of the Degree of Ionization on Weak Polyelectrolyte Multilayer Assembly. *Macromolecules* **2004,** *38* (1), 116-124.

44. Chen, C.-Y.; Chen, C.-Y., Stability constants of polymer-bound iminodiacetate-type chelating agents with some transition-metal ions. *J. Appl. Polym. Sci.* **2002,** *86* (8), 1986-1994.

45. Kaliyappan, T.; Swaminathan, C. S.; Kannan, P., Synthesis and characterization of a new metal chelating polymer and derived Ni(II) and Cu(II) polymer complexes. *Polymer* **1996,** *37* (13), 2865-2869.

46. Tian, F.; Roman, M. J.; Decker, E. A.; Goddard, J. M., Biomimetic design of chelating interfaces. *J. Appl. Polym. Sci.* **2015,** *132* (1), 41231.

47. Goon, I. Y.; Zhang, C.; Lim, M.; Gooding, J. J.; Amal, R., Controlled fabrication of polyethylenimine-functionalized magnetic nanoparticles for the sequestration and quantification of free Cu2+. *Langmuir* **2010,** *26* (14), 12247-52.

48. Cui, Z.; Lockman, P. R.; Atwood, C. S.; Hsu, C.-H.; Gupte, A.; Allen, D. D.; Mumper, R. J., Novel d-penicillamine carrying nanoparticles for metal chelation therapy in Alzheimer's and other CNS diseases. *European Journal of Pharmaceutics and Biopharmaceutics* **2005,** *59* (2), 263-272.

49. Sugiura, Y.; Tanaka, H., Studies on the Sulfur-containing Chelating Agents. XXV. Chelate Formation of Penicillamine and Its Related Compounds with Copper (II). *Chemical & Pharmaceutical Bulletin* **1970,** *18* (2), 368-373.

50. Bradshaw, M. P.; Barril, C.; Clark, A. C.; Prenzler, P. D.; Scollary, G. R., Ascorbic Acid: A Review of its Chemistry and Reactivity in Relation to a Wine Environment. *Critical Reviews in Food Science and Nutrition* **2011,** *51* (6), 479-498.

CHAPTER 4

PHOTO-CURABLE METAL-CHELATING COATINGS OFFER A SCALABLE APPROACH TO PRODUCTION OF ANTIOXIDANT ACTIVE PACKAGING*

Abstract

To enable removal of synthetic chelators in response to increasing consumer demand for clean label products, metal-chelating active food packaging technologies have been developed with demonstrated antioxidant efficacy in simulated food systems. However, prior work in fabrication of metal-chelating materials leveraged batch chemical reactions with limited industrial translatability. To improve the industrial translatability, we have designed a two-step laminated photo-grafting process to introduce metal chelating functionality onto common polymeric packaging materials. Iminodiacetic acid (IDA) functionalized materials were fabricated by photo-grafting poly(acrylic acid) onto polypropylene (PP) films, followed by a second photo-grafting process to graft-polymerize an IDA functionalized vinyl monomer (GMA-IDA). The photo-grafting was conducted under atmospheric conditions and was completed in two minutes. The resulting IDA functionalized metal-chelating material was able to chelate iron and copper, and showed antioxidant efficacy against ascorbic acid degradation, supporting its potential to be used synergistically with natural antioxidants for preservation of food and beverage products. The two-step photo-grafting process improves the throughput of active packaging coatings, enabling potential roll-to-roll fabrication of metal-chelating active packaging materials for antioxidant food packaging applications.

*Zhuangsheng Lin, Julie Goddard

Published in Journal of Food Science. 2018. 83, 367-376.

Introduction

Active food packaging provides additional functional properties beyond containment, protection and communication of the packaged goods, with the major purposes being reducing food waste and improving product safety.[1-2] According to a recent market analysis, the global revenue for active and intelligent packaging combined was estimated to be $31.1 billion in 2016 and was expected to grow steadily worldwide, surged by increasing consumer demand for smarter packaging solutions.[3] Emerging technologies in active packaging materials have been developed at the research laboratory scale, such as ferulic acid imprinted antioxidant hydrogels,[4] selenium incorporated free radical scavenging materials,[5] and natural antimicrobial incorporated materials.[6-7] However, for such emerging active packaging technologies to be realized commercially, many obstacles need to be addressed, such as industrial translatability, cost of production, effectiveness after storage, and heat sealing properties.

Metal-chelating active packaging represents an emerging active packaging technology that has been successfully demonstrated in concept.[8-9] Metal-chelating ligands such as carboxylic acid, hydroxamic acid, and iminodiacetic acid (IDA) have been immobilized onto food packaging materials (e.g. polypropylene (PP)).[8-10] Of these, hydroxamic acid and IDA ligands present highest stability constants for common transition metals in foods, such as iron and copper, and low stability constants for macro food minerals such as calcium, magnesium and sodium.[11] IDA has half the chemical structure of EDTA (Figure 1), and the presence of the secondary amine group allowed chemical tethering of the ligands to support materials bearing reactive chemical groups. IDA functionalized materials are expected to have the same amino-dicarboxylic acid ligands as EDTA,

permitting similar metal-chelating performance as EDTA in food systems. Indeed, the high specificity of the ligand to trace transition metals in food systems can enhance the chelating performance of the metal-chelating materials in complex food matrices.[12] In a recent study, IDA functionalized materials showed equivalent antioxidant efficacy as EDTA against lipid oxidation in emulsified oil systems in neutral to high acid conditions.[10] In comparison, metal-chelating materials with less specific chelating ligands (e.g. carboxylic acid) lost antioxidant efficacy in high acid conditions.[13]

The reported metal-chelating materials work by scavenging transition metals from aqueous and emulsified solutions to control transition metal induced oxidative spoilage, a major cause of product spoilage in emulsified oil systems.[14] Such metal-chelating active packaging materials offer an alternative to synthetic soluble chelators (e.g. ethylenediaminetetraacetic acid, EDTA) and address the increasing consumer demand for additive-free, clean-label products. Because this technology leverages covalently tethered metal-chelating ligands, the ligands are unlikely to migrate to the food. Such materials could therefore be regulated as a food contact substance, rather than a food additive, a potential regulatory benefit.[15]

Despite the promise of active packaging technologies, a significant hurdle exists in the translation of bench-scale synthesis routes to high-throughput, continuous coating or production operations. Indeed, traditional techniques for immobilization of metal-chelating ligands required organic chemical reactions to tether the ligands, with long-time, batch style reactions. Such batch chemical reactions have been reported for preparation of a range of metal-chelating materials, such as nanoparticles,[16] resins,[17-18] membranes[19-20] and fabrics.[21] In our previous studies, metal-chelating active packaging

materials were also fabricated via batch reactions in ligand solutions to tether metal-chelating ligands.[10, 22-23] For example, the IDA functionalized materials were prepared via a 10-hour chemical reaction in a concentrated IDA solution to tether IDA ligands to reactive surfaces bearing chlorine groups.[10] Therefore, despite the promising laboratory results of metal-chelating active packaging technologies, the industrial translatability of the technology remains limited. The overall goal of this work was therefore to design a new synthesis route to improve the throughput of introducing IDA metal chelating ligands onto polymer films.

Photo-curing is a low energy, high speed industrial coating process in which liquid coatings are cured onto solid supports by exposure to ultraviolet radiation and has potential for solvent-free roll-to-roll processing.[24 25] Photo-curing can be used to photo-graft vinyl monomers onto material surfaces to introduce added functionalities.[26-27] In our previous study, a laminated photo-grafting technique was investigated in order to graft acrylic acids from PP surface, resulting in carboxylic acid functionalized materials.[22] In the current study, a high-throughput fabrication method was designed to prepare IDA coated PP materials with metal-chelating properties, without the need for batch solution reaction (Figure 2). IDA functionalized monomers (GMA-IDA) were synthesized, which were then grafted onto food packaging materials via a two-step photo-grafting process. The two-step photo-grafting process eliminated the solution reaction step to tether ligands onto materials, and could potentially enable high-throughput roll-to-roll fabrication of metal-chelating materials. The material's ability to chelate trace transition metals (iron, copper) responsible for metal promoted oxidative

degradation in foods and beverages, and its antioxidant efficacy against ascorbic acid degradation were also investigated.

Materials and Methods

Materials

Polypropylene (PP) pellets (isotactic) were purchased from Scientific Polymer Products (Ontario, NY). L-ascorbic acid, cupric sulfate pentahydrate (99+%), ethylenediaminetetraacetic acid (EDTA) (disodium salt dehydrate), imidazole (99%), glycidyl methacrylate, benzophenone (99%), zincon monosodium salt, 3-(2-pyridyl)-5,6-diphenyl-1,2,4-triazine-p,p'-disulfonic acid disodium salt hydrate (ferrozine, 98%+), and toluidine blue O (TBO) were purchased from Sigma-Aldrich (St. Louis, MO). Isopropanol, acetone, methanol, sodium hydroxide, glacial acetic acid, hydrochloric acid (trace metal grade), trichloroacetic acid (TCA), oxalic acid dihydrate, sodium acetate trihydrate, 4-(2-hydroxyethyl)-1-piperazineethanesul-fonic acid (HEPES), sodium phosphate monobasic monohydrate, sodium carbonate anhydrous, sodium bicarbonate, ferric chloride hexahydrate, and 2,6-dichloroindophenol were purchased from Fisher Scientific (Fair Lawn, NJ). Iminodiacetic acid (IDA) (98+%) was purchased from Acros Organics (Morris Plains, NJ). Absolute ethanol was purchased from Pharmco-Aaper (Brook-field, CT). All chemicals and reagents were used as received without further purification. The IDA functionalized vinyl monomer, 2-propenoic acid, 2-methyl-,3-[bis-(carboxymethyl) amino]-2-hydroxypropyl ester (GMA-IDA), was synthesized according to a reported procedure.[28]

Preparation of iminodiacetic acid (IDA) functionalized materials

PP pellets were washed sequentially in isopropanol, acetone and water with

sonication (two cycles per solvent and 10 min per cycle), and then dried in a desiccator over anhydrous calcium sulfate. The cleaned pellets were sandwiched between two pieces of Kapton film and hot pressed into PP films of 330 ± 50 μm thickness using a Carver hot press (180 ^{o}C, 4.5 tons force). The PP films were cut into pieces of 5 x 5 cm^2 in size and then washed sequentially in isopropanol, acetone and water again with sonication. The cleaned PP films were dried in a desiccator before surface modifications. The metal-chelating materials were prepared via a two-step photo-grafting process as illustrated in Figure 2. In the first step, 0.4 mL of 50 v/v % acrylic acid, 2.5 wt % benzophenone in water solution was sandwiched between a glass slide (5 × 7 cm^2, Ted Pella Inc., Redding, CA) and a piece of 5 x 5 cm^2 PP film, and exposed to ultraviolet (UV) light for 30 s (365 nm, 225 mW/cm^2, Dymax EC, Dymax Corporation, Torrington, CT). The resulting acrylic acid functionalized PP (PP-*g*-PAA) films were rinsed with acetone and then washed in 60^{o}C DI water for 30 min. The washed PP-*g*-PAA films were blow-dried with an air gun and stored in a desiccator. In the second step, 0.4 mL of 80 v/v % GMA-IDA in water was sandwiched between a glass slide and a piece of PP-*g*-PAA film, followed by exposure to UV light for 90 s (365 nm, 225 mW/cm^2). The resulting IDA functionalized PP (PP-*g*-PIDA) films were washed in 60^{o}C DI water (three times, 30 min each wash) to remove un-grafted monomers and homo-polymers. The cleaned PP-*g*-PIDA were cut into coupons of 1x1 cm^2 in size and dried in a desiccator before further analysis.

Surface characterizations

The surface chemistry of native PP and modified PP films was characterized using attenuated total reflectance Fourier transform infrared (ATR−FTIR) spectroscopy.

Spectra were collected on an IRTracer-100 FTIR spectrometer (Shimadzu Scientific Instruments, Kyoto, Japan) with a diamond ATR crystal. Spectra collection was conducted at a resolution of 4 cm^{-1} (32 scans) using Happ-Genzel apodization, with air as a background spectrum. Surface morphology of the materials was observed under scanning electron microscopy (SEM). Film samples were coated with gold using a Cressington 108 sputter coater (Cressington Scientific, Watford, UK) and imaged at 10kV in a JEOL 6000 FXV SEM (JEOL Ltd. Akishima, Tokyo, Japan). Surface wettability of the materials was characterized using water contact angle analysis with an Attension Theta Optical Tensiometer (Biolin Scientific, Stockholm, Sweden). Advancing and receding water contact angles were measured according to a reported protocol.[29] Briefly, advancing water contact angles were measured by depositing deionized water onto substrate surfaces at rate of 0.5 µL/s, and the advancing water contact angles were recorded as the maximum contact angle before the contact line started to advance. Receding contact angles were measured after advancing angle measurement by withdrawing water at a rate of 0.5 µL/s, and the receding contact angles were recorded as the minimum contact angle before the contact line started to recede. Carboxylic acid densities of the materials were quantified using a TBO dye assay.[30] The materials were stored in 0.5 mM TBO dye solutions at pH 10.0 for 2 hours to allow the materials to absorb TBO dye. The absorbed TBO dye was then desorbed by storing the materials in an aliquot of 50 v/v % acetic acid in water solution. The amount of dye released to acetic acid solution was quantified by measuring absorbance at 633 nm, and compared to a standard curve of TBO dye in acetic acid solution. The carboxylic acid density was determined by assuming a 1:1 stoichiometric ratio between absorbed dye

and carboxylic acid.

Metal-chelating analysis

Iron (Fe^{3+}) and copper (Cu^{2+}) chelating capacities of the metal-chelating materials were analyzed using colorimetric ferrozine and zincon assays, respectively.[10, 31-32] Materials were incubated in 0.08 mM ferric chloride or cupric sulfate in 50 mM sodium acetate/imidazole solutions at pH 3.0-5.0 for 24 hours (22 ^{o}C, dark). Iron chelation was quantified by the reduction in solution Fe^{3+} concentration after 24 hours exposure to the materials. Briefly, a working reagent of a reducing solution (5 wt % hydroxylamine chloride and 10 wt % TCA) and a ferrozine solution (18 mM ferrozine in 50 mM HEPES (pH 7.0)) were added to the iron solution. The absorbance of the mixture was measured at 562 nm after 1 hour incubation and the Fe^{3+} concentration was calculated by comparison to a standard curve. Copper chelation was similarly quantified by adding an aliquot of 0.0625 mM zincon in 0.1 M sodium carbonate solution (pH 9.0) to copper solution before and after 24 hours exposure to the materials. The absorbance of the mixture was measured at 600 nm after 30 min incubation. The Cu^{2+} concentration was calculated by comparison to a standard curve prepared using cupric sulfate. The Fe^{3+} and Cu^{2+} chelating capacities of the metal-chelating materials were quantified by measuring the decrease in Fe^{3+} and Cu^{2+} concentrations of the buffered solutions after exposure to the films, with PP and PP-*g*-PAA films serving as controls. Materials stored in buffered metal ion solutions were rinsed with absolute ethanol, dried, and subjected to ATR-FTIR analysis to determine the dissociation behavior of the chelating ligand after metal-chelation.

Ascorbic acid degradation study

The antioxidant efficacy of the materials against ascorbic acid degradation was analyzed using an accelerated ascorbic acid degradation study.[10] Briefly, PP-*g*-PIDA films were stored in 20 mM ascorbic acid in 10 mM sodium acetate/imidazole solutions (pH 3.0 – 7.0) at 37°C, with blank ascorbic acid solution, native PP, PP-*g*-PAA and ascorbic acid solution containing 0.08 mM EDTA as controls. Each 1x1 cm^2 coupon was stored in 1 mL of buffered ascorbic acid solution in a sealed 10 mL GC vial. The vials were sampled every one to three days to measure the remaining ascorbic acid content during storage. The ascorbic acid content was quantified using a modified dichloroindophenol assay based on the Association of Official Analytical Chemists (AOAC) official method 967.21.[33] Briefly, 0.2 mL of ascorbic acid solution from each vial was added into 4.8 mL of 0.04 wt % oxalic acid, and 0.3 mL of the mixture was added to 4.7 mL of 0.2 mM dichloroindophenol solution. The absorbance of the mixture was measured immediately at 520 nm and ascorbic acid content was quantified by comparison to a standard curve of ascorbic acid prepared in buffered solutions.

Statistical Analysis

All statistical analyses were conducted using GraphPad Prism (La Jolla, CA). Reported ATR-FTIR spectra are representative of quadruplicate analysis (n=4 independent films). Reported scanning electron micrographs are representative of images acquired at random locations across quadruplicate coupons. Surface wettability analysis was conducted on quadruplicate coupons. Carboxylic acid density and metal-chelating analysis were conducted on sextuplicate coupons. Ascorbic acid content measurements were conducted in triplicate. Results of metal-chelating activity and ascorbic acid

degradation experiments are representative of at least 2 experiments repeated independently. Results of carboxylic acid density and metal-chelating capacity were subjected to analysis of variance (ANOVA) to compare difference using Fisher's least significant difference ($p<0.05$). Results of ascorbic acid degradation were fitted using first order degradation kinetic equations to calculate the degradation half-life of the treatments.

Results and Discussion

Surface characterization

The surface chemistry of coated and native, clean PP was characterized using ATR-FTIR (Figure 3). The native PP had absorption bands at 3000-2800 cm^{-1}, indicative of alkyl stretching vibrations from the saturated hydrocarbon bonds. Native PP also had bands at 1450 cm^{-1} and 1370 cm^{-1} from the bending vibrations of the saturated hydrocarbon bonds. The FTIR spectrum of the native PP surface was in agreement with previous reports.[22, 34] PP-*g*-PAA had a singlet absorption band at 1710 cm^{-1}, a broad absorption band at 3600-2400 cm^{-1}, and absorption bands at 1260-1160 cm^{-1}, which are characteristic of poly(acrylic acid) surface grafts (indicating stretching vibration of carbonyl bond, stretching vibration of O-H bond, and C-O related stretching vibrations, respectively) on PP.[22, 35] Grafting the IDA functionalized monomer, GMA-IDA, from PP-*g*-PAA in the secondary photo-curing step produced PP-*g*-PIDA films with doublet absorption bands at 1710 cm^{-1} and 1620 cm^{-1} (characteristic of protonated and deprotonated carboxylate groups, respectively), a broad absorption band at 3600-2400 cm^{-1} (indicative of O-H stretching vibration), and absorption bands at 1260-1160 cm^{-1} (indicative of C-O related stretching vibrations), as expected after introduction of the

IDA ligands.[10, 20] The alkyl C-H stretching vibration bands at 3000-2800 cm^{-1} from the native PP decreased with each photo-curing step, further confirming successful introduction of the surface grafts. The ATR-FTIR results suggested potential introduction of IDA ligands onto native PP surface via the two-step photo-grafting process.

The surface morphology of the materials was observed under SEM (Figure 4). Native PP film had a planar and relatively smooth surface, with minor peels likely an artefact of film preparation, in which hot pressed PP films were separated from Kapton films after pressing. The PP-*g*-PAA material exhibited surface wrinkling, which is in agreement with prior reports and likely a result of drying of hydrophilic surface grafts.[22, 36] PP-*g*-PIDA had distinct surface morphology from PP-*g*-PAA, with patches of patterned wrinkles uniformly distributed across the surface. The observed wrinkles were likely chain aggregations formed during the desiccation of the material. Nevertheless, surface imaging showed evidence of successful photo-grafting.

The surface wettability was analyzed using water contact angle analysis. The materials were dried in a desiccator prior to analysis. Advancing contact angles were recorded while a water droplet was added to the surface, while receding contact angles were recorded while the same droplet was withdrawn from the surface. Native PP was hydrophobic with a large advancing contact angle of 111.9 ± 2.5 ^{o} (Figure 5). PP-*g*-PAA was more hydrophilic than native PP, with an advancing contact angle of 81.6 ± 3.0 ^{o}. The advancing water contact angles of PP and PP-*g*-PAA materials were in agreement with previous reports and indicative of the successful grafting of poly(acrylic acid).[8, 22] PP-*g*-PIDA surface was the most water hydrophilic with a lowest advancing water

contact angle of 49.8 ± 2.9 °. The increase in water hydrophilicity of the PP-*g*-PIDA after immobilization of hydrophilic IDA ligands is in agreement with a previous report on IDA functionalized materials.[10] The receding water contact angles were measured and hysteresis (difference between advancing and receding angles) was calculated to give an indication of the interaction between probe fluid and surface.[37] Native PP had a high receding contact angle of 87.1 ± 4.5 °, which agreed with previous reports.[8, 22] Both PP-*g*-PAA and PP-*g*-PIDA had low receding contact angles of 17.4 ± 3.0 ° and 15.8 ± 1.2 °, respectively, and correspondingly high hysteresis degree (64.3 ± 10.2 ° and 34.0 ± 3.2 °, respectively) suggesting high interaction between water and the surfaces. Introduction of hydrophilic polymer grafts with hierarchical chemical structures (PAA grafts to which PIDA chains are further grafted) introduces a large number of hydrophilic moieties with which a water droplet can interact, resulting in the observed high hysteresis. These results support our hypothesis that PP-*g*-PIDA materials are able to effectively interact with aqueous solutions, supporting their ability to chelate ions from liquid to semi-liquid products.

The carboxylic acid density of the materials was quantified using a TBO dye assay. TBO is a cationic dye that is hypothesized to complex with carboxylic acid at 1:1 molar ratio.[30] Native PP did not present significant carboxylic acid content, as expected from a clean native PP coupon (Figure 6). PP-*g*-PAA had a carboxylic acid density of 75.5 ± 11.8 nmol/cm^2 and PP-*g*-PIDA had a carboxylic acid density of 127.4 ± 11.1 nmol/cm^2. The increase in carboxylic acid density after photo-grafting GMA-IDA suggests successful immobilization of IDA ligands, which supports the results observed in the ATR-FTIR analysis (Figure 3). The increase in carboxylic acid content corresponds to

an immobilization of approximately 25 nmol/cm^2 IDA ligands. For a half-liter package with approximately 600 cm^2, the amount of IDA on the surface would corresponds to approximately 4.4 ppm EDTA (assuming an EDTA molecular weight of 292.2 g/mol), below the FDA's maximum allowance (33 ppm in beverages, 75 ppm in salad dressings) ,[38] but well above the minimum concentration of EDTA (0.75 ppm) to have been reported to have a significant antioxidant effect in emulsified oil systems.[39]

The two-step photo-grafting process enabled immobilization of IDA ligands onto PP surface in atmospheric environment without the need for solution reactions. The surface modifications can be conducted on native PP films without any pretreatment (e.g. UV-ozone cleaning, plasma treatment and corona treatment) to enhance adhesion of surface coatings.[40] The two-step photo-grafting process can be completed in two-minutes in laboratory (325 mW/cm^2 UV lamp), which marks a huge improvement comparing to traditional synthesis techniques. Traditional techniques for immobilization of metal-chelating ligands onto solid support materials required organic chemical reactions to tether the ligands (e.g. Sn2 substitution reaction), with long reaction time in solutions containing concentrated ligand substrates. For example, in our previous studies, a 4-hour reaction in hydroxylamine and a 10-hour reaction in IDA solution were required to prepare hydroxamic acid and IDA functionalized metal-chelating materials, respectively.[10, 22-23] The photo-curing process has potential to be conducted as a roll-to-roll process, which enables preparation of metal-chelating materials on large scales for active packaging application.

Metal-chelating analysis

Iron and copper are the two most common transition metals in foods that contribute to

oxidative degradation (e.g. lipid oxidation, nutrient degradation).[14] Therefore, the metal-chelating activity of PP-*g*-PIDA towards Fe^{3+} and Cu^{2+} was investigated, with native PP and PP-*g*-PAA serving as controls (Figure 7). Materials were stored in buffered solutions spiked with transition metal ions at pH 3.0-5.0 for 24 hours to measure the total amount of ion chelation. Native PP did not contain metal-chelating ligands, therefore, had insignificant amount of metal-chelation. As indicated in Figure 6, PP-*g*-PAA contained 75.5 ± 11.8 nmol/cm^2 of carboxylic acids, yet did not chelate a significant amount of either Fe^{3+} or Cu^{2+} at pH 3.0 due to their protonation under low pH conditions.[41] The chelating capacity increased as the pH increased, due to gradual deprotonation of carboxylic acid groups. At pH 5.0, PP-*g*-PAA was capable of chelating 43.8 ± 7.0 nmol/cm^2 of Fe^{3+} and 78.8 ± 24.8 nmol/cm^2 of Cu^{2+}. The metal-chelating capacity of PP-*g*-PAA at pH 5.0 towards Fe^{3+} was in agreement with PP-*g*-PAA materials prepared in previous reports with similar carboxylic acid density [13, 42]. In contrast, PP-*g*-PIDA was effective against chelating both transition metal ions at all pH conditions tested. At pH 3.0, PP-*g*-PIDA chelated 47.5 ± 6.9 nmol/cm^2 of Fe^{3+} and 80.0 ± 23.3 nmol/cm^2 of Cu^{2+}. Compared with carboxylic acid, IDA is more specific to transition metal ions with higher stability constants to both Fe^{3+} and Cu^{2+}.[11] The immobilization of IDA improved the chelating performance of materials at pH 3.0. The metal-chelating capacity at pH 3.0 towards both metal ions per IDA content were in agreement with a previous report on IDA functionalized materials.[10] While PP-*g*-PIDA chelated transition metals at all tested pH values, its metal-chelating capacity increased as pH increased. At pH 5.0, PP-*g*-PIDA chelated 115.8 ± 19.5 nmol/cm^2 of Fe^{3+} and 241.0 ± 36.0 nmol/cm^2 of Cu^{2+}. The trend was in agreement with previous reports on

the performance of metal-chelating materials under different pH conditions.[19, 43] As pH value increases, ligands experience less competition from protons and become capable of chelating more metal ions. Many consumer products (e.g. salad dressings, natural beverages) that are prone to transition metal induced oxidative degradations have pH values below 5.0. The metal-chelating performance at different pH conditions is directly related to the antioxidant efficacy at corresponding pH conditions. In oxidation studies conducted in emulsified oil systems at pH 3.0, IDA functionalized materials retained antioxidant efficacy,[10] while PP-*g*-PAA materials lost antioxidant efficacy.[13] These results therefore suggest that the PP-*g*-PIDA materials would retain antioxidant efficacy at pH values down to pH 3.0.

To further demonstrate the performance of the PP-*g*-PIDA materials across a range of pH values, the dissociation behavior of the IDA ligands on PP-*g*-PIDA was analyzed using ATR-FTIR spectroscopy (Figure 8). The IDA ligand had characteristic doublet absorption bands at carbonyl stretching vibration region (1800-1500 cm^{-1}), with absorbance at 1710 cm^{-1} and 1620 cm^{-1} from protonated and deprotonated carboxylic acid groups, respectively (Figure 3). The dissociation of the carboxylic acid groups is affected by proton and metal ion concentrations of the environment making them suitable for characterization of dissociation behavior using FTIR spectroscopy.[10, 28, 44-45] As the pH of storage buffer increased from 3.0 to 5.0, the absorption band shifted towards 1620 cm^{-1}, a result of dissociation of the carboxylic acid groups (Figure 8). After Fe^{3+} chelation, the absorption bands also shifted towards 1620 cm^{-1} at all tested pH values (pH 3.0-5.0), a result of dissociation of the carboxylic acid groups. Importantly, Fe^{3+} was able to out-compete protons for the IDA ligands and allowed

some carboxylic acid groups to deprotonate. After Cu^{2+} chelation, the absorption bands shifted towards 1590 cm^{-1}, a result of dissociation of carboxylic acid groups as the protons were displaced by Cu^{2+}. The downshift of the carboxylate absorbance from 1620 cm^{-1} to 1590 cm^{-1} was potentially due to deprotonation of the tertiary amine group neighboring to the carboxylic acid groups on IDA ligands.[28, 46] The results suggested that PP-*g*-PIDA has specificity to both Fe^{3+} and Cu^{2+} ions and that the PIDA ligands form effective metal-chelate complexes.

Ascorbic acid degradation

Ascorbic acid is not only an important nutrient in foods (Vitamin C), but also is often used as a natural antioxidant in foods to prevent oxidation of other food components (e.g. lipids) [14, 47] and to reduce enzymatic browning.[48-49] Transition metals promote ascorbic acid degradation by inducing the oxidation of ascorbic acid to dehydroascorbic acid, which is unstable and undergo further degradation reactions.[50] Using a batch material synthesis method, we have previously demonstrated that metal-chelating materials can control ascorbic acid degradation by reducing the soluble transition metal content in the matrix.[10]

The antioxidant efficacy of PP-*g*-PIDA material was tested in ascorbic acid solutions, with native PP, PP-*g*-PAA and EDTA as controls. Accelerated oxidation studies were conducted at 37^{o}C using ascorbic acid in buffered solutions at pH 3.0, pH 5.0 and pH 7.0, representing high acid, low acid and neutral aqueous products, respectively. Importantly, the ascorbic acid solutions were not spiked with transition metals and, therefore, only intrinsic transition metals from chemicals, reagents and experimental supplies were present. The results of ascorbic acid degradation during storage are shown

in Figure 9. At pH 3.0, blank, native PP and PP-*g*-PAA treatments had the most rapid ascorbic acid degradation and the least retention of ascorbic acid after 11 days. PP-*g*-PIDA enhanced the stability of ascorbic acids and improved the ascorbic acid retention to 15.4 mM at day 11. EDTA was the most effective against ascorbic acid degradation among all treatments at pH 3.0. The results were in agreement with a previous report on the antioxidant efficacy of IDA functionalized materials at pH 3.0.[10] It was hypothesized that the metal-chelating material reduced soluble transition metal content partitioning them to the interface, while EDTA was able to reduce catalytic activity of transition metals by the formation of metal-chelate complex. At pH 3.0, PP-*g*-PAA had no effect on ascorbic acid degradation, in agreement with the metal chelation results (Figure 7) which indicated no significant Fe^{3+} or Cu^{2+} chelation at pH 3.0. At pH 5.0, blank and native PP treatments had the fastest ascorbic acid degradation among all treatments. EDTA had a similar degradation kinetic as blank and native PP treatments, and had a low ascorbic acid retention of 3.7 mM at the end of 8 days. EDTA had a dramatic reduction in antioxidant efficacy as the pH increased from 3.0 to 5.0. The pro-oxidative and anti-oxidative properties of EDTA depends on the concentrations of metal and EDTA.[51] At pH 5.0, EDTA might increase pro-oxidant activity of transition metal ions by increasing their solubility. PP-*g*-PAA delayed ascorbic acid degradation and exhibited a higher ascorbic acid retention than blank and native PP treatments at the end of the storage period. PP-*g*-PAA had improved metal-chelating activity towards both Fe^{3+} and Cu^{2+} as the pH increased from 3.0 to 5.0 (Figure 7), resulting in improved antioxidant efficacy. PP-*g*-PIDA was the most effective against ascorbic acid degradation at pH 5.0 and had the highest amount of ascorbic acid retention of 9.6 mM

at the end of 8-day storage period. At pH 7.0, EDTA became pro-oxidant and accelerated ascorbic acid degradation comparing to the blank and native PP treatments. The presence of EDTA might have promoted the ascorbic acid degradation via reactions associated with the Udenfriend system, where the EDTA accelerates ascorbic acid participates in hydroxylation reaction of aromatic compounds in the presence of iron and oxygen.[52] PP-*g*-PIDA and PP-*g*-PAA treatments exhibited similar ascorbic acid degradation kinetics and both treatments yielded the highest amount of ascorbic acid retention at the end of storage period. Prior studies reported that surface grafted poly(acrylic acid) had a surface pKa value of 6.45.[41] Therefore, at pH 7.0, the carboxylic acid groups on PP-*g*-PAA were highly deprotonated, and could bind soluble metal ions through non-specific ionic interactions.

The ascorbic acid degradation results suggested the PP-*g*-PIDA material was effective against ascorbic acid degradation. The soluble metal-chelator, EDTA, was only effective at low pH conditions, and lost antioxidant efficacy as the pH increased. Ascorbic acid is often used in food products as an antioxidant to control oxidation of food components (e.g. lipids, colorants and phenolic compounds). Metal-chelating materials have shown efficacy to control oxidative degradation of lipids and lycopene (a natural red colorant).[10, 23] PP-*g*-PIDA prepared in a two-step photo-curing process amenable to roll-to-roll processing may work synergistically with ascorbic acid to improve oxidative stability of aqueous and semi-aqueous products (e.g. juice, jams and salad dressings).

Conclusions

In this work, iminodiacetic acid (IDA) based coatings were prepared by a two-

step photo-grafting process using an IDA functionalized vinyl monomer. The two-step photo-grafting process eliminated the need for lengthy batch chemical reactions. This material fabrication technique can potentially be adopted as a high-throughput roll-to-roll photo-curing process for large-scale fabrication of the metal-chelating active packaging materials. The photo-grafting technique may also be applied to large-scale surface immobilization of other bio-active compounds, such as antimicrobial and catalytic agents. The IDA functionalized materials exhibited pH dependent metal chelating capacity and antioxidant efficacy against ascorbic acid degradation. Metal-chelating active packaging technology can potentially be used to control transition metal induced oxidative degradation of ascorbic acids in aqueous products (e.g. beverages and salad dressings). The technology may also be used synergistically with natural antioxidants such as ascorbic acids to control oxidative degradations in consumer products. However, the surface with IDA functionality is lack of heat sealing property and further studies are to be conducted to tailor the thermal physical properties and to improve heat sealing. Future studies also aim to determine the chelating performance and antioxidant efficacies in complex food matrices (e.g. in the presence of competitive ions) and to test the non-migratory properties as potential food contact substances.

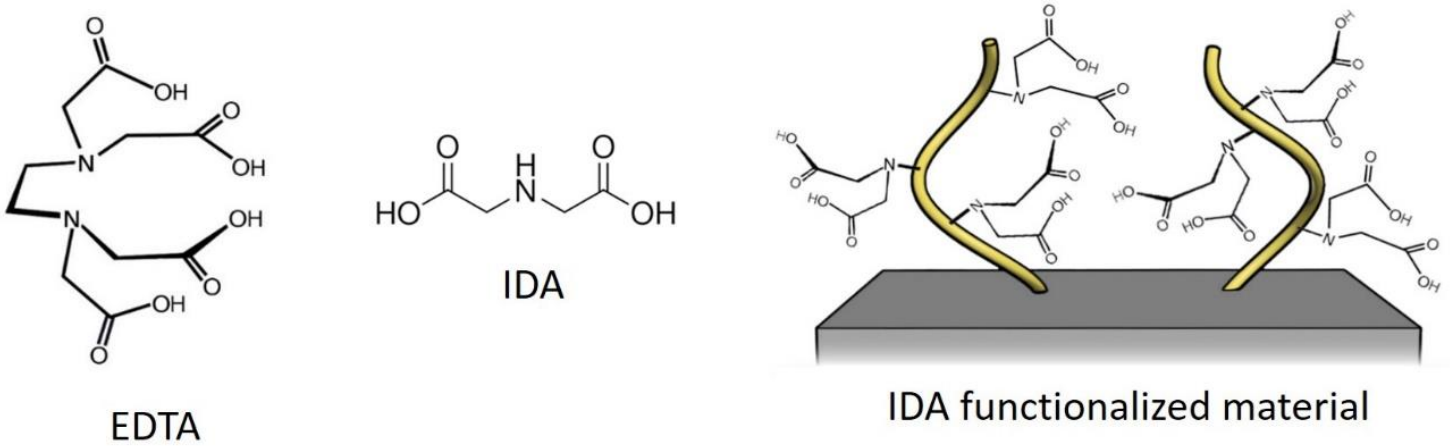

Figure 4.1. Chemical structure of ethylenediamine tetraacetic acid (EDTA) and iminodiacetic acid (IDA), and illustration of IDA functionalized metal-chelating materials.

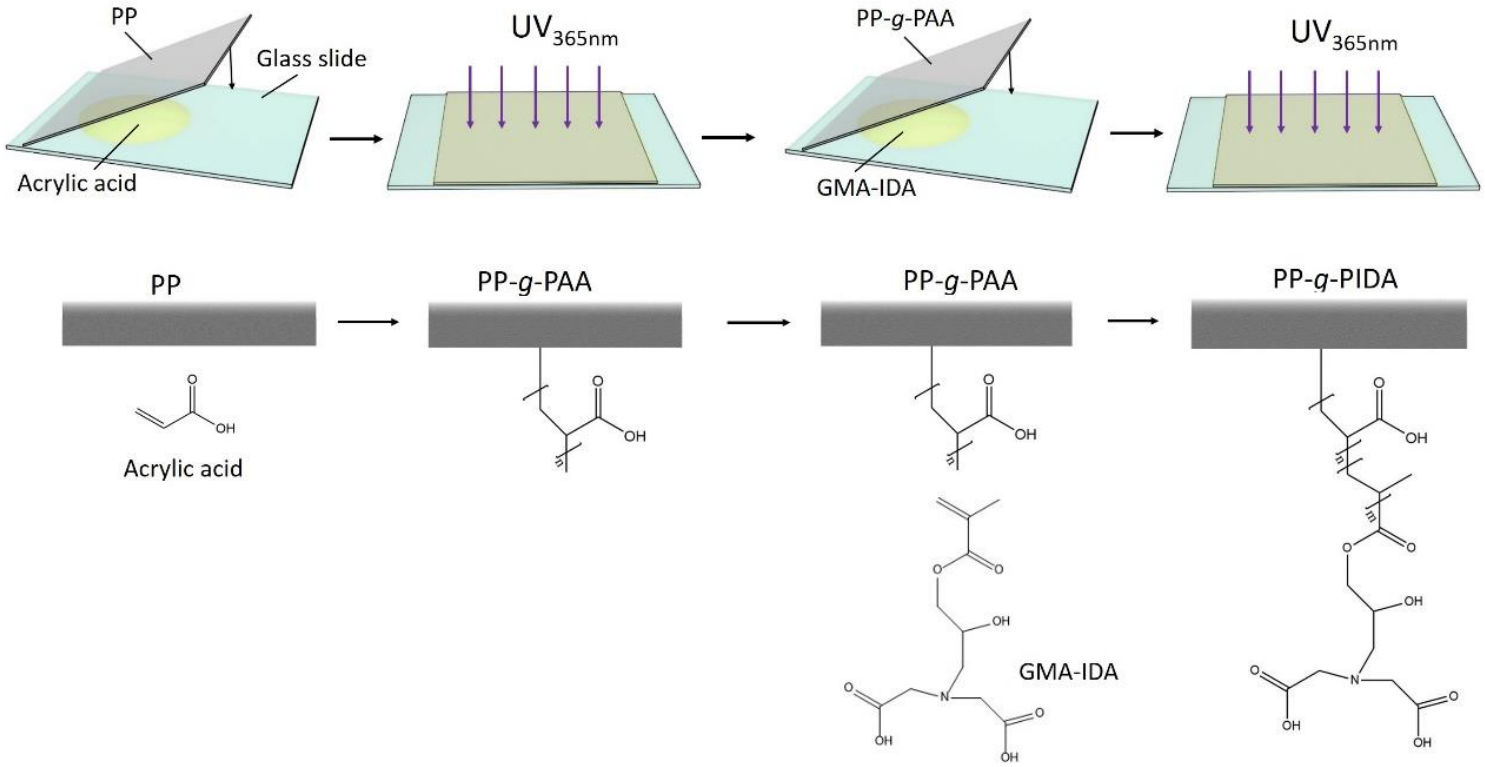

Figure 4.2. Synthesis scheme of metal-chelating PP-*g*-PIDA materials via a two-step laminated photo-grafting process.

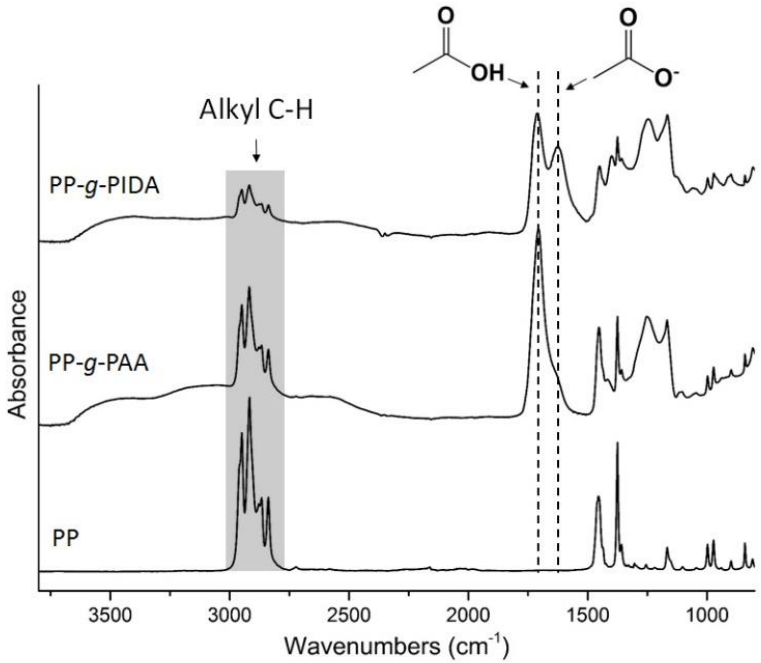

Figure 4.3. AFR-FTIR spectrum of PP, PP-*g*-PAA and PP-*g*-PIDA materials.

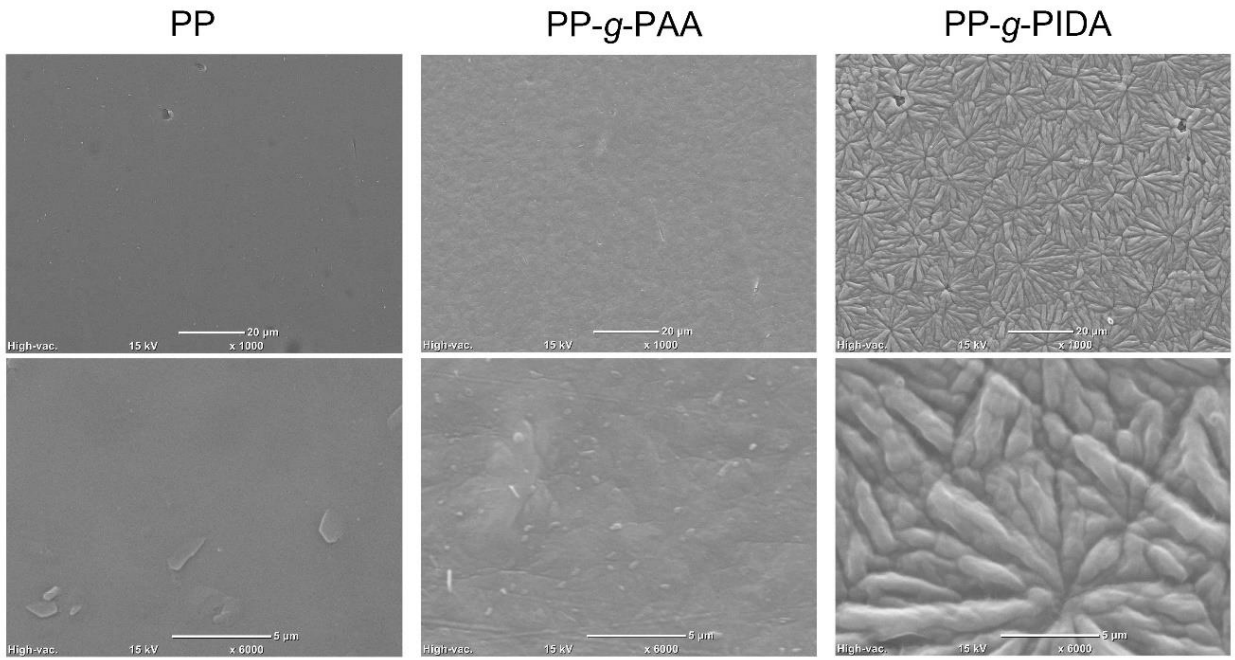

Figure 4.4. Representative electron micrographs of PP, PP-*g*-PAA and PP-*g*-PIDA. Top: x1000 magnification. Bottom: x6000 magnification.

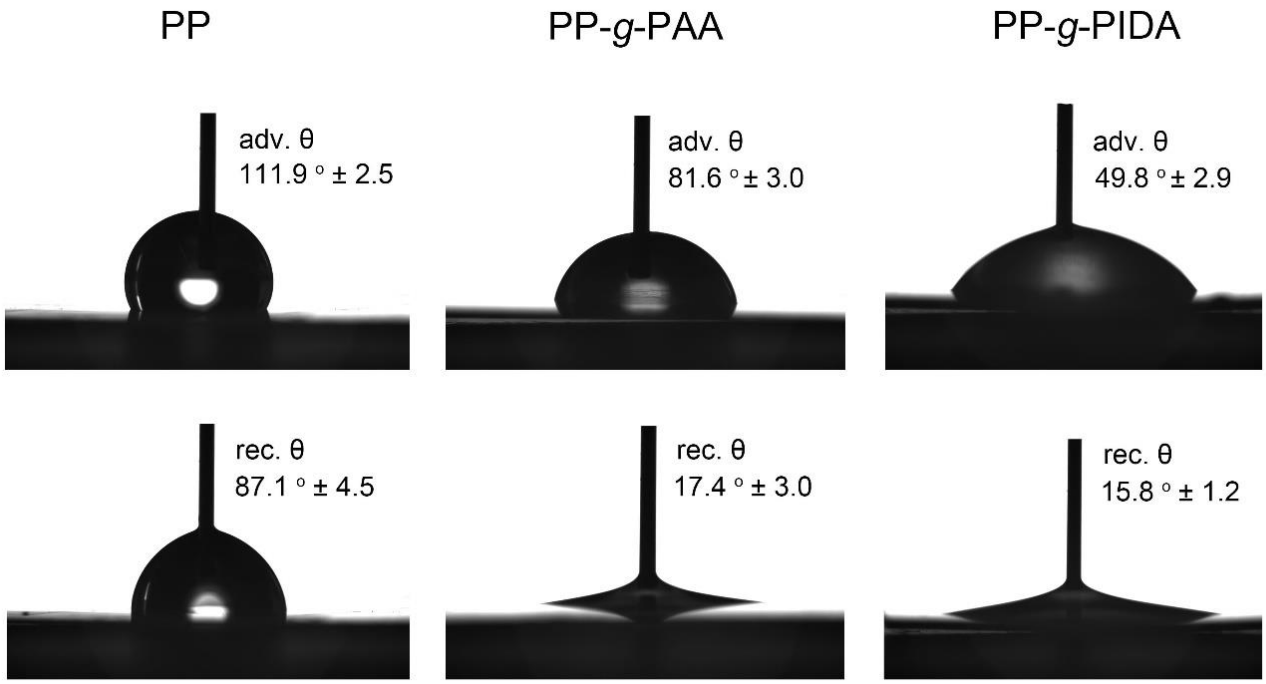

Figure 4.5. Advancing water contact angles (top) and receding water contact angles (bottom) of PP, PP-*g*-PAA and PP-*g*-PIDA.

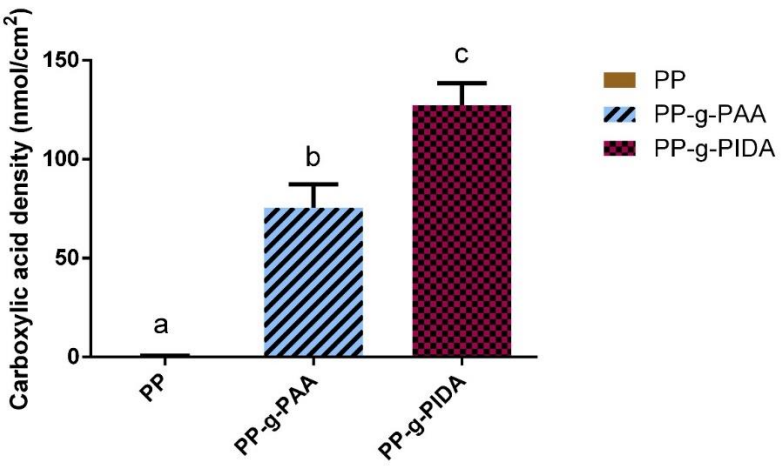

Figure 4.6. Carboxylic acid density analysis of PP, PP-*g*-PAA and PP-*g*-PIDA materials.

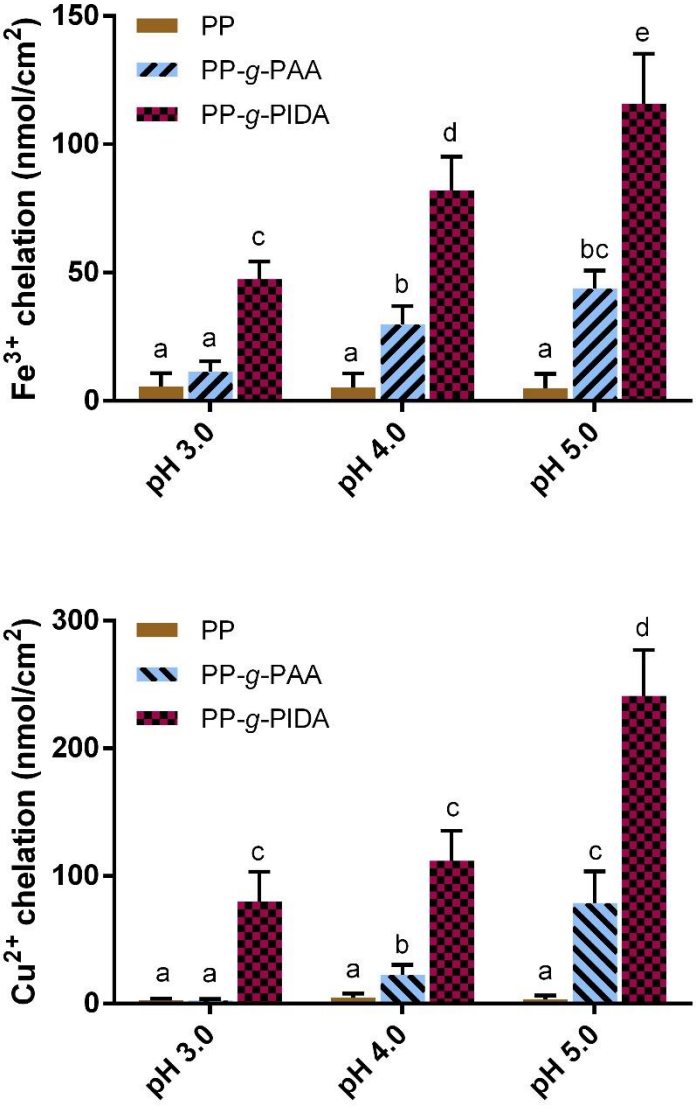

Figure 4.7. Ferric ion chelating capacity (top) and cupric ion chelating capacity analysis (bottom) of PP, PP-*g*-PAA and PP-*g*-PIDA at pH 3.0-5.0.

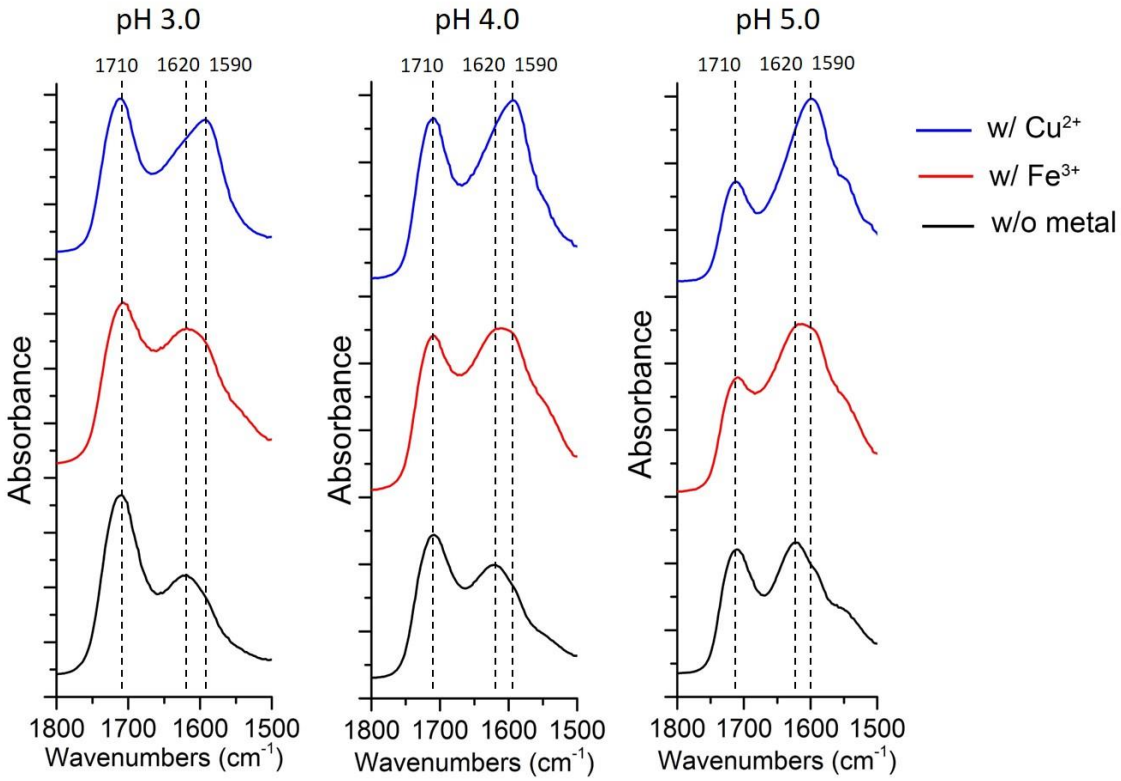

Figure 4.8. ATR-FTIR spectrum of carboxylic acid groups on PP-*g*-PIDA materials before and after metal-chelation.

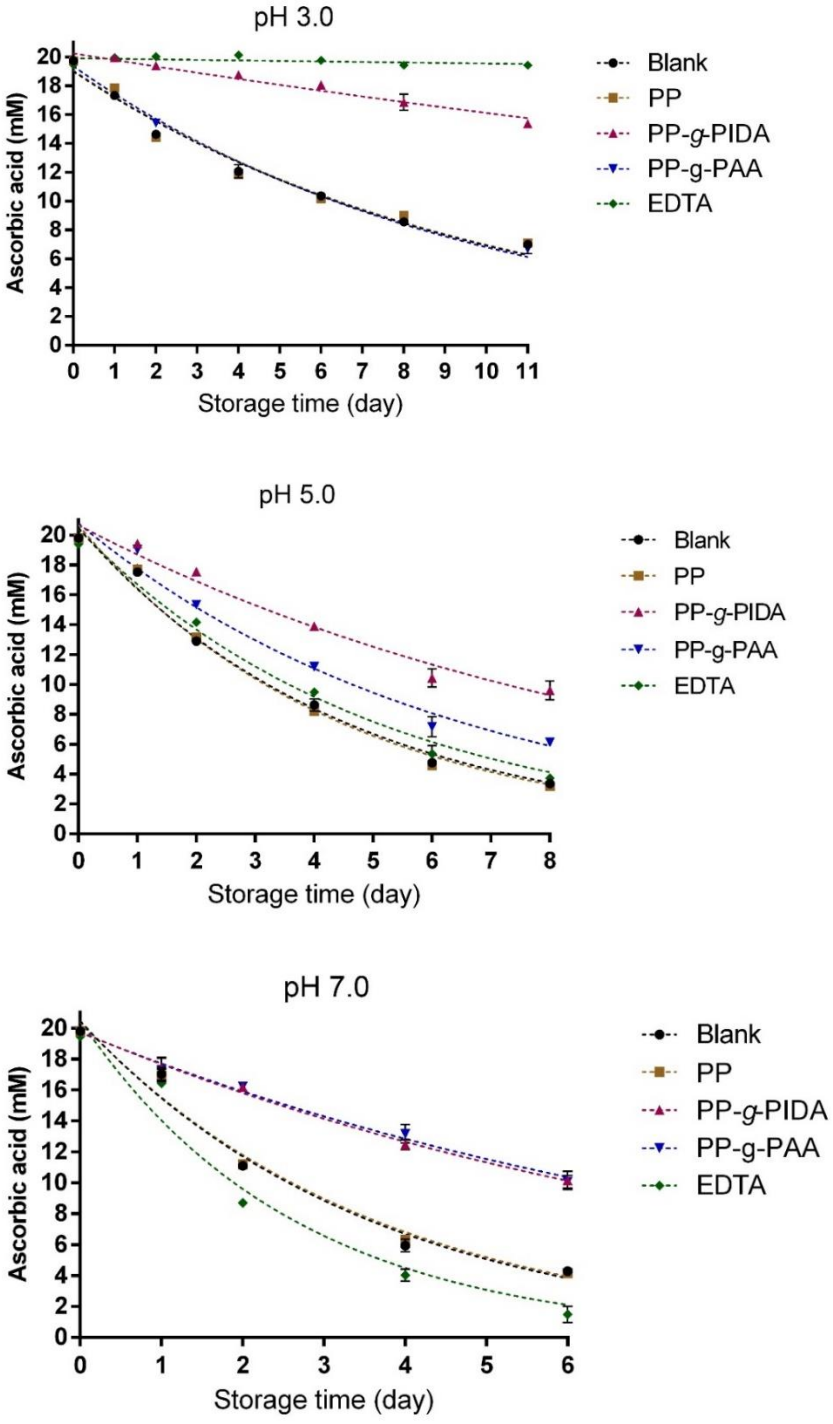

Figure 4.9. Ascorbic acid degradation in buffered ascorbic acid solutions at pH 3.0, pH 5.0 and pH 7.0, stored at 37ºC.

REFERENCES

1. Brody, A. L.; Bugusu, B.; Han, J. H.; Sand, C. K.; McHugh, T. H., Innovative food packaging solutions. *Journal of food science* **2008,** *73* (8), R107-R116.

2. Gómez-Estaca, J.; López-de-Dicastillo, C.; Hernández-Muñoz, P.; Catalá, R.; Gavara, R., Advances in antioxidant active food packaging. *Trends Food Sci. Technol.* **2014,** *35* (1), 42-51.

3. Anonymous *Smart Packaging Market Report 2016-2026*; Visiongain: 2016.

4. Benito-Pena, E.; Gonzalez-Vallejo, V.; Rico-Yuste, A.; Barbosa-Pereira, L.; Cruz, J. M.; Bilbao, A.; Alvarez-Lorenzo, C.; Moreno-Bondi, M. C., Molecularly imprinted hydrogels as functional active packaging materials. *Food Chem* **2016,** *190*, 487-94.

5. Vera, P.; Echegoyen, Y.; Canellas, E.; Nerín, C.; Palomo, M.; Madrid, Y.; Cámara, C., Nano selenium as antioxidant agent in a multilayer food packaging material. *Analytical and Bioanalytical Chemistry* **2016,** *408* (24), 6659-6670.

6. Moshe, I.; Weizman, O.; Natan, M.; Jacobi, G.; Banin, E.; Dotan, A.; Ophir, A., Multiphase thermoplastic hybrid for controlled release of antimicrobial essential oils in active packaging film. *Polymers for Advanced Technologies* **2016,** *27* (11), 1476-1483.

7. Duran, M.; Aday, M. S.; Zorba, N. N. D.; Temizkan, R.; Büyükcan, M. B.; Caner, C., Potential of antimicrobial active packaging ‘containing natamycin, nisin, pomegranate and grape seed extract in chitosan coating’ to extend shelf life of fresh strawberry. *Food and Bioproducts Processing* **2016,** *98*, 354-363.

8. Tian, F.; Decker, E. A.; Goddard, J. M., Control of lipid oxidation by nonmigratory active packaging films prepared by photoinitiated graft polymerization. *J. Agric. Food. Chem.* **2012,** *60* (31), 7710-7718.

9. Tian, F.; Decker, E. A.; Goddard, J. M., Controlling lipid oxidation via a biomimetic iron chelating active packaging material. *J. Agric. Food. Chem.* **2013,** *61* (50), 12397-12404.

10. Lin, Z.; Roman, M. J.; Decker, E. A.; Goddard, J. M., Synthesis of Iminodiacetate Functionalized Polypropylene Films and Their Efficacy as Antioxidant Active-Packaging Materials. *J. Agric. Food. Chem.* **2016,** *64* (22), 4606-4617.

11. Martell, A. E.; Robert, M. S., *Critical stability constants*. Plenum Press: New York, 1974.

12. Ogiwara, Y.; Roman, M. J.; Decker, E. A.; Goddard, J. M., Iron chelating active packaging: Influence of competing ions and pH value on effectiveness of soluble and immobilized hydroxamate chelators. *Food Chem.* **2016,** *196*, 842-847.

13. Tian, F.; Decker, E. A.; McClements, D. J.; Goddard, J. M., Influence of non-migratory metal-chelating active packaging film on food quality: impact on physical and chemical stability of emulsions. *Food Chem.* **2014,** *151*, 257-265.

14. McClements, D. J.; Decker, E. A., Lipid Oxidation in Oil-in-Water Emulsions: Impact of Molecular Environment on Chemical Reactions in Heterogeneous Food Systems. *Journal of food science* **2000,** *65* (8), 1270-1282.

15. Koontz, J., Packaging Technologies to Control Lipid Oxidation. In *Oxidative Stability and Shelf Life of Foods Containing Oils and Fats*, Hu M, J. C., Ed. Academic Press and AOCS Press: 2016; pp 479-517.

16. Goon, I. Y.; Zhang, C.; Lim, M.; Gooding, J. J.; Amal, R., Controlled fabrication of polyethylenimine-functionalized magnetic nanoparticles for the sequestration and quantification of free Cu2+. *Langmuir* **2010,** *26* (14), 12247-52.

17. Atzei, D.; Ferri, T.; Sadun, C.; Sangiorgio, P.; Caminiti, R., Structural Characterization of Complexes between Iminodiacetate Blocked on Styrene−Divinylbenzene Matrix (Chelex 100 Resin) and Fe(III), Cr(III), and Zn(II) in Solid Phase by Energy-Dispersive X-ray Diffraction. *Journal of the American Chemical Society* **2001,** *123* (11), 2552-2558.

18. El-Nahhal, I.; Zaggout, F.; Nassar, M.; El-Ashgar, N.; Maquet, J.; Babonneau, F.; Chehimi, M., Synthesis, Characterization and Applications of Immobilized Iminodiacetic Acid-Modified Silica. *Journal of Sol-Gel Science and Technology* **2003,** *28* (2), 255-265.

19. Yamada, K.; Nagano, R.; Hirata, M., Adsorption and desorption properties of the chelating membranes prepared from the PE films. *J. Appl. Polym. Sci.* **2006,** *99* (4), 1895-1902.

20. Zhu, J.; Sun, G., Facile fabrication of hydrophilic nanofibrous membranes with an immobilized metal-chelate affinity complex for selective protein separation. *ACS applied materials & interfaces* **2014,** *6* (2), 925-32.

21. Kavaklı, P. A.; Kavaklı, C.; Güven, O., Preparation and characterization of Fe(III)-loaded iminodiacetic acid modified GMA grafted nonwoven fabric adsorbent for anion adsorption. *Radiation Physics and Chemistry* **2014,** *94*, 105-110.

22. Lin, Z.; Decker, E. A.; Goddard, J. M., Preparation of metal chelating active packaging materials by laminated photografting. *Journal of Coatings Technology and Research* **2016,** *13* (2), 395-404.

23. Roman, M. J.; Decker, E. A.; Goddard, J. M., Retaining Oxidative Stability of Emulsified Foods by Novel Nonmigratory Polyphenol Coated Active Packaging. *J Agric Food Chem* **2016,** *64* (27), 5574-82.

24. Ligon, S. C.; Husár, B.; Wutzel, H.; Holman, R.; Liska, R., Strategies to Reduce Oxygen Inhibition in Photoinduced Polymerization. *Chem. Rev.* **2013,** *114* (1), 557-589.

25. Ahn, S. H.; Guo, L. J., High-Speed Roll-to-Roll Nanoimprint Lithography on Flexible Plastic Substrates. *Advanced Materials* **2008,** *20* (11), 2044-2049.

26. Decker, C.; Zahouily, K., Surface modification of polyolefins by photografting of acrylic monomers. *Macromol. Symp.* **1998,** *129* (1), 99-108.

27. Yang, W.; Rånby, B., Radical Living Graft Polymerization on the Surface of Polymeric Materials. *Macromolecules* **1996,** *29* (9), 3308-3310.

28. Chen, C.-Y.; Chen, C.-Y., Stability constants of polymer-bound iminodiacetate-type chelating agents with some transition-metal ions. *J. Appl. Polym. Sci.* **2002,** *86* (8), 1986-1994.

29. Korhonen, J. T.; Huhtamaki, T.; Ikkala, O.; Ras, R. H., Reliable measurement of the receding contact angle. *Langmuir* **2013,** *29* (12), 3858-63.

30. Kang, E. T.; Tan, K. L.; Kato, K.; Uyama, Y.; Ikada, Y., Surface Modification and Functionalization of Polytetrafluoroethylene Films. *Macromolecules* **1996,** *29* (21), 6872-6879.

31. Rush, R. M.; Yoe, J. H., Colorimetric Determination of Zinc and Copper with 2-Carboxy-2-hydroxy-5-sulfoformazylbenzene. *Analytical Chemistry* **1954,** *26* (8), 1345-1347.

32. Dawson, M. V.; Lyle, S. J., Spectrophotometric determination of iron and cobalt with Ferrozine and dithizone. *Talanta* **1990,** *37* (12), 1189-1191.

33. Horwitz, W.; Association of Official Analytical, C., Official methods of analysis of the Association of Official Analytical Chemists. *Official methods of analysis of the Association of Official Analytical Chemists.* **1970**.

34. Morent, R.; De Geyter, N.; Leys, C.; Gengembre, L.; Payen, E., Comparison between XPS- and FTIR-analysis of plasma-treated polypropylene film surfaces. *Surface and Interface Analysis* **2008,** *40* (3-4), 597-600.

35. Wu, T.; Gong, P.; Szleifer, I.; Vlček, P.; Šubr, V.; Genzer, J., Behavior of Surface-Anchored Poly(acrylic acid) Brushes with Grafting Density Gradients on Solid Substrates: 1. Experiment. *Macromolecules* **2007,** *40* (24), 8756-8764.

36. Fasce, L. A.; Costamagna, V.; Pettarin, V.; Strumia, M. C.; Frontini, P. M., Poly (acrylic acid) surface grafted polypropylene films: near surface and bulk mechanical response. **2008**.

37. Gao, L.; McCarthy, T. J., Wetting 101°†. *Langmuir* **2009,** *25* (24), 14105-14115.

38. Anonymous, TITLE 21--FOOD AND DRUGS. In *CITE: 21CFR172.120*, Regulations, C. o. F., Ed. 2017.

39. Alamed, J.; McClements, D. J.; Decker, E. A., Influence of heat processing and calcium ions on the ability of EDTA to inhibit lipid oxidation in oil-in-water emulsions containing omega-3 fatty acids. *Food Chem.* **2006,** *95* (4), 585-590.

40. Bastarrachea, L.; Wong, D.; Roman, M.; Lin, Z.; Goddard, J., Active Packaging Coatings. *Coatings* **2015,** *5* (4), 771.

41. Roman, M. J.; Decker, E. A.; Goddard, J. M., Fourier transform infrared studies on the dissociation behavior of metal-chelating polyelectrolyte brushes. *ACS applied materials & interfaces* **2014,** *6* (8), 5383-7.

42. Roman, M. J.; Tian, F.; Decker, E. A.; Goddard, J. M., Iron chelating polypropylene films: Manipulating photoinitiated graft polymerization to tailor chelating activity. *J. Appl. Polym. Sci.* **2014,** *131* (4), 39948.

43. Dinu, M. V.; Dragan, E. S., Heavy metals adsorption on some iminodiacetate chelating resins as a function of the adsorption parameters. *Reactive and Functional Polymers* **2008,** *68* (9), 1346-1354.

44. Tseng, J.-Y.; Chang, C.-Y.; Chang, C.-F.; Chen, Y.-H.; Chang, C.-C.; Ji, D.-R.; Chiu, C.-Y.; Chiang, P.-C., Kinetics and equilibrium of desorption removal of copper from magnetic polymer adsorbent. *Journal of Hazardous Materials* **2009,** *171* (1–3), 370-377.

45. Dong, R.; Lindau, M.; Ober, C. K., Dissociation Behavior of Weak Polyelectrolyte Brushes on a Planar Surface. *Langmuir* **2009,** *25* (8), 4774-4779.

46. Kaliyappan, T.; Swaminathan, C. S.; Kannan, P., Synthesis and characterization of a new metal chelating polymer and derived Ni(II) and Cu(II) polymer complexes. *Polymer* **1996,** *37* (13), 2865-2869.

47. Uluata, S.; McClements, D. J.; Decker, E. A., How the Multiple Antioxidant Properties of Ascorbic Acid Affect Lipid Oxidation in Oil-in-Water Emulsions. *J. Agric. Food. Chem.* **2015,** *63* (6), 1819-1824.

48. Sapers, G. M.; Hicks, K. B.; Phillips, J. G.; Garzarella, L.; Pondish, D. L.; Matulaitis, R. M.; McCormack, T. J.; Sondey, S. M.; Seib, P. A.; Ei-Atawy, Y. S., Control of Enzymatic Browning in Apple with Ascorbic Acid Derivatives, Polyphenol Oxidase Inhibitors, and Complexing Agents. *Journal of food science* **1989,** *54* (4), 997-1002.

49. Pizzocaro, F.; Torreggiani, D.; Gilardi, G., INHIBITION of APPLE POLYPHENOLOXIDASE (PPO) BY ASCORBIC ACID, CITRIC ACID and SODIUM CHLORIDE. *Journal of Food Processing and Preservation* **1993,** *17* (1), 21-30.

50. Bradshaw, M. P.; Barril, C.; Clark, A. C.; Prenzler, P. D.; Scollary, G. R., Ascorbic Acid: A Review of its Chemistry and Reactivity in Relation to a Wine Environment. *Critical Reviews in Food Science and Nutrition* **2011,** *51* (6), 479-498.

51. Decker, E. A., Antioxidant mechanisms. In *Food lipids: chemistry, nutrition and biotechnology.*, Akoh, C., Min DB, Ed. Marcel Dekker: New York, 1998; pp p 397-421.

52. Udenfriend, S.; Clark, C. T.; Axelrod, J.; Brodie, B. B., Ascorbic acid in aromatic hydroxylation. *J Biol Chem* **1954,** *208*, 731-738.

CHAPTER 5

PHOTOCURABLE COATINGS PREPARED BY EMULSION POLYMERIZATION PRESENT CHELATING PROPERTIES*

Abstract

Herein, we present a method to synthesize a photocurable metal chelating copolymer coating via emulsion polymerization to enable a facile coat/cure preparation of metal chelating materials. The copolymer coating was a poly(*n*-butyl acrylate) based polymer (79 mol %) synthesized by emulsion polymerization, with iminodiacetic acid (2 mol %) and benzophenone moieties (19 mol %) to impart metal chelating and photocrosslinking properties, respectively. The copolymer was applied onto polypropylene films and was photocured (365 nm, 225 mW/cm^2, 180s) to produce metal chelating film. The resulting metal chelating film had activity towards Fe^{3+} by chelating 10.9 ± 1.9 nmol/cm^2, 47.9 ± 5.3 nmol/cm^2, and 156.0 ± 13.8 nmol/cm^2 of Fe^{3+} at pH 3.0, pH 4.0, and pH 5.0, respectively. The metal chelating film controlled transition metal induced ascorbic acid degradation by extending half-life of ascorbic acid degradation from 6 days to 20 days at pH 3.0, and from 3 days to 6 days at pH 5.0, demonstrating its potential as an antioxidant active packaging material. Despite the introduction of polar iminodiacetic acid chelating moieties, the poly(*n*-butyl acrylate) based coatings retained low surface energies (24.0 mN/m) necessary to mitigate fouling and enable product release in packaging applications. The photocurable polymer coatings as reported here enable scalable production of active materials with metal chelating functionality.

*Zhuangsheng Lin, Julie M. Goddard

Submitted to Colloids and Surfaces B: Biointerfaces

Introduction

Synthetic metal chelators (e.g. ethylenediamine tetraacetic acid (EDTA)) are often used in shelf-stable consumer products to control transition metal induced oxidative degradation. In response to the increasing consumer demand for natural and 'clean label' consumer products,[1] our research group has developed an active packaging technology to serve as an alternative to synthetic additives (Figure 5.1).[2-8] In particular, metal chelating moieties (e.g. carboxylic acids, hydroxamic acid, and iminodiacetic acid) have been introduced to polymer surfaces to partition transition metal ions and prevent their reactivity. Our studies suggest that the metal chelating active packaging materials are effective in controlling transition metal induced oxidative degradation of labile components, with demonstrated performance in retaining stability of lipids,[2-3, 5-7] ascorbic acids[3-4] and lycopene.[5] By utilizing covalent immobilization chemistries, such active packaging technologies are considered non-migratory (or immobilized) and thus can potentially be regulated in the U.S.A. by the Food and Drug Admission (FDA) as food contact substance (FCS), rather than as direct additives.[9] Other than active packaging, metal chelating materials have application in heavy metal removal in water treatment,[10-12] protein separation,[13-14] and catalytic chemistry.[15-16] However, preparation of these materials has typically relied on extensive, complicated material preparation steps to tether metal chelating ligands, including degassing,[6-7, 10, 17] batch chemical reactions,[3, 5, 11, 13] and long-time thermal curing processes,[15, 18] thus limiting the commercial availability of the materials, especially in the area of active packaging.

Photocuring (i.e. light-induced hardening of monomeric or polymeric substances) has been widely adopted in the printing and coating industries due to its low energy, high

speed, and solvent-free processing.[19] Photocurable copolymers have been reported in recent years for preparation of a range of functional coatings (e.g. antimicrobial,[20-21] antifouling,[22] biopatterning,[23] adhesives,[24-25] surface bound lubricants,[26] and other polymer thin films[27-29]). Photocurable copolymers permit introduction of a target functional group (e.g. antimicrobial, lubricant) via a simple coat/cure process, without the need for degassing or batch chemical reactions typical of grafting-from style surface modifications. Benzophenone is the most commonly reported photocrosslinker used in photocurable copolymers,[20, 24-26, 28] and monomeric benzophenone and its derivatives have been used in ink formulations for paper and paperboard food packaging.[30] When exposed to UV light (365 nm), benzophenone is excited to its biradical state, which can abstract a hydrogen from neighboring C-H bond and permit formation of a new, stable C-C bond.[31] Benzophenone derivatives can be introduced into copolymers and are not prone to oxygen inhibition, enabling atmospheric photocuring without the need for degassing.[19] Benzophenone moieties can further covalently crosslink with polymeric substances rich in alkyl groups (e.g. polypropylene, polyethylene) via photocuring.

Iminodiacetic acid (IDA) is a metal chelating ligand used in commercial metal chelating resins and membranes for heavy metal removal.[11, 32] IDA has half of the chemical structure of EDTA, and is a tridentate metal chelator with specificity to transition metals common in foods and beverages (e.g. iron). IDA derived metal chelating active packaging materials have been explored due to IDA's high affinity to iron (log K=10.72 for Fe^{3+}) and low affinity to common multivalent ions in foods, such as calcium (log K=2.59 for Ca^{2+}) and magnesium (log K=2.98 Mg^{2+}),[33] supporting its potential efficacy in complex food matrices. We have previously demonstrated the antioxidant efficacy of

IDA functionalized materials against both transition metal-induced lipid oxidation and ascorbic acid degradation in simulated food systems.[3-4] However, by introducing only polar IDA ligands, the resulting coating presented a swellable, hydrogel like morphology, unsuitable for application as a packaging material for which product release is required.

In this work, we prepare a poly(*n*-butyl acrylate) based copolymer coating with IDA and benzophenone moieties to impart metal-chelating and photocrosslinking, respectively, via emulsion copolymerization (Figure 5.2). Poly(*n*-butyl acrylate) based copolymers are FDA approved as indirect additives for food contact applications (e.g. non-stick coatings for cooking pans[34]),[9] and as a polymer base to control the thermal mechanical properties and to control the surface energy of the coating. Poly(n-butyl acrylate) based copolymers have been prepared by emulsion polymerization to prepare functional polymer coatings for application in antimicrobial,[35] UV-shielding,[36] and corrosion protection.[37] Emulsion copolymerization is a water-based polymerization system and has been widely used for preparation of latex paints, adhesives, print inks, and coatings with reduced emission of volatile organic compounds (VOC).[38] Copolymers comprised of IDA and poly(*n*-butyl acrylate) have been produced via emulsion copolymerization with applications in antimicrobial,[39] oxygen scavenging,[40] and semi-conductive[41] materials; however, such materials had limited stability in aqueous environments due to the lack of crosslinkers. The photocurable metal chelating copolymer coating technology prepared in this study will enable a simple coat/cure preparation of metal chelating materials. The resulting coatings were characterized for surface chemistry, thickness, chelating capacity, and surface energy. Their antioxidant

efficacy against transition metal-induced ascorbic acid degradation and stability in food simulants were also tested.

Materials and methods

Materials

Polypropylene pellets (isotactic) were purchased from Scientific Polymer Products (Ontario, NY). L-ascorbic acid, EDTA (disodium salt dihydrate), imidazole (99%), glycidyl methacrylate (97%), zincon monosodium salt, 3-(2-pyridyl)-5,6-diphenyl-1,2,4-triazine-p,p'-disulfonic acid disodium salt hydrate (ferrozine, 98%+), toluidine blue O (TBO), *n*-butyl acrylate (99+%), methacryloyl chloride (97%), 4-hydroxybenzophenone (98%), and potassium persulfate (99+%) were purchased from Sigma-Aldrich (St. Louis, MO). Isopropanol, acetone, methanol, sodium hydroxide, glacial acetic acid, hydrochloric acid (trace metal grade), trichloroacetic acid (TCA), oxalic acid dihydrate, sodium acetate trihydrate, 4-(2-hydroxyethyl)-1-piperazineethanesul-fonic acid (HEPES), sodium phosphate monobasic monohydrate, sodium carbonate anhydrous, sodium bicarbonate, ferric chloride hexahydrate, and 2,6-dichloroindophenol were purchased from Fisher Scientific (Fair Lawn, NJ). Iminodiacetic acid (IDA) (98+%) was purchased from Acros Organics (Morris Plains, NJ). Absolute ethanol was purchased from Pharmco-Aaper (Brook-field, CT). Nitric acid (trace metal grade) was purchased from VWR Chemicals (Radnor, PA). All chemicals and reagents were used as received without further purification. 2-propenoic acid, 2-methyl-,3-[bis-(carboxymethyl) amino]-2-hydroxypropyl ester (GMA-IDA) and 4-benzoyphenyl methacrylate (BPM) were synthesized according to reported procedures.[28, 42].

Preparation of photocurable metal chelating copolymer

The photocurable metal chelating polymer, poly (2-propenoic acid,2-methyl-,3-[bis-(carboxymethyl) amino]-2-hydroxypropyl ester-*co*-*n*-butyl acrylate-*co*-4-benzoylphenyl methacrylate) (GMA-IDA-*co*-BA-*co*-BPM) was synthesized by emulsion copolymerization of GMA-IDA, *n*-butyl acrylate and BPM monomers (Figures 5.2, 5.3A). Emulsion polymerization is a free radical polymerization of vinyl monomers (oil phase) commonly conducted in water as a continuous phase. In this work, the amphiphilic nature of the GMA-IDA monomer permitted surfactant-free emulsion polymerization. Briefly, in a 300 mL reaction vessel equipped with an overhead mixer and a condenser, GMA-IDA (2.7 g, 48 w/w % monomer in water) and potassium persulfate (0.39 g) were dissolved in deionized (DI) water (126 mL). BPM (2.4 g) was dissolved in *n*-butyl acrylate (9.66 g) and the mixture was added into the reaction vessel. The mixture in the reaction vessel was purged with nitrogen gas for 20 min with stirring and was brought to 70^{o}C using an oil bath. The reaction continued at 70^{o}C for 20 hours in the dark with stirring. The crude copolymer emulsion was centrifuged at 3000 g force for 15 min to remove polymer precipitates. The supernatant was dialyzed in DI water using a 20 kDa regenerated cellulose dialysis membrane to remove unreacted GMA-IDA. The retentate was further purified by dialysis in methanol to remove unreacted *n*-butyl acrylate and BPM, and to introduce methanol as a co-solvent. The retentate was centrifuged at 3000 g force for 15 min to remove polymer precipitates. The supernatant containing the purified copolymer was collected and stored in a refrigerator until coating application (Figure 5.3B). The yield of the reaction was 47.6 %. The dispersed phase of the copolymer emulsion contained 42.4 mg/mL of

copolymer, and the continuous phase contained 75 v/v % of methanol as co-solvent. The particle size distribution and the electrical charge of polymer emulsion were analyzed using a Zetasizer Nano ZS (Malvern Instruments, Ltd., Worcestershire, U.K.). To conduct NMR analysis, the polymer emulsion was dialyzed in DI water and lyophilized to collect dried GMA-co-BA-co-BPM copolymer. Nuclear Magnetic Resonance (NMR) spectrum of the copolymer was collected in DMSO-d_6 at 130^{o}C in a Varian INOVA-600 spectrometer (Palo Alto, CA).

Preparation of metal chelating film

Metal chelating films were prepared by coating GMA-IDA-*co*-BA-*co*-BPM copolymer onto heat-pressed polypropylene films followed by photocuring (Figure 5.3B). Polypropylene films were prepared by pressing polypropylene pellets into polypropylene films according to previous reports.[3-4] To prepare the metal chelating films, an aliquot of GMA-IDA-*co*-BA-*co*-BPM copolymer emulsion was applied onto polypropylene films (20 µL/cm^2 of copolymer coating unless otherwise noted). As the solvent evaporated and the copolymer coalesced, a clear and glossy polymer coating was formed. The coating was crosslinked and bound to the polypropylene film by exposure to UV irradiation (365 nm, 225 mW/cm^2 flux) for 180 s. The completion of the benzophenone photocrosslinking reaction was monitored by following absorption spectrum at 270-290 nm[20, 23] during the photocuring process (0-200 s UV exposure time) using a Synergy Neo2 Hybrid Multi-Mode Reader (BioTek Instruments, Winooski, VT). The photocured metal chelating coating on polypropylene was further washed in hot DI water at 60^{o}C three times (30 min each) to remove any unattached polymers.

Surface characterization

Surface chemistry of the coated materials was characterized using attenuated total reflectance Fourier transform infrared (ATR−FTIR) spectroscopy and X-ray photoelectron spectroscopy (XPS). ATR-FTIR spectra were collected on an IRTracer-100 FTIR spectrometer (Shimadzu Scientific Instruments, Kyoto, Japan) equipped with an ATR crystal. Spectra were collected at a resolution of 4 cm^{-1} (32 scans) using Happ-Genzel apodization, with air as background spectra. XPS spectra were collected on a SSX-100 (Surface Science Instruments) with operation pressure at around $2x10^{-9}$ Torr. Photoelectrons were collected at a 55° emission angle using a monochromatic Al Kα X-ray (1486.6 eV) with 1 mm diameter beam size. Electron kinetic energy was determined using a hemispherical analyzer with a pass energy of 150 V for wide/survey scans. Surface morphology and coating thickness were characterized using scanning electron microscopy (SEM). Surfaces and cross-sections were sputter-coated with gold (Cressington Scientific, Watford, UK) and imaged at 10 kV in a JEOL 6000 FXV SEM (JEOL Ltd. Akishima, Tokyo, Japan). Surface wettability and surface energy of the materials were analyzed using contact angle analysis using an Attension Theta Optical Tensiometer (Biolin Scientific, Stockholm, Sweden). Advancing and receding water contact angles were measured according to a reported protocol.[43] Briefly, advancing water contact angles were measured by depositing DI water onto substrate surfaces at rate of 0.5 µL/s and receding contact angles were measured after advancing angle measurement by withdrawing water at a rate of 0.5 µL/s. Surface energy of the materials was determined using a Zisman plot method.[44] Advancing contact angles were collected using water, acetone, ethylene glycol and glycerol as probe fluids to calculate the surface energy. Carboxylic acid densities of the materials were quantified using a TBO

dye assay.[45] The materials were stored in 0.5 mM TBO dye solutions at pH 10.0 for 24 hours to absorb TBO dye, followed by rinsing in water adjusted to pH 10.0 by sodium hydroxide to remove loosely bound dye. The complexed TBO dye was then desorbed by storing the materials in 50 v/v % acetic acid in water solutions. The amount of dye released to acetic acid solution was quantified by measuring absorbance at 633 nm, and compared to a standard curve of TBO dye in acetic acid solution. The carboxylic acid density was determined by assuming a 1:1 stoichiometric ratio between absorbed dye and carboxylic acid.

Metal chelating analysis

Iron chelating capacity of materials was analyzed using inductively coupled plasma-mass spectrometry (ICP-MS) and a colorimetric ferrozine assay according to previous protocols.[7, 46] To conduct ICP-MS analysis, materials were stored in 0.06 mM ferric chloride in 50 mM sodium acetate/imidazole buffer (pH 3.0, 4.0 and pH 5.0) in the dark for 72 hours. The materials were rinsed with absolute ethanol and dried in a desiccator. The materials (approximately 140 mg) were digested in 5 mL of nitric acid (trace metal grade) in a microwave oven (Milestone Srl, Milan, Italy) (ramp to 210 ^{o}C for 20 min, hold at 210 ^{o}C for 20 min and cool for 10 min). Digested samples were diluted with DI water and were stored in a refrigerator until analysis. ICP-MS analysis was conducted on an Agilent 7500 series ICP-MS equipped with an Agilent ASX-500 autosampler (Agilent, Waltham, MA). Calibration standards were prepared with iron solutions (1000 ppm ICP−MS Standard, Sigma-Aldrich, St. Louis, MO). To conduct the ferrozine assay, materials were incubated in 0.08 mM ferric chloride in 50 mM sodium acetate/imidazole buffer (pH 4.0, 72 hours, room temperature, dark) to chelate

ferric ions. Ferric ion concentration in the buffered solution remaining after storage was quantified by adding a reducing agent (5 wt % hydroxylamine chloride and 10 wt % TCA) and ferrozine solution (18 mM ferrozine in 50 mM HEPES (pH 7.0)). The absorbance of the mixture was measured at 562 nm after 1 hour incubation and the ferric ion concentration was calculated by comparison to a standard curve prepared using ferric chloride.

Antioxidant efficacy

The performance of the metal chelating films was evaluated by analyzing the antioxidant efficacy against ascorbic acid degradation according to previous protocols.[3-4] Metal chelating films (1x1 cm^2 coupons) were stored in 1 mL of ascorbic acid solution (20 mM ascorbic acid in 10 mM sodium acetate/imidazole buffer, at both pH 3.0 and pH 5.0) at 37^oC in 10 mL glass vials sealed with septum caps. Blank ascorbic acid solutions, ascorbic acid solutions incubated with polypropylene, and ascorbic acid solutions with 0.08 mM EDTA (23.4 ppm equivalent, molecular weight 292.2 g/mol) were used as controls. The ascorbic acid content during the storage was analyzed using a modified Association of Official Analytical Chemists (AOAC) official method 967.21.[47] Briefly, 0.2 mL of the ascorbic acid solution was mixed with 4.8 mL 0.04 wt % oxalic acid in water, followed by adding 0.3 mL of this ascorbic acid/oxalic acid mixture into 4.7 mL of 0.2 mM dichloroindophenol in water solution. The absorbance was measured immediately at 520 nm and ascorbic acid content was calculated by comparing to ascorbic acid standards. The changes in ascorbic acid contents during storage were fitted to a first order degradation rate equation to determine degradation half-lives and rate coefficients.

Graft stability

Coating stability was assessed by incubating metal chelating films in food simulants in accordance with a reported FDA guideline for premarket approval of food contact substances.[48] Metal chelating films (1x1 cm^2 coupons) were stored in 1.55 mL of DI water, 3 wt % acetic acid, 10 v/v % ethanol and corn oil, simulating aqueous, acidic, alcoholic, and fatty food systems, respectively, for 10 days at 40^oC. After storage, films were rinsed with absolute ethanol and DI water, and were dried in a desiccator. The surface chemistry and surface morphology of the metal chelating films were analyzed using ATR-FTIR and SEM and compared to spectra and micrographs of freshly coated films to assess for stability.

Statistics

GMA-IDA-*co*-BA-*co*-BPM copolymer emulsion was prepared at least three times, with uniformity in surface chemistry, metal-chelating activity and antioxidant efficacy, indicating reproducibility of the coating formulation. Surface analysis, metal chelating assays, and ascorbic acid degradation study were performed using quadruplicate samples of metal chelating films prepared by a single representative batch of copolymer emulsion. The reported ATR-FTIR spectra are representative of four spectra collected across quadruplicate separately prepared samples. Reported scanning electron micrographs are representative of images acquired at random locations on quadruplicate samples. Results of surface wettability and surface energy, carboxylic acid density, metal chelating analysis and ascorbic acid degradation experiments are representative of at least two experiments repeated independently. Results of coating thickness, carboxylic acid density and metal chelating capacity were subjected to

analysis of variance (ANOVA) to compare difference using Fisher's least significant difference ($p<0.05$) in GraphPad Prism 6.0 (La Jolla, CA).

Results and discussion

Copolymer characterization

The photocurable metal chelating copolymer, GMA-IDA-*co*-BA-*co*-BPM, was synthesized by surfactant-free emulsion polymerization. GMA-IDA-*co*-BA-*co*-BPM is a poly(*n*-butyl acrylate) based copolymer with IDA and benzophenone moieties (Figure 5.2), where IDA serves as a metal chelator and benzophenone serves as a photocrosslinker (Figure 5.3). The copolymer latex was stable as polymer emulsion in water and in aqueous environment with methanol as a co-solvent without the need for surfactants, likely due to the amphiphilic nature of the GMA-IDA moieties, in agreement with other reports.[39-41] The mean diameter of the resulting copolymer latex was determined to be 470.9 ± 5.2 nm. The copolymer latex had a slightly negative surface charge of -1.67 ± 0.26 mV, which was likely from the partially deprotonated IDA moieties that served to stabilize the copolymer latex. The proton NMR spectrum of the copolymer was collected in DMSO-d_6 at 130^{o}C (Figure 5.4). Chemical shifts at 0.86 ppm, 1.50 ppm, 1.55 ppm, 4.00 ppm were assigned to the butyl acrylate moieties. Chemical shifts at 7.28 ppm, 7.50 ppm, 7.76 ppm were assigned to the aromatic protons from BPM moieties. The GMA-IDA moieties did not show apparent NMR signals, suggesting a low molar composition of GMA-IDA in the copolymer. The molar composition of BA and BPM was determined to be 79 % and 19 %, respectively, using NMR spectroscopy. The composition of GMA-IDA moieties in the copolymer was determined to be 2 % by measuring the carboxylic acid content in the copolymer

coating. The determination of molar composition of each monomeric moiety is described in detail in SI.

The copolymer coating was applied onto polypropylene surface to form a clear and glossy uncured coating, which was futher photocured by exposure to UV-light. The photocuring capability of the GMA-IDA-*co*-BA-*co*-BPM copolymer was analyzed by monitoring the absorption spectrum at 270-290 nm, which decreases in intensity with increased crosslinking of benzophenone.[20, 23] The uncured coating had a strong absorption maximum at 270 nm. As the coating was exposed to UV-light (365 nm, 225 mW/cm^2), the absorption band at 270 nm decreased (Figure 5.5A), suggesting successful benzophenone crosslinking. The mechanism of this crosslinking reaction was explained by Dorman and Prestwich.[31] As benzophenone absorbs photons at 365 nm, the carbonyl group is induced to a biradical triplet state, which abstracts a hydrogen from a neighboring C-H bond and forms two free radicals. The two free radicals then form a new C-C bond and create a crosslink. Since alkyl groups are abundant on the surface of polypropylene and on the poly(*n*-butyl acrylate) based copolymer, the benzophenone moieties were hypothesized to crosslink to the surface of polypropylene substrate and within the polymer coating, making the coating stable against delamination from the polypropylene after photocuring. It is worthwhile to note that poly(*n*-butyl acrylate) based copolymer coatings with IDA moieties but without benzophenone moieties prepared in our preliminary experiments failed to form stable coatings on polypropylene after exposure to UV-light.

Surface Characterization

The surface chemistry of metal chelating film was characterized using ATR-

FTIR spectroscopy, with polypropylene film as control (Figure 5.6A). Polypropylene had characteristic absorption bands at 3000-2800 cm^{-1} (C-H stretch), and at 1450 cm^{-1} and 1370 cm^{-1} (C-H bend). Metal chelating film had an absorption band at 3000-2800 cm^{-1} (C-H stretch), a strong absorption band at 1710 cm^{-1}, a small shoulder at 1620 cm^{-1} (C=O stretch), and absorption bands at 1260-1160 cm^{-1} (C-O-C stretch). These absorption bands are characteristic for poly(*n*-butyl acrylate) based materials.[36, 39] The small shoulder at 1620 cm^{-1} suggests the presence of IDA ligands, as deprotonated IDA ligands are known to absorb at this wavenumber.[3, 42] The dissociation behavior of the coating was further investigated by monitoring the C=O stretch region (1800-1520 cm^{-1}) after storing the metal chelating film in aqueous solutions of pH values ranging from 1.0 to 12.0 (Figure 5.6B). As the pH increased from pH 1.0 to pH 5.0, the absorption band at 1620 cm^{-1} increased as a result of deprotonation of carboxylic acid groups on IDA. The absorption band further shifted from 1620 cm^{-1} to 1570 cm^{-1} as the pH increased from pH 5.0 to pH 12.0, potentially due to further deprotonation of tertiary amine group on IDA. The change in FTIR spectrum in different pH conditions was in agreement with the ligand dissociation behavior studied in a previous report.[3] The ATR-FTIR results suggested successful coating of GMA-IDA-*co*-BA-*co*-BPM copolymer on polypropylene with absorbance bands and dissociation behavior typical of immobilized IDA ligands.

The surface chemistry of the metal chelating films was further characterized by analyzing the atomic percentage of the coating surface using XPS. The surface of the metal chelating film contained 84.6 ± 1.9 % of carbon and 15.4 ± 1.9 % of oxygen, while the nitrogen content was under the limit of detection. The low nitrogen content

on the surface agreed with the low content of IDA moieties (2 mol %) in the copolymer. This analyzed atomic percentage was also in agreement with the theoretical 79 % of carbon, 20 % of oxygen and 1 % of nitrogen based on the composition of the copolymer coating as determined by NMR and dye assays for functional groups.

The surface wettability and surface energy of the metal chelating film was analyzed using contact angle analysis, with native polypropylene film as control (Table 5.1). Surface energy was calculated using a Zisman plot method.[44] The native polypropylene surface had an advancing water contact angle and a receding water contact angle of 108.0 ± 1.4° and 82.9 ± 2.1°, respectively, and a surface energy of 20.4 mN/m, in agreement with previous reports.[4, 8, 49] The metal chelating film had an advancing water contact angle of 102.4 ± 0.3°. The high advancing water contact angle was in agreement with the reported hydrophobicity of poly(*n*-butyl acrylate) based materials.[50] The advancing water contact angle of metal chelating film prepared using the copolymer coating was more hydrophobic than materials prepared by grafting-from techniques in previous studies.[3-4, 8] The metal chelating film had a low receding water contact angle of 19.1 ± 1.6°, and a high hysteresis degree (83.4 ± 1.7°), indicative of strong interactions between the water and the surface.[51] The surface energy of the metal chelating film was determined to be 24.0 mN/m, which was higher than the 20.4 mN/m of uncoated polypropylene, but importantly lower than the 30 mN/m surface energy limit to be considered non-fouling materials.[52] The low surface energy of this coating is important for product release in packaging applications.

The surface morphologies of the native polypropylene and metal chelating film were imaged using SEM (Figure 5.7A and B). Native polypropylene had a relatively

smooth surface while the application and curing of the copolymer coating introduced a uniform surface with a slight increase in surface roughness. The cross-section of the copolymer coating was imaged under SEM to observe the thickness of coatings prepared using different amounts of copolymers (Figure 5.7C, D, E and F). The thickness of copolymer coating increased as the amount of coating increased. The effect of the amount of coating on coating thickness was quantified and reported in Figure 5.8A. The metal chelating film prepared using 10 μl/cm^2 of copolymer coating had a coating thickness of 4.3 ± 0.1 μm, while the thickness increased to 19.4 ± 0.2 μm when 80 μl/cm^2 of coating was used. The carboxylic acid density of the metal chelating film with increasing coating thickness was quantified using a TBO dye assay (Figure 5.8B). The carboxylic acid density increased as the amount of coating increased. The metal chelating film prepared using 10 μl/cm^2 of copolymer coating had a carboxylic acid density of 96.2 ± 6.6 nmol/cm^2, and increased to 753.9 ± 91.7 nmol/cm^2 when 80 μl/cm^2 of coating was used. These results suggest that the IDA ligands were present and available for metal chelation throughout the coating, again supporting the observed high hysteresis value. At a preparation in which 20 μl/cm^2 coating was applied to the polypropylene film, the thickness was measured to be 7.9 ± 0.5 μm, with a measured carboxylic acid density of 221.7 ± 37.3 nmol/cm^2 carboxylic acids. This density of carboxylic acids is equivalent to approximately110 nmol/cm^2 of IDA ligand. For a half-liter package with approximately 600 cm^2, 110 nmol/cm^2 available IDA ligands corresponds to approximately 19.4 ppm EDTA (molecular weight 292.2 g/mol), above the minimum concentration of EDTA (0.75 ppm) to give a significant antioxidant effect in emulsified oil systems.[53] These results suggest that both the coating thickness and

resulting chelating capacity can be tailored by application of different amount of copolymer coating, therefore, manufacturers have the ability to control the chelating capacity and antioxidant efficacy for target applications (e.g. active packaging).

Metal Chelation

The metal chelating capacity of the film coated by the GMA-IDA-*co*-BA-*co*-BPM copolymer emulsion was quantified by storing the materials in 0.06 mM Fe^{3+} buffered solutions (pH 3.0-5.0) for 72 hours. The materials were acid digested and the Fe^{3+} content in the digest was analyzed using ICP-MS (Figure 5.9A). Metal chelating films prepared using 20 µL/cm^2 of coating had a ferric ion chelating capacity of 10.9 ± 1.9 nmol/cm^2, 47.9 ± 5.3 nmol/cm^2 and 156.0 ± 13.8 nmol/cm^2, at pH 3.0, pH 4.0 and pH 5.0, respectively, with minimal ferric ion chelation by the uncoated polypropylene, suggesting that the observed metal chelation was a result of ligand specific interactions and not precipitation or adsorption. The chelating capacity of the metal chelating film increased with increasing pH value, in agreement with prior studies on the effect of pH on chelating activities of IDA ligands.[11, 32, 54]. The effect of the amount of coating on the metal chelating activity at pH 4.0 was analyzed (Figure 5.9B). The amount of Fe^{3+} chelation increased as the amount of coating increased, in agreement with the observed increase in carboxylic density with increasing coating thickness. The metal chelating film prepared using 10 µl/cm^2 of coating chelated 19.8 ± 5.2 nmol/cm^2 of Fe^{3+}, which increased to 134.3 ± 7.7 nmol/cm^2 of Fe^{3+} when 80 µl/cm^2 of coating was applied. These results suggested that the IDA ligands present within the coating interior were able to chelate Fe^{3+}, and that the metal chelating capability of the materials can be readily tailored by adjusting the thickness of copolymer coating.

Antioxidant efficacy

The antioxidant efficacy of the metal chelating film was characterized by analyzing its ability to control ascorbic acid degradation. It has been well established that transition metals promote oxidative degradation of labile components of packaged goods; in food systems, ascorbic acid degradation can occur by metal promoted oxidation of ascorbic acid to dehydroascorbic acid.[55] Dehydroascorbic acid is relatively unstable and can undergo further degradation reactions. Previous studies suggested that metal chelating materials controlled ascorbic acid degradation in aqueous solutions by a hypothesized mechanism of scavenging transition metals from the system.[3-4] Metal chelating films prepared by coating and curing the copolymer emulsion described above were stored in ascorbic acid solutions at pH 3.0 and pH 5.0 at 37^{o}C, with blank ascorbic acid solution (no film), ascorbic acid solution with clean polypropylene films, and ascorbic acid solution containing EDTA as controls (Figure 5.10). Ascorbic acid degradation was observed to follow a first order degradation kinetic in agreement with other reports.[56] At pH 3.0, the ascorbic acid in blank and polypropylene treatments degraded the fastest, with a shortest degradation half-life of 6 days. In contrast, introduction of the metal chelating coating slowed ascorbic acid degradation and extended the degradation half-life to 20 days. EDTA was the most effective against ascorbic acid degradation at pH 3.0 and had the highest ascorbic acid retention at the end of the storage period. At pH 5.0, the blank, polypropylene and EDTA treatments showed similar ascorbic acid degradation kinetics with a degradation half-life of around 3 days. The loss in antioxidant efficacy of EDTA against ascorbic acid degradation at slightly acidic pH was in agreement with our previous report[4] which suggested that

EDTA loses antioxidant efficacy as transition metal solubility increases. The metal chelating films controlled ascorbic acid degradation and improved the degradation half-life to 6 days at pH 3.0. The metal chelating film showed antioxidant efficacy against ascorbic acid degradation at both pH conditions tested, outperforming EDTA at pH 3.0. The results suggested the metal chelating film could potentially serve as an antioxidant active packaging material to control transition metal induced oxidative degradation.

Coating stability study

To demonstrate the stability of the photocured metal chelating polymer coating on polypropylene against delamination under conditions typical of packaged goods, the metal chelating films were stored in food simulants of water, 3% acetic acid, 10% alcohol and corn oil, representing aqueous, acidic, alcoholic and fatty foods, respectively.[48] After 10 days of storage at 40^{o}C, surface chemistry and morphology were analyzed and compared to that of freshly coated and cured films to assess potential change in surface chemistry and delamination of the coating. The metal chelating films stored in water, 10% alcohol and corn oil had similar ATR-FTIR spectra as freshly prepared metal chelating materials . Metal chelating film stored in 3% acetic acid had a slight decrease in the absorption band at 1650 cm^{-1}, which is characteristic for IDA functionalized materials in acidic environment due to protonation of IDA, and not indicative of delamination or hydrolysis (Figure 5.6). The ATR-FTIR analysis showed no change in surface chemistry, suggesting the chemical stability of the metal chelating film after prolonged exposure to a range of conditions typical of food, beverage, and packaged consumer product systems. Scanning electron micrographs showed no signs of delamination or flaking, suggesting the physical stability of the metal chelating film.

These coating stability studies suggest that the metal chelating films were stable against delamination or decomposition after prolonged exposure to acidic, alcoholic, fatty, or fatty systems.

Conclusion

In this work, we describe a method to synthesize a GMA-IDA-*co*-BA-*co*-BPM copolymer via emulsion polymerization, which can be applied onto polymer films by a simple coat/cure preparation to produce metal chelating materials with antioxidant character. The IDA chelating moieties were capable of chelating transition metal ions, with chelating capacity tunable by coating thickness. The benzophenone moieties enabled rapid photocuring, resulting in a robust, uniformly applied coating. The integration of poly(*n*-butyl acrylate) permitted a final coating with surface energy values sufficiently low to be considered low fouling and suitable for product release, an important parameter in active packaging applications. Despite the low surface energy and the high hydrophobicity, the high contact angle hysteresis suggested sufficient interaction of IDA ligands, which was supported by the efficacy of the materials in both chelating ferric ions and inhibiting transition metal induced ascorbic acid degradation. The photocured coating on polypropylene was stable both chemically and physically after exposure to fatty, alcoholic, acidic, and aqueous product simulants, supporting its stability in active packaging applications. The photocurable polymer coatings as reported here enables scalable production of active materials with metal chelating functionality. The copolymer coating can potentially be applied onto plastic films and bottles via industrially scalable coat/cure processes for the manufacture of metal chelating active packaging.

Table 5.1. Water contact angle and surface energy measurements.

	Adv. Contact angle (θ)	Rec. Contact Angle (θ)	Hysteresis (θ)	Surface energy (mN/m)
Polypropylene	108.0 ± 1.4	82.9 ± 2.1	25.0 ± 3.2	20.4
Metal chelating film	102.4 ± 0.3	19.1 ± 1.6	83.4 ± 1.7	24.0

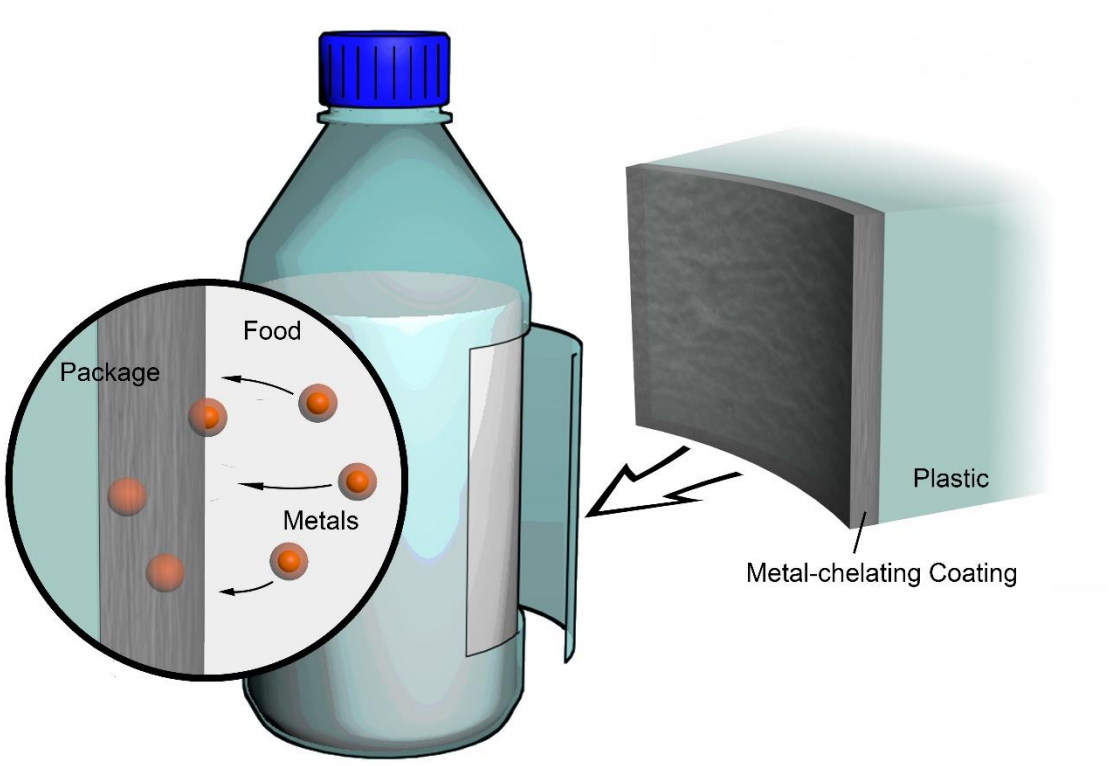

Figure 5.1. Conceptual illustration of metal chelating active packaging materials in food packaging application.

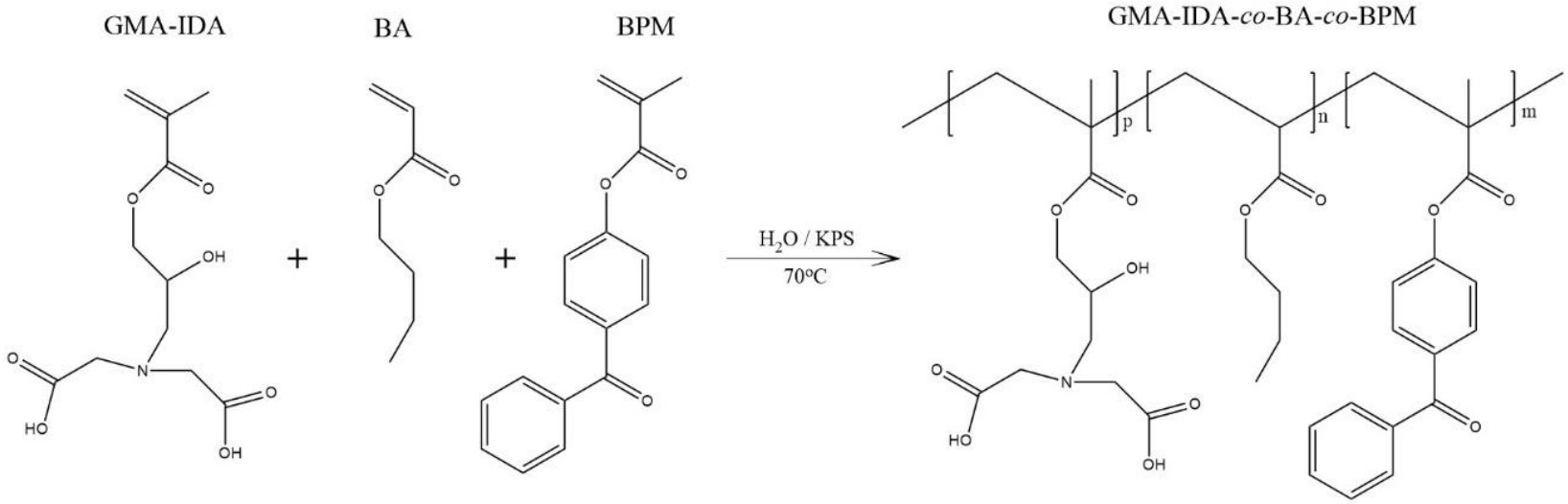

Figure 5.2. Synthesis of poly(2-propenoic acid,2-methyl-,3-[bis-(carboxymethyl) amino]-2-hydroxypropyl ester-*co*-*n*-butyl acrylate-*co*-4-benzoylphenyl methacrylate) (GMA-IDA-*co*-BA-*co*-BPM) by emulsion polymerization of 2-propenoic acid, 2-methyl-,3-[bis-(carboxymethyl) amino]-2-hydroxypropyl ester (GMA-IDA), *n*-butyl acrylate (BA) and 4-benzoylphenyl methacrylate (BPM).

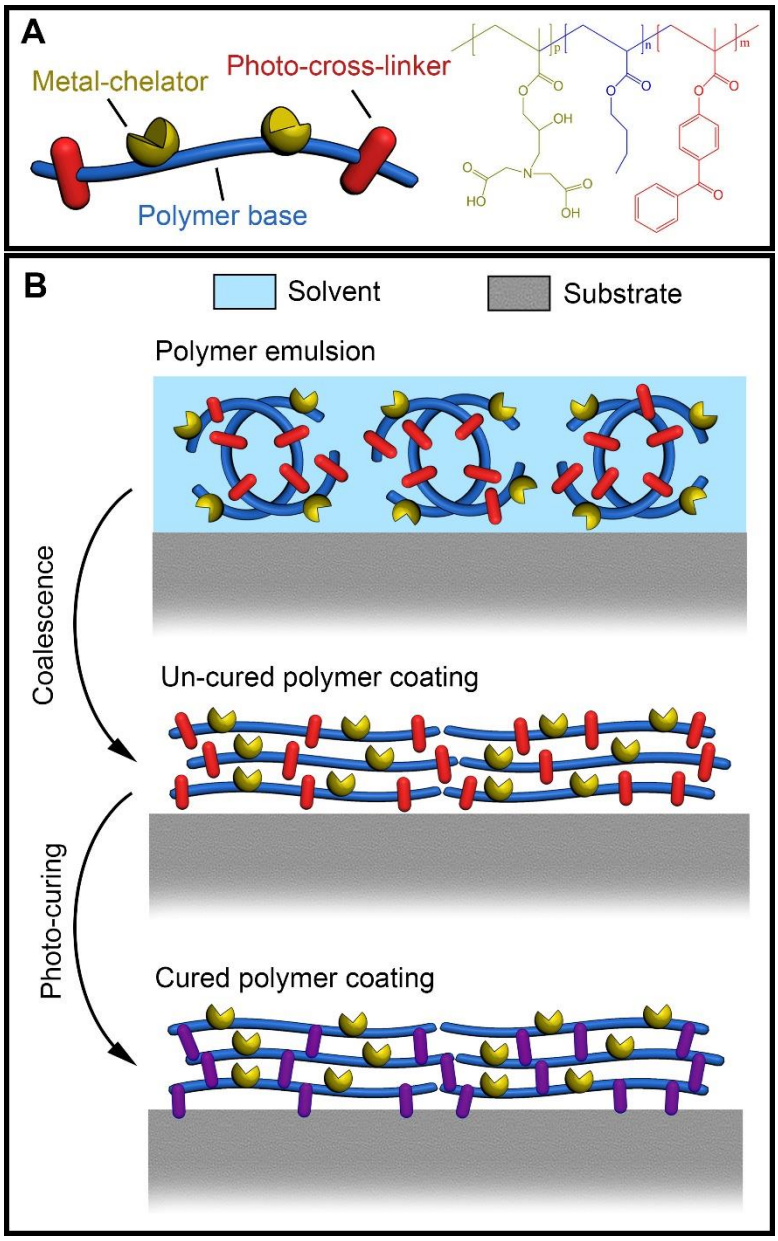

Figure 5.3. Conceptual illustration of the photocurable metal chelating polymer (A) and the process of preparing metal chelating films using the photocurable metal chelating coating (B).

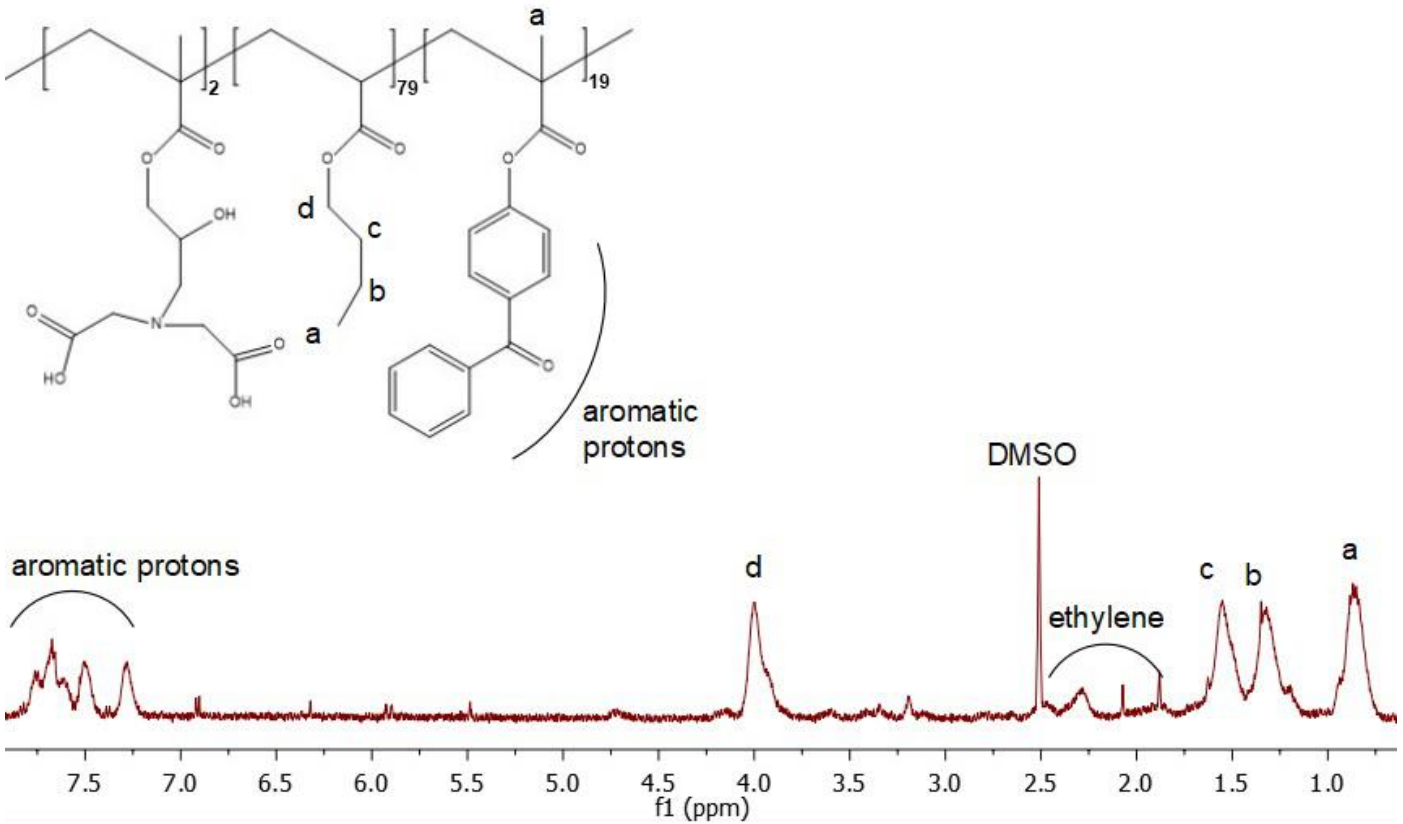

Figure 5.4. Proton NMR spectrum of GMA-IDA-*co*-BA-*co*-BPM polymer collected in DMSO-d_6 (130 ^{o}C, 600 MHZ).

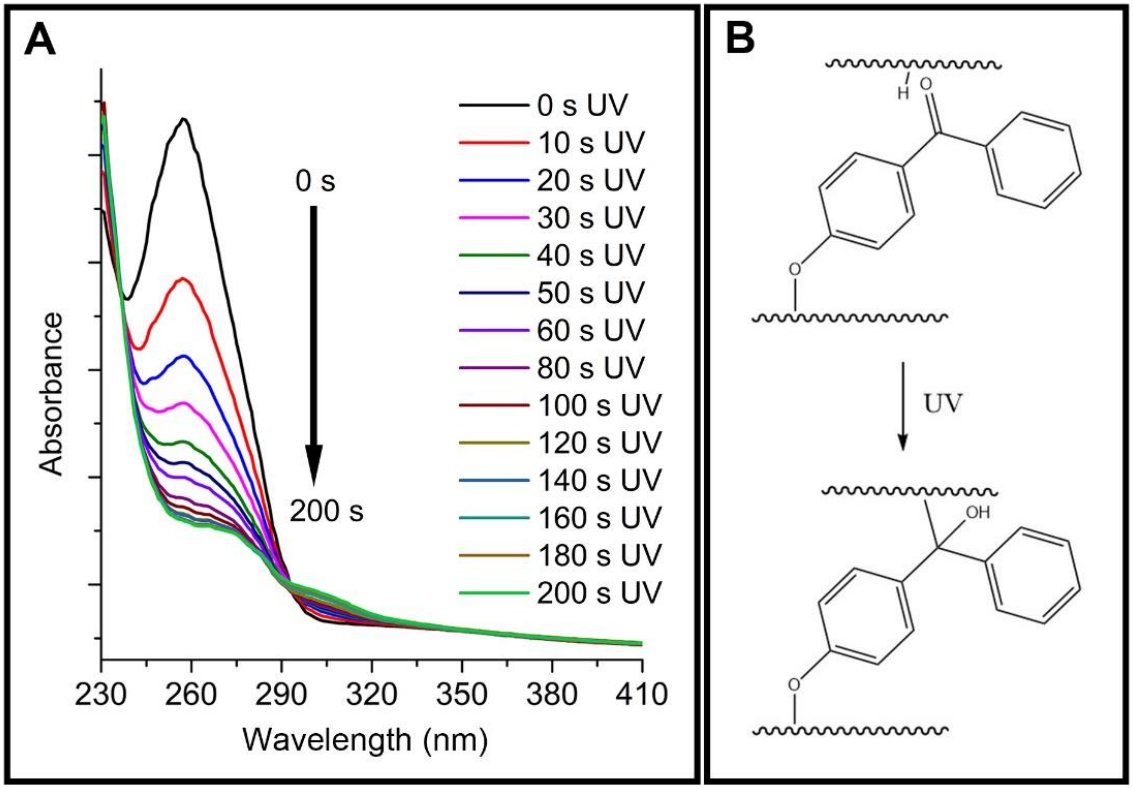

Figure 5.5. Benzophenone absorption spectra during UV-curing (A) and cross-linking reaction of the benzophenone moiety during UV-curing (B).

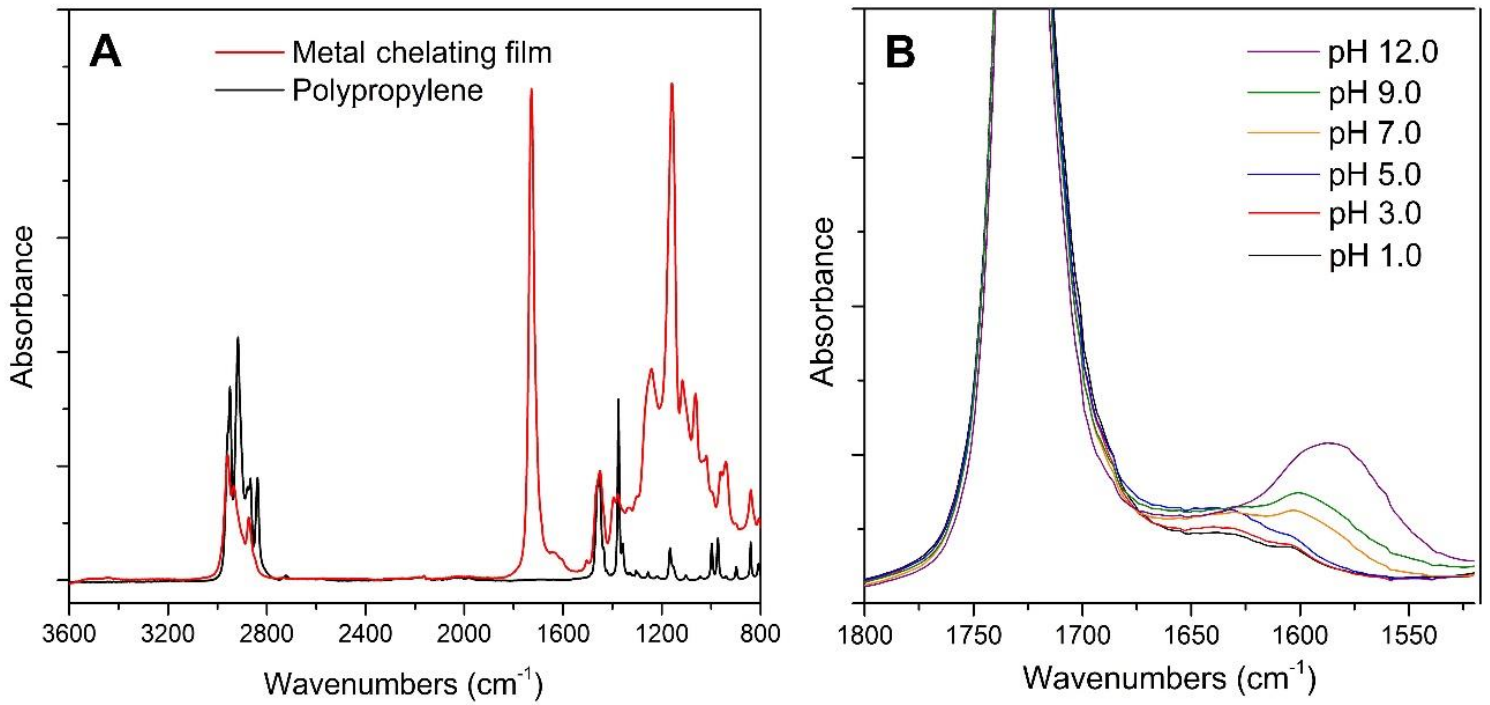

Figure 5.6. ATR-FTIR spectrum of metal chelating film and polypropylene (A) and ATR-FTIR spectrum of the carbonyl stretching vibration region of metal chelating films under different pH conditions (B).

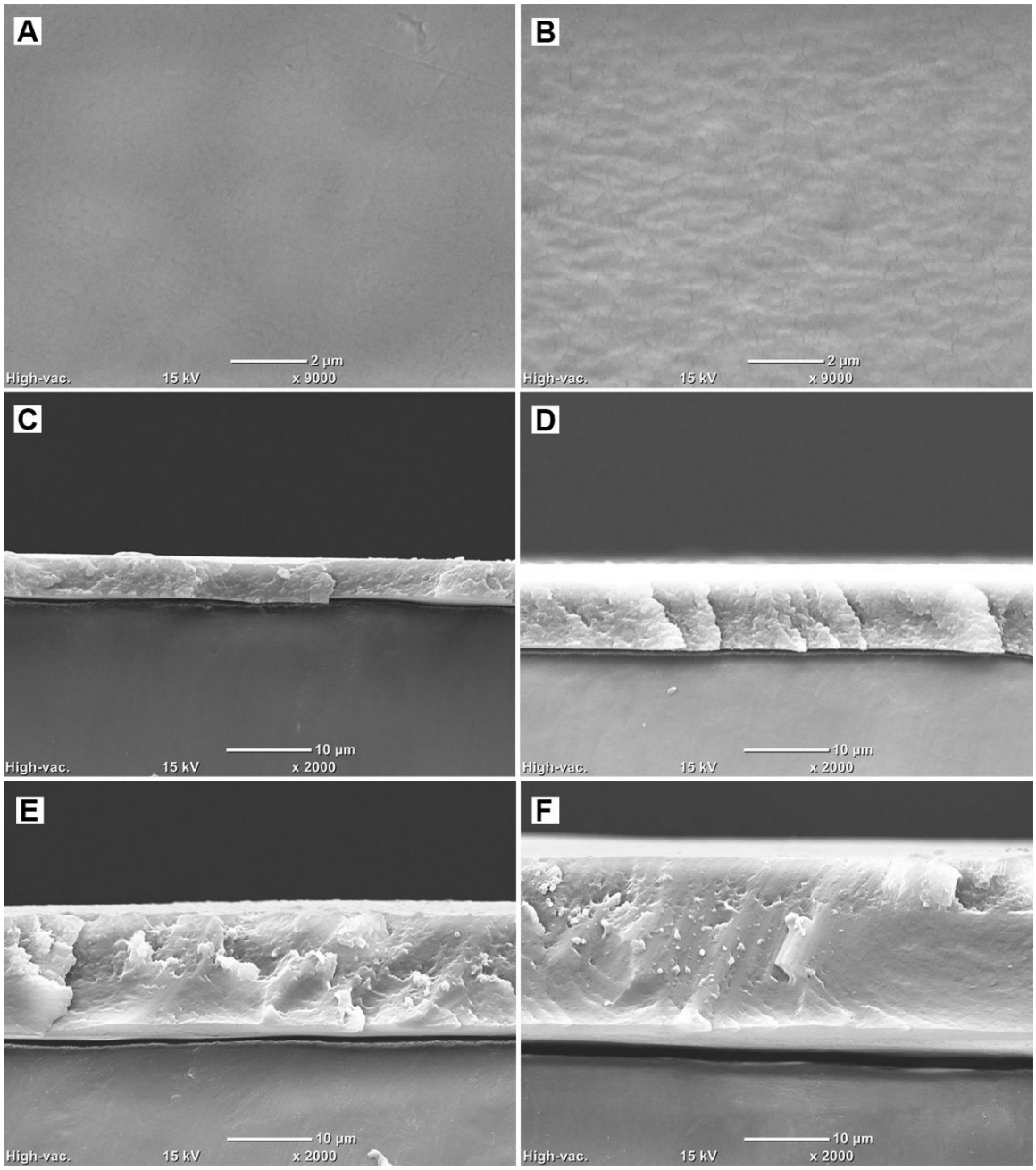

Figure 5.7. Representative surface micrographs of polypropylene (A), and metal chelating film (B); cross-sectional micrographs of metal chelating film prepared using 10 µL/cm^2 (C), 20 µL/cm^2 (D), 40 µL/cm^2 (E), and 80 µL/cm^2 (F) of coating.

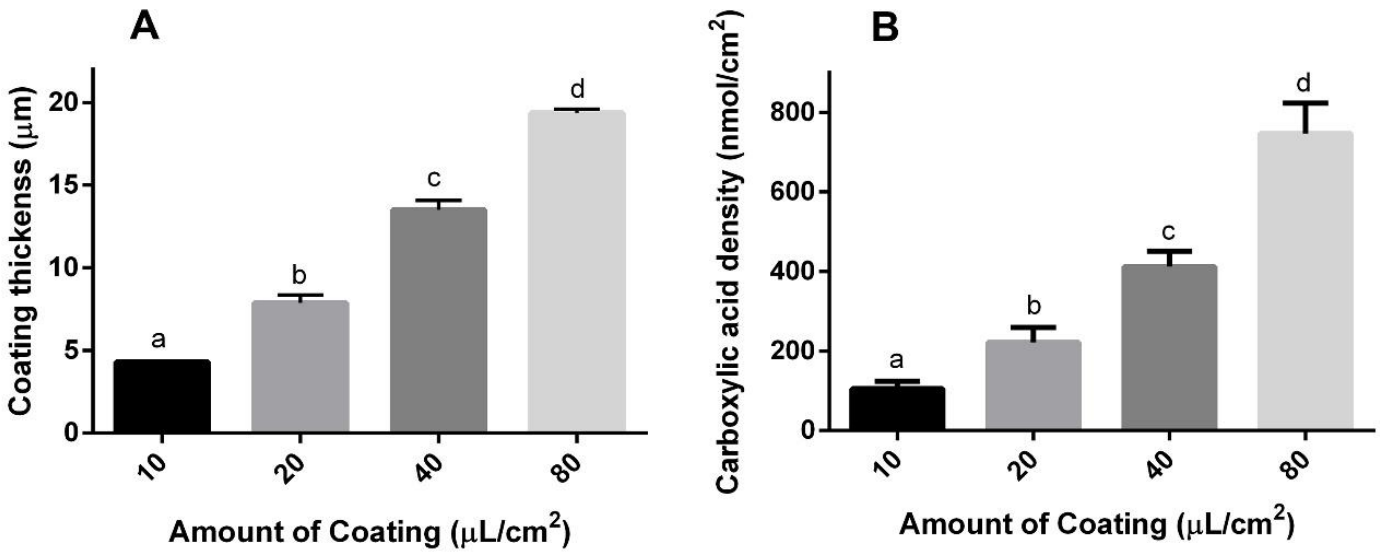

Figure 5.8. Effect of the amount of coating on the coating thickness (A), carboxylic acid density (B). Means are significantly different (Fisher's least significant difference, $P<0.05$) if they share different superscript in the same chart.

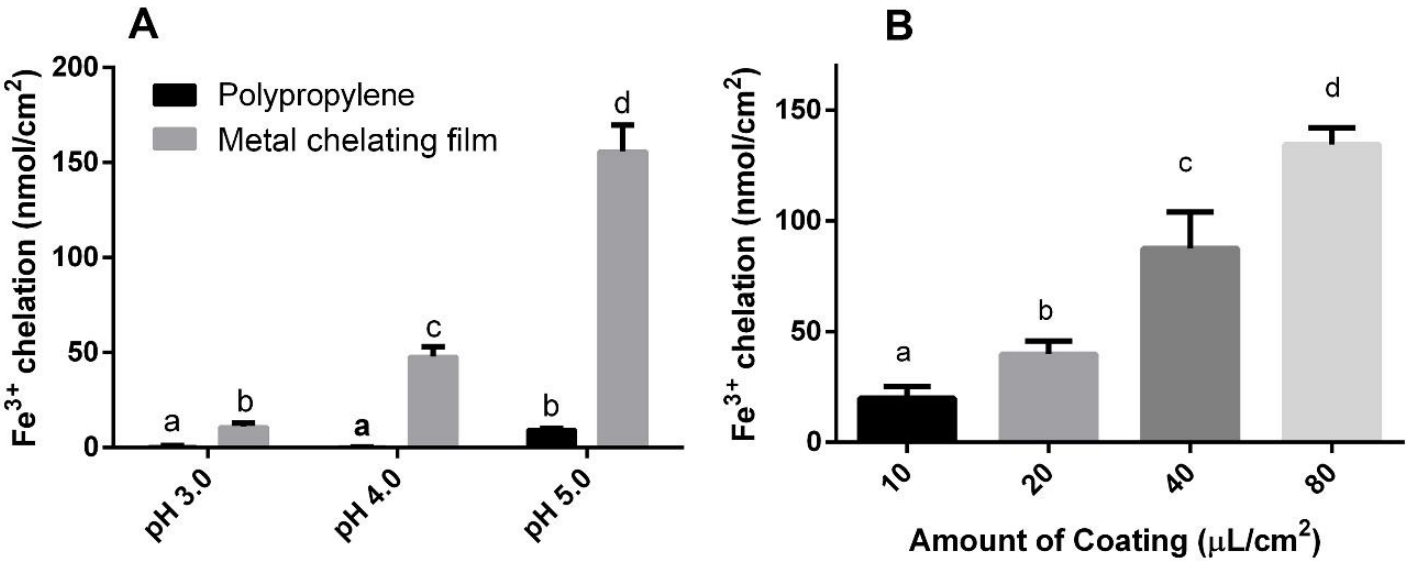

Figure 5.9. Measurement of Fe^{3+} chelating capacity of metal chelating films (prepared using 20 μL/cm^2 of coating) in 0.06 mM ferric chloride solutions (pH 3.0-5.0) after 72 hours of storage (A). Effect of the amount of coating on Fe^{3+} chelation analyzed at pH 4.0 (B). Means are significantly different (Fisher's least significant difference, $P<0.05$) if they share different superscript in the same chart.

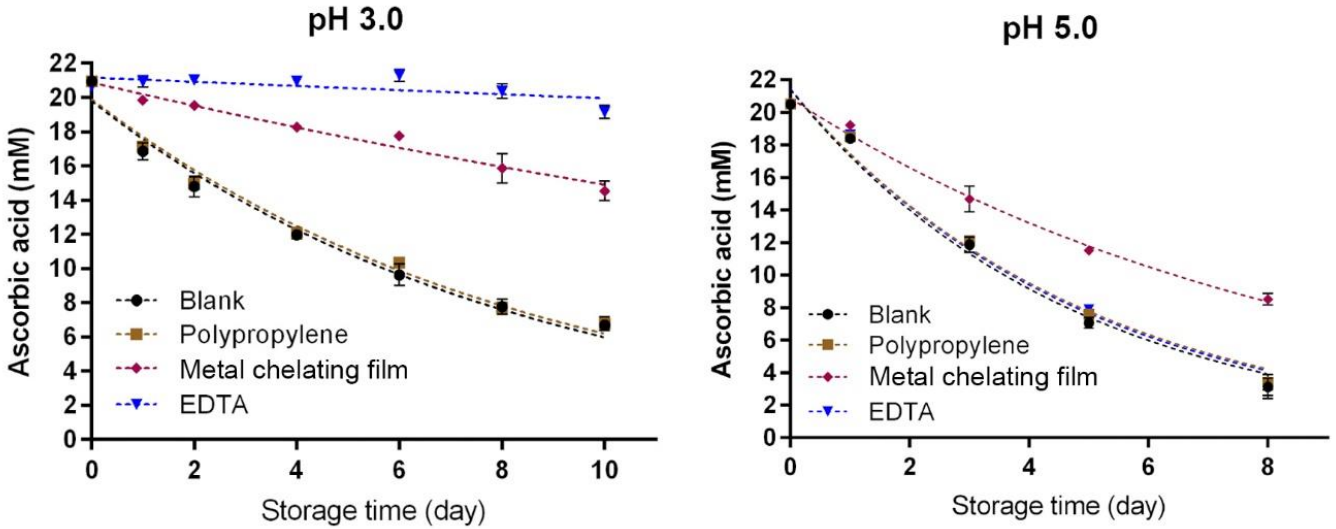

Figure 5.10. Control of ascorbic acid degradation using the metal chelating film (prepared using 20 µL/cm^2 of coating) at pH 3.0 and pH 5.0 (stored at 37^{o}C).

REFERENCES

1. Asioli, D.; Aschemann-Witzel, J.; Caputo, V.; Vecchio, R.; Annunziata, A.; Naes, T.; Varela, P., Making sense of the "clean label" trends: A review of consumer food choice behavior and discussion of industry implications. *Food Res Int* **2017,** *99* (Pt 1), 58-71.

2. Tian, F.; Decker, E. A.; Goddard, J. M., Control of lipid oxidation by nonmigratory active packaging films prepared by photoinitiated graft polymerization. *J. Agric. Food. Chem.* **2012,** *60* (31), 7710-7718.

3. Lin, Z.; Roman, M. J.; Decker, E. A.; Goddard, J. M., Synthesis of Iminodiacetate Functionalized Polypropylene Films and Their Efficacy as Antioxidant Active-Packaging Materials. *J. Agric. Food. Chem.* **2016,** *64* (22), 4606-4617.

4. Lin, Z.; Goddard, J., Photo-Curable Metal-Chelating Coatings Offer a Scalable Approach to Production of Antioxidant Active Packaging. *Journal of food science* **2018,** *83* (2), 367-376.

5. Roman, M. J.; Decker, E. A.; Goddard, J. M., Retaining Oxidative Stability of Emulsified Foods by Novel Nonmigratory Polyphenol Coated Active Packaging. *J Agric Food Chem* **2016,** *64* (27), 5574-82.

6. Johnson, D. R.; Tian, F.; Roman, M. J.; Decker, E. A.; Goddard, J. M., Development of Iron-Chelating Poly(ethylene terephthalate) Packaging for Inhibiting Lipid Oxidation in Oil-in-Water Emulsions. *J. Agric. Food. Chem.* **2015,** *63* (20), 5055-5060.

7. Tian, F.; Decker, E. A.; Goddard, J. M., Controlling lipid oxidation via a biomimetic iron chelating active packaging material. *J. Agric. Food. Chem.* **2013,** *61* (50), 12397-12404.

8. Lin, Z.; Decker, E. A.; Goddard, J. M., Preparation of metal chelating active packaging materials by laminated photografting. *Journal of Coatings Technology and Research* **2016,** *13* (2), 395-404.

9. Anonymous, TITLE 21--FOOD AND DRUGS. In *CITE: 21CFR172.120*, Regulations, C. o. F., Ed. 2017.

10. Li, T.; Chen, S.; Li, H.; Li, Q.; Wu, L., Preparation of an ion-imprinted fiber for the selective removal of Cu2+. *Langmuir* **2011,** *27* (11), 6753-8.

11. Yamada, K.; Nagano, R.; Hirata, M., Adsorption and desorption properties of the chelating membranes prepared from the PE films. *J. Appl. Polym. Sci.* **2006,** *99* (4), 1895-1902.

12. Kavaklı, P. A.; Kavaklı, C.; Güven, O., Preparation and characterization of Fe(III)-loaded iminodiacetic acid modified GMA grafted nonwoven fabric adsorbent for anion adsorption. *Radiation Physics and Chemistry* **2014,** *94*, 105-110.

13. Zhu, J.; Sun, G., Facile fabrication of hydrophilic nanofibrous membranes with an immobilized metal-chelate affinity complex for selective protein separation. *ACS applied materials & interfaces* **2014,** *6* (2), 925-32.

14. Sun, L.; Dai, J.; Baker, G. L.; Bruening, M. L., High-Capacity, Protein-Binding Membranes Based on Polymer Brushes Grown in Porous Substrates. *Chem. Mater.* **2006,** *18* (17), 4033-4039.

15. Mentbayeva, A.; Ospanova, A.; Tashmuhambetova, Z.; Sokolova, V.; Sukhishvili, S., Polymer-metal complexes in polyelectrolyte multilayer films as catalysts for oxidation of toluene. *Langmuir* **2012,** *28* (32), 11948-55.

16. Rahim, M. A.; Islam, M. S.; Bae, T. S.; Choi, W. S.; Noh, Y.-Y.; Lee, H.-J., Metal Ion-Enriched Polyelectrolyte Complexes and Their Utilization in Multilayer Assembly and Catalytic Nanocomposite Films. *Langmuir* **2012,** *28* (22), 8486-8495.

17. Tian, F.; Decker, E. A.; Goddard, J. M., Development of an iron chelating polyethylene film for active packaging applications. *J. Agric. Food. Chem.* **2012,** *60* (8), 2046-2052.

18. Katsumi Mizuguchi, S.; Yoshitaka Okuda, H.; Hiroshi Miwa, I.; Hidefumi Okuda, T. Metal Chelate Compound and Curable Coating Compoistion Therefrom. 4,861,839, 1989.

19. Ligon, S. C.; Husár, B.; Wutzel, H.; Holman, R.; Liska, R., Strategies to Reduce Oxygen Inhibition in Photoinduced Polymerization. *Chem. Rev.* **2013,** *114* (1), 557-589.

20. Dhende, V. P.; Samanta, S.; Jones, D. M.; Hardin, I. R.; Locklin, J., One-step photochemical synthesis of permanent, nonleaching, ultrathin antimicrobial coatings for textiles and plastics. *ACS applied materials & interfaces* **2011,** *3* (8), 2830-7.

21. Hsu, B. B.; Klibanov, A. M., Light-Activated Covalent Coating of Cotton with Bactericidal Hydrophobic Polycations. *Biomacromolecules* **2011,** *12* (1), 6-9.

22. Liu, Q.; Singha, P.; Handa, H.; Locklin, J., Covalent Grafting of Antifouling Phosphorylcholine-Based Copolymers with Antimicrobial Nitric Oxide Releasing Polymers to Enhance Infection-Resistant Properties of Medical Device Coatings. *Langmuir* **2017,** *33* (45), 13105-13113.

23. Baek, N. S.; Kim, Y. H.; Han, Y. H.; Offenhausser, A.; Chung, M. A.; Jung, S. D., Fine neurite patterns from photocrosslinking of cell-repellent benzophenone copolymer. *J Neurosci Methods* **2012,** *210* (2), 161-8.

24. Nanjundan, S.; Unnithan, C. S.; Selvamalar, C. S. J.; Penlidis, A., Homopolymer of 4-benzoylphenyl methacrylate and its copolymers with glycidyl methacrylate: synthesis, characterization, monomer reactivity ratios and application as adhesives. *Reactive and Functional Polymers* **2005,** *62* (1), 11-24.

25. Janko, M.; Jocher, M.; Boehm, A.; Babel, L.; Bump, S.; Biesalski, M.; Meckel, T.; Stark, R. W., Cross-Linking Cellulosic Fibers with Photoreactive Polymers: Visualization with Confocal Raman and Fluorescence Microscopy. *Biomacromolecules* **2015,** *16* (7), 2179-87.

26. Li, K.; Pandiyarajan, C. K.; Prucker, O.; Rühe, J., On the Lubrication Mechanism of Surfaces Covered with Surface-Attached Hydrogels. *Macromolecular Chemistry and Physics* **2016,** *217* (4), 526-536.

27. Lehaf, A. M.; Moussallem, M. D.; Schlenoff, J. B., Correlating the compliance and permeability of photo-cross-linked polyelectrolyte multilayers. *Langmuir* **2011,** *27* (8), 4756-63.

28. Schlemmer, C.; Betz, W.; Berchtold, B.; Ruhe, J.; Santer, S., The design of thin polymer membranes filled with magnetic particles on a microstructured silicon surface. *Nanotechnology* **2009,** *20* (25), 255301.

29. Toomey, R.; Freidank, D.; Rühe, J., Swelling Behavior of Thin, Surface-Attached Polymer Networks. *Macromolecules* **2004,** *37* (3), 882-887.

30. Anderson, W.; Castle, L., Benzophenone in cartonboard packaging materials and the factors that influence its migration into food. *Food Additives & Contaminants* **2003,** *20* (6), 607-618.

31. Dorman, G.; Prestwich, G. D., Benzophenone Photophores in Biochemistry. *Biochemistry* **1994,** *33* (19), 5661-5673.

32. Dinu, M. V.; Dragan, E. S., Heavy metals adsorption on some iminodiacetate chelating resins as a function of the adsorption parameters. *Reactive and Functional Polymers* **2008,** *68* (9), 1346-1354.

33. Martell, A. E.; Robert, M. S., *Critical stability constants*. Plenum Press: New York, 1974.

34. Bate, T. J., Non-stick coating and method of forming same. Google Patents: 2005.

35. Ye, W.; Leung, M. F.; Xin, J.; Kwong, T. L.; Lee, D. K. L.; Li, P., Novel core-shell particles with poly(n-butyl acrylate) cores and chitosan shells as an antibacterial coating for textiles. *Polymer* **2005,** *46* (23), 10538-10543.

36. Suma, K. K.; Jacob, S.; Joseph, R., Studies on the effect of nano-TiO2 on vinyl acetate–butyl acrylate latex-based surface coating. *Materials Science and Engineering: B* **2010,** *168* (1–3), 254-258.

37. Gustavsson, J. M.; Innis, P. C.; He, J.; Wallace, G. G.; Tallman, D. E., Processable polyaniline-HCSA/poly(vinyl acetate-co-butyl acrylate) corrosion protection coatings for aluminium alloy 2024-T3: A SVET and Raman study. *Electrochimica Acta* **2009,** *54* (5), 1483-1490.

38. Steward, P. A.; Hearn, J.; Wilkinson, M. C., An overview of polymer latex film formation and properties. *Advances in Colloid and Interface Science* **2000,** *86* (3), 195-267.

39. Chen, C.-Y.; Chen, C.-Y., Formation of silver nanoparticles on a chelating copolymer film containing iminodiacetic acid. *Thin Solid Films* **2005,** *484* (1-2), 68-72.

40. Wang, C.-C.; Cheng, M.-H.; Chen, C.-Y.; Chen, C.-Y., Facilitated transport of molecular oxygen in cobalt-chelated copolymer membranes prepared by soap-free emulsion polymerization. *Journal of Membrane Science* **2002,** *208* (1–2), 133-145.

41. Chu, Y.-C.; Wang, C.-C.; Chen, C.-Y., A new approach to hybrid CdS nanoparticles in poly(BA-co-GMA-co-GMA-IDA) copolymer membranes. *Journal of Membrane Science* **2005,** *247* (1-2), 201-209.

42. Chen, C.-Y.; Chen, C.-Y., Stability constants of polymer-bound iminodiacetate-type chelating agents with some transition-metal ions. *J. Appl. Polym. Sci.* **2002,** *86* (8), 1986-1994.

43. Korhonen, J. T.; Huhtamaki, T.; Ikkala, O.; Ras, R. H., Reliable measurement of the receding contact angle. *Langmuir* **2013,** *29* (12), 3858-63.

44. Kabza, K. G.; Gestwicki, J. E.; McGrath, J. L., Contact Angle Goniometry as a Tool for Surface Tension Measurements of Solids, Using Zisman Plot Method. A Physical Chemistry Experiment. *Journal of Chemical Education* **2000,** *77* (1), 63.

45. Uchida, E.; Uyama, Y.; Ikada, Y., Sorption of low-molecular-weight anions into thin polycation layers grafted onto a film. *Langmuir* **1993,** *9* (4), 1121-1124.

46. Dawson, M. V.; Lyle, S. J., Spectrophotometric determination of iron and cobalt with Ferrozine and dithizone. *Talanta* **1990,** *37* (12), 1189-1191.

47. Horwitz, W.; Association of Official Analytical, C., Official methods of analysis of the Association of Official Analytical Chemists. *Official methods of analysis of the Association of Official Analytical Chemists.* **1970**.

48. Guidance for Industry: Preparation of Premarket Submissions for Food Contact Substances: Chemistry Recommendations. http://www.fda.gov/Food/GuidanceRegulation/GuidanceDocumentsRegulatoryInformation/ucm081818.htm#i (accessed last visited 11/17/2015).

49. Bastarrachea, L. J.; Goddard, J. M., Antimicrobial Coatings with Dual Cationic and N-Halamine Character: Characterization and Biocidal Efficacy. *J. Agric. Food. Chem.* **2015,** *63* (16), 4243-4251.

50. Letey, J., Measurement of contact angle, water drop penetration time, and critical surface tension. **1969**.

51. Gao, L.; McCarthy, T. J., Wetting 101°†. *Langmuir* **2009,** *25* (24), 14105-14115.

52. Kota, A. K.; Kwon, G.; Tuteja, A., The design and applications of superomniphobic surfaces. *NPG Asia Materials* **2014,** *6* (7), e109.

53. Alamed, J.; McClements, D. J.; Decker, E. A., Influence of heat processing and calcium ions on the ability of EDTA to inhibit lipid oxidation in oil-in-water emulsions containing omega-3 fatty acids. *Food Chem.* **2006,** *95* (4), 585-590.

54. Ling, C.; Liu, F. Q.; Xu, C.; Chen, T. P.; Li, A. M., An integrative technique based on synergistic coremoval and sequential recovery of copper and tetracycline with dual-functional chelating resin: roles of amine and carboxyl groups. *ACS applied materials & interfaces* **2013,** *5* (22), 11808-17.

55. Bradshaw, M. P.; Barril, C.; Clark, A. C.; Prenzler, P. D.; Scollary, G. R., Ascorbic Acid: A Review of its Chemistry and Reactivity in Relation to a Wine Environment. *Critical Reviews in Food Science and Nutrition* **2011,** *51* (6), 479-498.

56. Burdurlu, H. S.; Koca, N.; Karadeniz, F., Degradation of vitamin C in citrus juice concentrates during storage. *Journal of Food Engineering* **2006,** *74* (2), 211-216.

CHAPTER 6

OVERALL CONCLUSIONS & OPPORTUNITIES FOR NEXT STEPS

Metal chelating materials have been used in many applications such as heavy metal removals, protein purification, chromatography and biosensors. The potential use of metal chelating materials as active packaging materials has not been demonstrated until 2012, by the Goddard Research Group. When I joined the group in the summer of 2014 to work on the metal chelating active packaging project, my group members, Fang Tian, Maxine Roman, David Johnson, and Yoshiko Ogiwara had done a lot of proof of concept research synthesizing metal chelating films and testing the chelating and antioxidant performances in simulated food systems. The antioxidant efficacy of metal chelating materials was initially demonstrated in emulsified oil systems using carboxylic acid functionalized polypropylene films (PP-*g*-PAA). Because carboxylic acid ligands had low specificity to transition metals, the resulting material had limited chelating and antioxidant efficacy in complex matrices (e.g. environment with competing ions). The team had then developed a hydroxamic acid functionalized material (PP-*g*-PHA). The hydroxamic acid ligand is known to have high specificity to iron comparing to carboxylic acid ligand, and, as a result, PP-*g*-PHA films had improved chelating and antioxidant performance in high acid conditions. However, the synthesis of PP-*g*-PHA material was quite complicated. Briefly, to synthesize PP-*g*-PHA, the research team had to first initiate native polypropylene coupons using benzophenone in a degassed environment using UV-light. The benzophenone functionalized coupons were placed in methyl acrylate solutions, degassed, and then exposed to UV-light to

graft poly(methyl acrylate) from the coupons. The poly(methyl acrylate) functionalized coupons were washed overnight in a Soxhlet apparatus using acetone. The following day, the washed coupons were reacted in a hydroxylamine solution for 4 hours to convert the methyl ester to hydroxamic acid. The whole process took around 2 days, and was simply too complicated for scaling up. Therefore, my mission as a Ph.D. student was to develop new synthesis techniques that would improve the scalability of the materials.

It is not easy to synthesize metal chelating materials. In fact, the majority of metal chelating ligands are hydrophilic, and it seems that the more specific the ligands are to transition metals, the more hydrophilic they are. Tethering a hydrophilic ligand onto an inert solid support material with retained performance and the requirement that they not to come off in aqueous environments are not trivial. Many people had also reported synthesis of metal chelating materials in literature articles and industry patents. However, they were mostly intended for chelating resins, membranes, and sensors, where scalability was not a priority.

There were two major hurdles in the preparation process of PP-*g*-PAA and PP-*g*-PHA materials. The first one was the degassing prior to the UV-exposure, and the second one was the solution reaction during the post-graft modification. Indeed, photo-assisted graft polymerization of vinyl monomers is prone to oxygen inhibition, and many graft-from reactions in literature had been conducted in degassed environments. However, in literature, there were several groups of researchers who skipped the degassing process, and, instead, conducted the reaction by sandwiching the vinyl

monomers within two films. Therefore, I adopted the laminated photografting technique to replace the degassing process (Chapter 2). The laminated photografting technique enabled potential roll-to-roll preparation of photo-functionalized materials and was a huge improvement comparing to previous process.

Meanwhile, I also explored iminodiacetic acid (IDA) as an metal chelating ligand for active packaging applications. Comparing to other metal chelating ligands (i.e. carboxylic acid, hydroxamic acid, catechol) that our team had investigated, IDA has several advantages of 1) high specificity to metals, 2) high commercial availability, 3) high stability and robustness, 4) ease of chemical modification. To prove the efficacy of IDA functionalized materials for active food packaging application, I made reactive chloride functionalized propylene films using laminated photografting and tethered IDA ligand onto the surface using a 10-hour chemical reaction (Chapter 3). The resulting IDA functionalized materials were as effective as EDTA at controlling lipid oxidation in emulsified oil systems at pH 3.0. The IDA functionalized material was also capable of controlling transition metal induced ascorbic acid degradation. Performance wise, the IDA functionalized materials had better antioxidant efficacy than materials functionalized with either carboxylic acid, hydroxamic acid or catechol. For example, carboxylic acid functionalized materials did not control lipid oxidation at pH 3.0, hydroxamic acid functionalized material did not control lipid oxidation as well as EDTA and it did not control ascorbic acid degradation, and catechol functionalized material had stability issues at pH 3.0.

Despite the promise of laminated photografting technique and the IDA

functionalized materials, the several-hour-long solution reaction still presented a major hurdle. In a lot of literature articles and industry patents, whether it was for metal chelating resins or membranes, solution reactions were often needed to tether the metal chelating ligands. To remove the solution modification process, the metal chelating ligands should be pre-attached to some anchoring system and then apply the anchoring system to the solid support using a speed chemistry. With this idea in mind, I synthesized IDA functionalized vinyl monomer (GMA-IDA) and attached the GMA-IDA monomer onto support materials using laminated photografting (Chapter 4). The use of GMA-IDA and laminated photografting enabled potential scalable production of metal chelating materials without degassing or batch reaction in solution. However, the material was hydrophilic and swellable, which may not be ideal for food packaging application. Although the surface grafts were chemically bound to the surface, there remained the potential to migrate into the food system. A nice analogy is that of human hair: despite our many hairs grown on our heads, we still manage to lose around 100 strands of them per day. In addition, migration of monomeric GMA-IDA may also present a safety concern. Migration of monomeric compounds from polymeric matrices have been notorious issues in food packaging industries. To name a few, migration of bisphenol A from polycarbonate coating on metal cans, migration of vinyl chloride from PVC containers, and migration of styrene from Styrofoam cups.

An alternative plan was to tether the metal chelating ligand onto polymeric anchoring system instead of monomeric anchoring system, and to develop a metal chelating polymer. There are three possible ways to incorporate the metal chelating

polymer onto solid support materials, 1) cast the polymer onto the substrate as a coating, 2) co-extrude the polymer with the substrate, 3) use the polymer as is and forget about the substrate. Taking into considerations the resources our laboratory had access to at the time of 2016, the first option was the most direct approach.

Metal chelating polymers were not hard to find in literature. In the biomedical field, people had synthesized metal chelating polymers for heavy metal chelation therapy. In the biology field, people had extracted metal chelating polymers secreted by natural organisms that they used to combat iron deficient conditions. In fact, metal chelating polymers, such as polyethyleneimine, are directly available from commercial suppliers. However, the most of the metal chelating polymers are soluble in water, and they have to be somehow immobilized onto the substrates. Therefore, crosslinkers have to be incorporated into these polymers to enable surface attachment.

Photocuring is widely used in printing and coating industry as a speed curing process, and benzophenone has often been used as a photocrosslinker in many photocurable polymeric coating formulations. Benzophenone also has several advantage of being used in our food active packaging application. First of all, benzophenone is inexpensive and has already been widely used many ink formulations in food package labels. Secondly, benzophenone is chemically robust and does not degrade easily by heat. Thirdly, benzophenone crosslinks with substrates rich in alkyl groups (e.g. common plastic materials for food packaging). Fourthly, the photocrosslinking reaction take place in atmospheric environment and the reaction is irreversible. Therefore, I decided to develop a photocurable metal chelating polymer

with IDA as metal chelator and benzophenone as photocrosslinker. I managed to synthesize a poly(*n*-butyl acrylate) copolymer with IDA and benzophenone moieties (Chapter 5). The copolymer was synthesized by emulsion copolymerization of *n*-butyl acrylate, GMA-IDA (the IDA functionalized vinyl monomer I used in Chapter 4), and 4-benzoyphenyl methacrylate (BPM, a benzophenone functionalized vinyl monomer). With emulsion polymerization, the reaction took place in water and the resulting polymer was insoluble in water but formed stable micelles. The polymer latex can be casted onto plastic substrates as a coating and photocured to immobilize the coating to the surface. The photocurable metal chelating copolymer technology enables scalable coat/cure preparation of metal chelating materials without the need of inert gas environment or batch solution reaction.

The photocurable metal chelating polymer coating technology was not only novel at the time, but was also non-obvious from perspectives of both chemical design and synthesis process. From the perspective of chemical design, all the building blocks used in the polymer design are inexpensive, necessary and effective. The advantages of IDA and benzophenone moieties has been justified above. Poly(*n*-butyl acrylate) served as a polymer based in the polymer design and is important to control the thermal mechanical properties of the coating. In addition, poly(*n*-butyl acrylate) based copolymers are FDA approved for coating application at food contact surfaces. It would be very difficult to come up with a polymer chemistry for our coating application that is better than the current design, in terms of economy, efficacy, and stability. From the perspective of synthesis process, emulsion polymerization is a water based

polymerization technique that gives low emission of volatile organic compounds (VOC) and is very favorable in industrial settings. In addition, emulsion polymerization may present the only synthesis technique to produce the polymer chemistry. Notable trials and fails during the development process are mentioned in Appendix. Additional optimizations (e.g. distillation and precipitation) may be needed to efficiently remove unreacted monomers and homopolymers after polymerization. Pre-homogenization of the monomers may be used to give better between-batch consistencies.

Moving forward, the safety of the photocurable metal chelating polymer coating and the antioxidant efficacy in real food systems still needs investigation. Migration of monomeric compounds in the coating formulation has to be determined before receiving premarket approval as a food contact substance. Migration of monomeric compounds can potentially be eliminated by 1) effectively removing unreacted monomers upon completion of polymerization and 2) photocuring to polymerize the vinyl monomers within the polymer matrix. In real food systems, the presence of competing ions and macromolecules such as proteins may present challenge for the coating to retain chelating and antioxidant efficacy.

Despite the reported progress in overcoming fundamental challenges in scalability, and the unknowns in material safety and performance in real food systems, the major challenge lies in the market value of the metal chelating active packaging technology. The metal chelating active packaging technology control transition metal induced oxidative degradations of labile components in consumer products and serves as an alternative to current technologies such as soluble metal chelator (e.g. EDTA) and

refrigeration. It is important and challenging to justify that such active packaging technology is advantageous over current technologies. Indeed, the metal chelating active packaging technology potentially provides a clean label approach to shelf-stable consumer products that are susceptible to transition metal induced oxidative degradations. However, the value of being clean label, shelf-stable and oxidative stable versus the cost of packaging material and the environmental impact has to be justified as well. Other than active packaging approach, it may be more cost effective and environmentally friendly to consider developing recyclable metal chelating resins as food processing aids.

APPENDIX A

Notable trials and fails during the development of the photocurable metal chelating copolymer in Chapter 5 are described in this Appendix.

The initial idea was to prepare a metal-chelating polymer based on polyethylene amine (PEI) (Figure A1.1). The amine groups on PEI ware converted to IDA groups by reacting PEI with bromoacetic acids. The resulting modified PEI showed metal-chelating activity, as was confirmed by adding the polymer into Fe^{3+} solutions followed by analyzing the remaining Fe^{3+} content after removal of polymer by centrifugal membranes. However, upon application of the polymer onto polypropylene surface as a coating, the coating was swellable and was soluble in aqueous solutions.

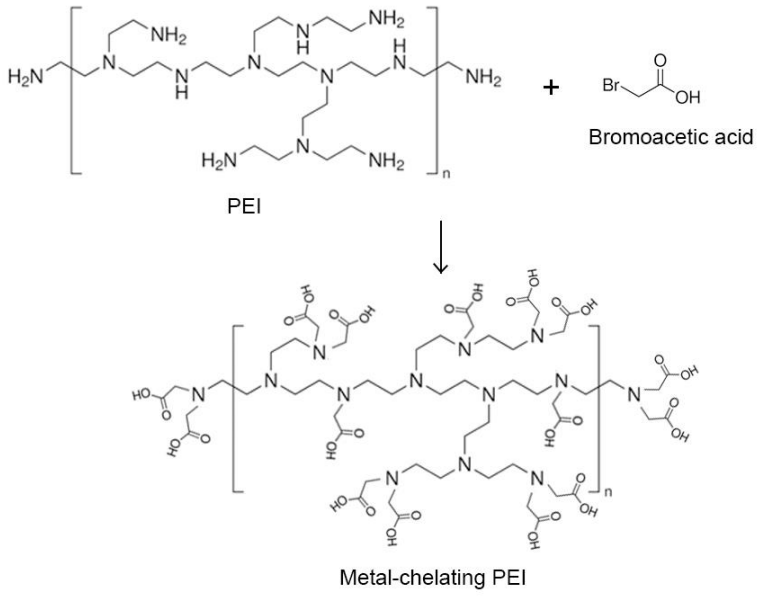

Figure A1.1. Synthesis of metal-chelating PEI polymer.

The next attempt was to control the solubility of the metal chelating polymer

and to prepare polymers that were insoluble in water. A poly(n-butyl acrylate) based copolymer with IDA functionality was synthesized by emulsion polymerization of *n*-butyl acrylate and GMA-IDA in water (Figure A1.2). The resulting polymer was insoluble in water but formed a stable colloid dispersion. Upon casting the polymer latex onto polypropylene surface, the polymer formed a clear coating after drying. However, upon contacting water, the polymer delaminated and reverted to its latex form. The instability of the polymer coating in aqueous environment was potentially caused by the hydrophilic IDA groups. It became apparent that crosslinking moieties had to be incorporated into the polymer, in order to immobilize the polymer coating to a substrate.

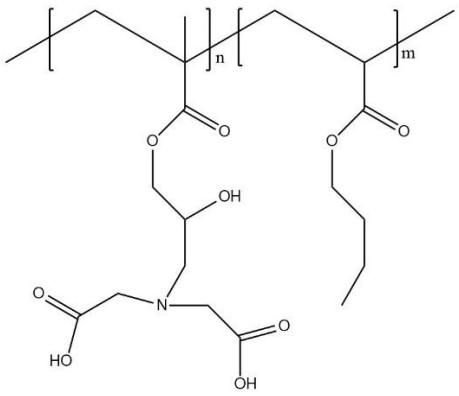

Figure A1.2. Structure of GMA-IDA-co-BA polymer.

An epoxy group was incorporated into the copolymer to give a poly(*n*-butyl acrylate) based copolymer with GMA-IDA and glycidyl methacrylate moieties (Figure A1.3). The polymer was again synthesized by emulsion copolymerization. The polymer latex was coated on polypropylene-graft-maleic anhydride (PP-*g*-MAA) surface and cured the coating by heat to allow cross-linking reaction between epoxy and maleic

anhydride groups. However, the cured coating was still unstable in aqueous environment like the one in Figure A1.2. Although some polymers might have been fixed to the PP-g-MAA surface, the polymers that were not in direct contact with PP-g-MAA surface might have not. The epoxy groups were able to have across-linking reactions with primary and secondary amines, which were not present in the polymer. It became apparent that the crosslinker has to not only crosslink with the substrate, but also crosslink with the polymer to improve the coating stability.

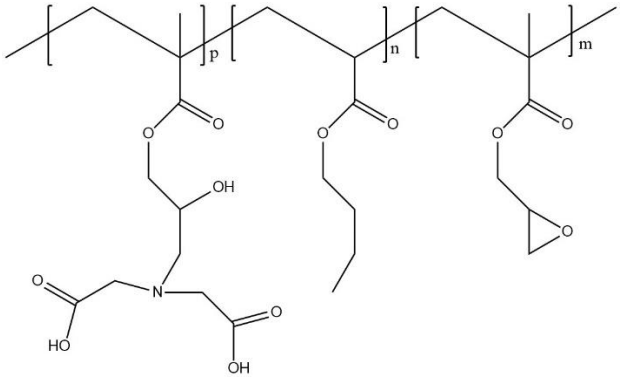

Figure A1.3. Structure of GMA-IDA-co-BA-co-GMA polymer.

The epoxy group was replaced by a photocrosslinker, 4-benzoyl-3-hydroxyphenyl methacrylate (BHMA). BHMA was purchased from a commercial supplier, and it contains a benzophenone derivative as a photocrosslinker. Benzophenone is known to photocrosslink with alkyl groups rich in both the polymer and polypropylene substrate. The GMA-IDA-co-BA-co-BHMA copolymer was synthesized by emulsion copolymerization (Figure A1.4). The polymer latex was casted onto polypropylene surface and formed a clear coating upon solvent evaporation. The

coating was exposed to UV-light to photocure the coating. However, the photocured coating was unstable in water and could be washed away by water. The instability was hypothesized to be the inefficiency of the photocrosslinker. However, it may also be that the polymer contained too much GMA-IDA or too little BHMA.

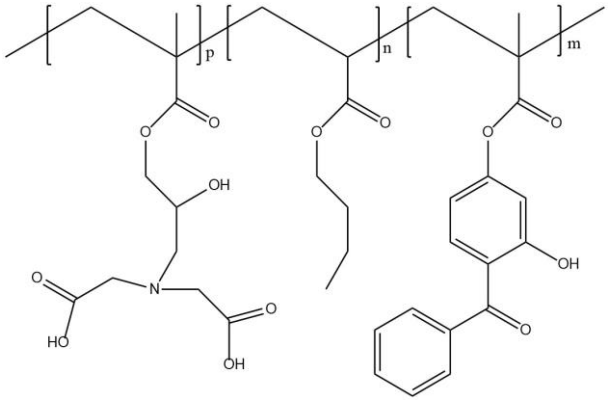

Figure A1.4. Structure of GMA-IDA-*co*-BA-*co*-BHMA.

The BHMA monomer was then replaced by a 4-benzoylphenyl methacrylate (BPM), which was synthesized in our laboratory. The GMA-co-BA-co-BPM copolymer was again synthesized by emulsion copolymerization (Figure A1.5). The photocured polymer coated formed on polypropylene surface was stable in water and could not be washed away by water. I have also attempted adjusting the content of the GMA-IDA and BPM in the formulation. However, too much GMA-IDA or too little BPM both led to the instability of the photocured coating.

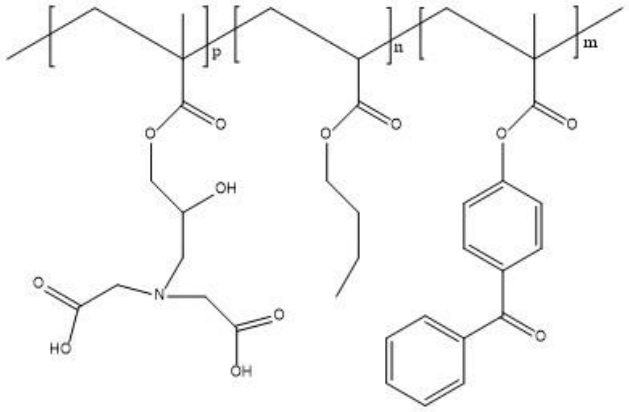

Figure A1.5. Structure of GMA-IDA-co-BA-co-BPM.

In addition, the poly(n-butyl acrylate) polymer base was replaced by polystyrene. The GMA-IDA-*co*-St-*co*-BPM was synthesized by emulsion copolymerization (Figure A1.6). The polymer latex was casted onto polypropylene surface, however, upon drying, the coating became some white powdery aggregates. Polystyrene has high glass transition temperature and may not be suitable for coating application.

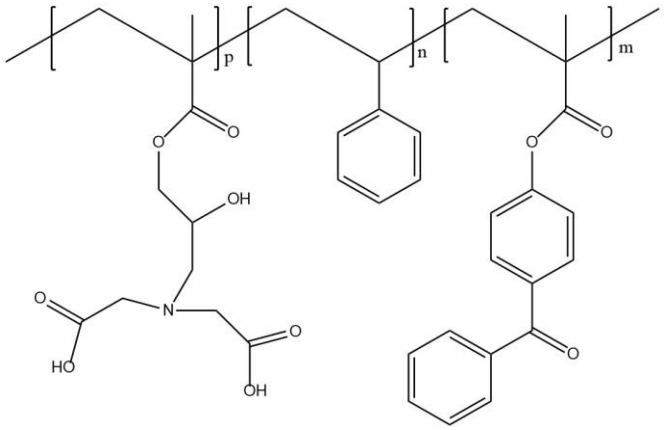

Figure A1.6. Structure of GMA-IDA-*co*-St-*co*-BPM.

Alternative synthesis routes were attempted to synthesize the photocurable metal chelating polymer, GMA-IDA-*co*-BA-*co*-BPM illustrated in Figure A1.5. An epoxy functionalized precursor polymer, GMA-*co*-BA-*co*-BPM, was synthesized by single electron transfer – living radical polymerization (SET-LRP) in DMSO. The precursor polymer was then reacted with IDA to tether the metal chelating ligand (Figure A1.7). However, the proposed reaction was unsuccessful because a solvent system that would dissolve both the precursor polymer and the IDA could not be found. Reaction was attempted in DMSO, DMSO/water, DMF/water, however, reaction was unsuccessful in these solvents.

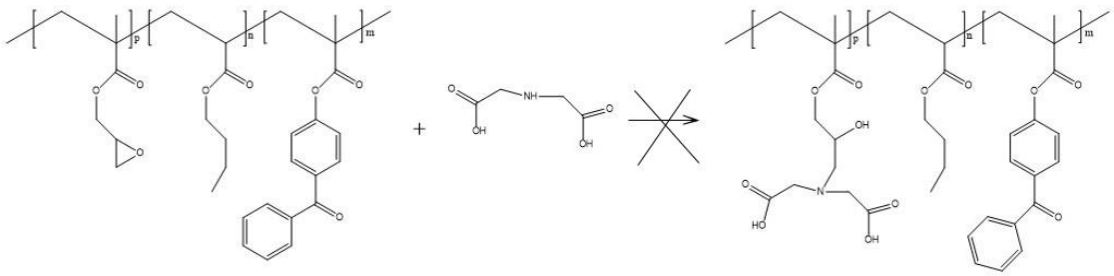

Figure A1.7. Proposed reaction to tether IDA onto GMA-*co*-BA-*co*-BPM that failed.

Ethylenediamine (EDA) is soluble in water and many organic solvent including DMSO and DMF. EDA and precursor polymer were dissolved in DMF and reacted at 30^{o}C or 70^{o}C for 24 hours to allow ring opening reaction (Figure A1.8). However, the resulting polymer lost benzophenone moieties as suggested by proton NMR spectroscopy. It was hypothesized that EDA might have cleaved the ester bond on the BPM moieties.

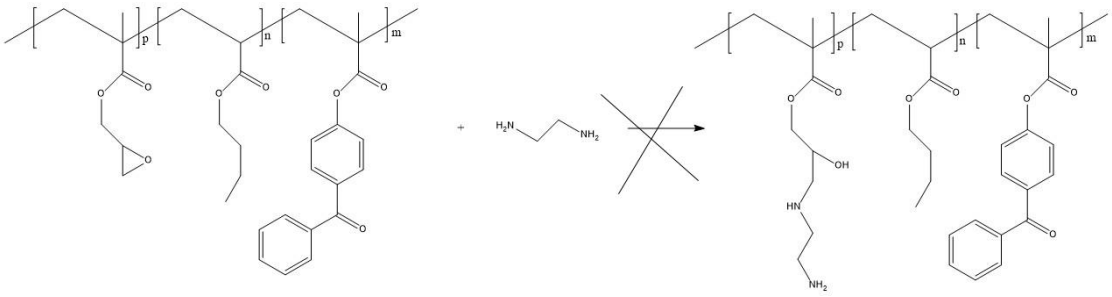

Figure A1.8. Proposed reaction to tether EDA onto GMA-*co*-BA-*co*-BPM that failed.

APPENDIX B

FACILE PREPARATION OF EPOXIDE FUNCTIONALIZED SURFACES VIA PHOTOCURABLE COPOLYMER COATINGS AND SUBSEQUENT IMMOBILIZATION OF IMINODIACETIC ACIDS*

Abstract

Herein, we report a simple coat/cure preparation of epoxide functionalized surfaces using a photocurable copolymer technology. The photocurable copolymer, poly(glycidyl methacrylate-*co*-butyl acrylate-*co*-4-benzoyphenyl methacrylate) (GBB) was synthesized by single electron transfer-living radical polymerization (SET-LRP). Three copolymers, GBB(1), GBB(2) and GBB(3) with epoxide contents of 22 mol %, 63 mol %, and 91 mol %, respectively, were cast onto polypropylene films and photocured by UV-light exposure. Subsequently, iminodiacetic acids (IDA) were immobilized onto the GBB coated materials via a ring opening reaction. The IDA functionalized coatings, GBB(1)-IDA, GBB(2)-IDA, GBB(3)-IDA presented IDA contents of 1.47 ± 0.08 nmol/cm^2, 18.67 ± 1.46 nmol/cm^2, and 49.05 ± 2.88 nmol/cm^2, respectively, which increased as the epoxide content increased. The IDA functionalized GBB coatings exhibited metal chelating capability towards transition metals (e.g. iron and copper). The reported photocurable copolymer technology offers a facile and tunable preparation of epoxide functionalized surfaces, with potential extended applications in biopatterning, active packaging, and nanotechnology.

*Zhuangsheng Lin, Yiren Zhang, Christopher Ober, Julie Goddard

To be submitted to Journal of Materials Chemistry C

Introduction

Epoxide groups are often functionalized onto solid support materials, such as membranes[1] and resins[2] for a wide range of applications in surface modification. The surface pendent epoxide groups can undergo subsequent ring opening reactions with nucleophilic compounds such as amines, thiols, aromatic alcohols, sulfites.[3-6] As a result, the epoxide functionalized surfaces have demonstrated versatile applications in areas such as adhesion[7], crosslinking[8], and absorption of waste chemicals[5], protein immobilization[9], metal chelation[10-11], cell capturing[12], and antimicrobial coatings[6]. Epoxide functionalized surfaces are commonly prepared via radical polymerization of glycidyl methacrylate[1, 4, 13-15] which presents a significant hurdle to large scale manufacturing (e.g. roll-to-roll) due to the multi-step treatment. Alternative epoxide functionalization techniques, such as plasma modifications[9, 16], have been investigated to enable facile fabrications of epoxide functionalized materials.

Photocurable copolymers permit introduction of a target functional group via a simple coat/cure process, without the need for multi-step preparation processes, and have been used to prepare functional coatings for applications, such as antimicrobial,[17-18] antifouling,[19] biopatterning,[20] surface bound lubricants[21], and metal-chelation[22]. These copolymers contain bioactive moieties to impart functionality and photocrosslinking moieties to impart photocuring capability. Benzophenone is commonly incorporated into photocurable copolymers as photocrosslinker via copolymerization of a synthetic vinyl monomer, 4-benzoylphenyl methacrylate.[17, 21-25] Benzophenone is a chemically robust photocrosslinker that enables photo-initiated

crosslinking under atmospheric conditions. UV light (365 nm) induces excitation of benzophenone to biradical state, which can abstract a hydrogen from neighboring C-H bond and permit formation of a new C-C bond.[26] Benzophenone functionalized copolymers are ideal for photocurable copolymer coatings on polymeric substances rich in alkyl groups (e.g. common plastic materials).

In this study, we report a coat/cure preparation of epoxide functionalized surfaces using a photocurable copolymer coating technology. The copolymers, poly(glycidyl methacrylate-*co*-butyl acrylate-*co*-4-benzoyphenyl methacrylate) (GBB) were synthesized by single electron transfer-living radical polymerization (SET-LRP) of glycidyl methacrylate (GMA), butyl acrylate (BA), and 4-benzoylphenyl methacrylate (BPM). The epoxide content in the GBB copolymers was controlled by adjusting the GMA to BA ratios. The photocuring capability of the GBB copolymers were demonstrated on polypropylene films.

Iminodiacetic acid (IDA) is a metal chelating ligand with specificity to transition metals (e.g. iron, copper). IDA contains a secondary amine group that can be attached to the surface pendent epoxide groups via ring opening reactions.[1, 3] IDA functionalized materials have been demonstrated to perform well in an wide array of applications including water treatment[1, 27-28], protein binding [29-32] and active food packaging[33-34]. In this study, epoxide functionalized materials prepared using the photocurable GBB copolymers were subjected to further functionalization to immobilize IDA chelating ligands. The surface chemistry, wetting properties and chelating capacities of the materials before and after IDA immobilization were analyzed.

Experimental

Materials

Polypropylene (PP) pellets (isotactic) from Scientific Polymer Products (#130, Ontario, NY) were pressed into PP films (330 ± 50 μm thickness) using a hot press (180°C, 10000 lbs force) according to previous procedures.[33, 35]. Sodium iminodiacetate dibasic monohydrate (≥95%), imidazole (99%), glycidyl methacrylate (97%), zincon monosodium salt, 3-(2-pyridyl)-5,6-diphenyl-1,2,4-triazine-p,p'-disulfonic acid disodium salt hydrate (ferrozine, 98%+), toluidine blue O (TBO), *n*-butyl acrylate (99+%), methacryloyl chloride (97%), 4-hydroxybenzophenone (98%), aluminum oxide, tris[2-(dimethylamino)ethyl]amine (Me_6TREN) (97%), and ethyl α-bromoisobutyrate (EBiB) (98%) were purchased from Sigma-Aldrich (St. Louis, MO). Isopropanol, acetone, methanol, sodium hydroxide, glacial acetic acid, hydrochloric acid (trace metal grade), trichloroacetic acid (TCA), oxalic acid dihydrate, sodium acetate trihydrate, 4-(2-hydroxyethyl)-1-piperazineethanesul-fonic acid (HEPES), sodium carbonate anhydrous, sodium bicarbonate, and ferric chloride hexahydrate were purchased from Fisher Scientific (Fair Lawn, NJ). Glycidyl methacrylate and *n*-butyl acrylate were purified using aluminum oxide to remove inhibitors. All other chemicals and reagents were used as received without further purification. 4-benzoyphenyl methacrylate (BPM) were synthesized according to reported procedures[22, 24].

Copolymer synthesis

Poly(glycidyl methacrylate-*co*-butyl acrylate-*co*-4-benzoyphenyl methacrylate) (GBB) copolymers were synthesized via single-electron transfer living radical

polymerization (SET-LRP) (Figure A2.1). Briefly, in a Schlenk tube, a mixture of monomers (10.00 mmol total) containing GMA, BA, and BPM were dissolved in 3 mL of DMSO. Three different monomer feed compositions were used to synthesize GBB(1), GBB(2) and GBB(3) with target epoxide contents of 85 mol %, 55 mol % and 25 mol %, respectively. The monomer compositions in the feed are summarized in Table 1. Aliquots of Me_6TREN (4.81 µL, 18 µmol), EBiB (14.66 µL, 100 µmol), and copper bromide (2.23 mg, 10 µmol) were added as catalysts. The mixture was degassed under nitrogen for 30 min. A copper wire was then added into the mixture under nitrogen protection. The mixture was allowed to polymerize at 25^{o}C for 18 hours in dark and was then precipitated in methanol. The polymer was cleaned by precipitating in an excess amount of methanol two times and was dried a fume hood for 48 hours. Nuclear Magnetic Resonance (NMR) spectra of the copolymers were collected in DMSO-d6 in a Varian INOVA-400 spectrometer (Palo Alto, CA). Gel permeation chromatography (GPC) analysis was conducted in a Waters GPC system (Milford, MA) equipped with a Waters 410 differential refractive index detector, using THF as mobile phase.

Surface functionalization

GBB copolymers were spin coated onto PP films followed by UV-curing (Figure A2.1B). Briefly, GBB copolymers were dissolved in THF at a concentration of 50 mg/mL. An aliquot of 1 mL copolymer in THF was cast onto PP film (5x5 cm^2) by spin coating (30s at 100 rpm, 30s at 200 rpm, 30s at 500 rpm, and 30s at 1000 rpm). The coated films were exposed to UV-light (365 nm, 225 mW/cm^2) for 180 s to photocure the coatings. The photocrosslinking reaction of benzophenone moieties was monitored

by following absorption spectrum at 270-290 nm during the photo-curing process (0-240 s UV-exposure time) using a Synergy Neo2 Hybrid Multi-Mode Reader (BioTek Instruments, Winooski, VT). GBB coated materials were subjected to a subsequent IDA functionalization via epoxide ring-opening. Briefly, in a glass reactor equipped with a condenser and an overhead mixer, the GBB coated films were submerged in 0.45 M IDA in DMSO/water (1:1 v/v) solution. The reaction continued for 18 hours at 80^{o}C with vigorous stirring. The IDA functionalized GBB coatings were rinsed in DI water and dried in a desiccator until further analysis.

Surface characterization

Surface chemistry of the coated materials was characterized using attenuated total reflectance Fourier transform infrared (ATR−FTIR) spectroscopy and X-ray photoelectron spectroscopy (XPS). ATR-FTIR spectra were collected on an IRTracer-100 FTIR spectrometer (Shimadzu Scientific Instruments, Kyoto, Japan) at a resolution of 4 cm^{-1} (32 scans) backgrounded against air. XPS spectra were collected on a SSX-100 (Surface Science Instruments) with operation pressure at around $2x10^{-9}$ Torr. Photoelectrons were collected at a 55° emission angle using a monochromatic Al Kα X-ray (1486.6 eV) with 1 mm diameter beam size. Electron kinetic energy was determined using a hemispherical analyzer with a pass energy of 50 V for high resolution scans. Surface morphologies were observed using scanning electron microscopy (SEM). Surfaces were sputter-coated with gold (Cressington Scientific, Watford, UK) and imaged at 10 kV in a JEOL 6000 FXV SEM (JEOL Ltd. Akishima, Tokyo, Japan). Surface wettability of the materials was analyzed using an Attension Theta Optical

Tensiometer (Biolin Scientific, Stockholm, Sweden). Advancing and receding water contact angles were measured according to a reported protocol.[36] Advancing and receding water contact angles were measured at a depositing and withdrawing rate of 0.5 μL/s double distilled water. Surface IDA content of the materials were quantified using a TBO dye assay.[37] The materials were stored in 0.5 mM TBO dye solutions (pH 10.0) for 24 hours to absorb TBO dye. The absorbed TBO dye was then desorbed in 50 v/v % acetic acid in water solutions. The amount of dye released to acetic acid solution was quantified by measuring absorbance at 633 nm, and compared to a standard curve of TBO dye in acetic acid solution. The IDA density was determined by assuming a 2:1 stoichiometric ratio between absorbed dye and IDA.

Metal chelating analysis

Iron and copper chelating activities of the materials were analyzed using colorimetric ferrozine and zincon assays, respectively.[34, 38-39] Materials were incubated in 0.08 mM ferric chloride or cupric sulfate in 50 mM sodium acetate/imidazole solutions at pH 4.0 for 24 hours (22 ^{o}C, dark) to permit iron and copper chelation, respectively. Iron chelation was quantified by the reduction in Fe^{3+} concentration after 24-hour exposure to the materials. Briefly, 0.5 mL of iron solution was mixed with 0.25 mL of ferrozine solution (18 mM ferrozine in 50 mM HEPES (pH 7.0)) and 0.25 mL of reducing solution (5 wt % hydroxylamine chloride and 10 wt % TCA). Fe^{3+} concentration was determined by measuring the absorbance of the mixture at 562 nm after 1 hour incubation. Copper chelation was quantified by the reduction in Cu^{2+} concentration after 24-hour exposure to the materials. Briefly, 0.3 mL of copper solution

was mixed with 0.7 mL of zincone solution (0.0625 mM zincon in 0.1 M sodium carbonate solution (pH 9.0)). Cu^{2+} concentration was determined by measuring the absorbance of the mixture at 600 nm after 30 min incubation.

Statistics

GBB copolymer synthesis, coating preparation, and IDA functionalization were conducted at least two times, with uniformity in polymer and surface chemistry urface analysis and metal chelating assays were performed using quadruplicate samples prepared by a representative batch of each copolymer. The reported ATR-FTIR and XPS spectra are representative of four spectra collected across quadruplicate samples. Reported scanning electron micrographs are representative of images acquired at random locations on quadruplicate samples. Results of dynamic water contact angles, surface IDA content, and metal chelating analysis were subjected to analysis of variance (ANOVA) to compare difference using Tukey method ($p<0.05$) in GraphPad Prism 6.0 (La Jolla, CA).

Results and discussion

Copolymer chemistry

The chemistry of the photocurable epoxide functionalized copolymer, poly(glycidyl methacrylate-*co*-butyl acrylate-*co*-4-benzoyphenyl methacrylate) (GBB), was analyzed using proton NMR spectroscopy (Figure A2.2). Chemical shifts at 0.76 ppm, 0.94 ppm were assigned to protons on the methyl groups on GMA, BA, and BPM. Chemical shifts at 1.31 ppm, 1.52 ppm, 3.96 ppm were assigned to BA moieties. Chemical shifts at 2.61 ppm, 2.77 ppm, 3.69 ppm, 4.26 ppm were assigned to GMA

moieties. The chemical shifts at 7.31 ppm to 7.83 ppm were assigned to the aromatic protons on the BPM moieties. The composition of GMA, BA, and BPM moieties were determined using the integrated peak area under 2.61 ppm and 2.77 ppm (e), 1.31 ppm and 1.52 ppm (b and c), and the aromatic protons, respectively. GBB(1) contained 22 mol % of GMA, 70 mol % of BA, and 8 mol % of BPM. GBB(2) contained 64 mol % of GMA, 27 mol % of BA and 9 mol % of BPM. GBB(3) contained 91 mol % of GMA and 9 mol % of BPM. The molar composition of the GBB copolymers were in agreement with the molar composition of the monomers in the feeds (Table A2.1). The epoxide content in the copolymers correlated to the molar composition of the GMA in the feed. The results suggested the epoxide content in the copolymers was controllable using the SET-LRP reactions. The benzophenone moieties in GBB(1), GBB(2) and GBB(3) were controlled at 8-9 mol % to give them equivalent photocuring performance. The weight average molecular weight (Mw) and polydispersity index (PDI) of the three GBB copolymers was determined using gel permeation chromatography (GPC). GBB(1), GBB(2) and GBB(3) had Mw of 16-18 kDa, and were monodispersed with a relatively low polydispersity index of 1.2. The NMR and GPC results suggested successful synthesis of the GBB copolymers with tunable epoxide content and controllable molecular weight using the SET-LRP reactions.

Photocuring

To test the photocuring capability of the GBB copolymers, the copolymers were spin coated onto polypropylene films and photocured by exposure to UV-light (365 nm, 225 mW/cm^2). Benzophenone moieties are able to crosslink with neighboring alkyl

groups (C-H bonds)[26], and are hypothesized to cross-link within both the copolymer coating and with PP surfaces. The photocrosslinking reaction was monitored by a decrease in absorption at 270-290 nm during photocuring.[17, 20] The un-cured coating had a strong absorption band at 270 nm, characteristic of uncured benzophenone, which decreased as the UV exposure time increased (Figure A2.3), suggesting crosslinking reaction of the benzophenone moieties. The change in the absorption spectrum was minimal as the UV-exposure time exceeded 160s, suggesting completion of the photocuring. The photocured GBB copolymer coatings were stable on PP films and the coatings were insoluble in organic solvents that would dissolve the copolymers (e.g. DMSO, DMF, THF, and acetone). The results suggest that the GBB copolymers were photocurable and stable after application and coating onto plastic substrates (e.g. PP).

Surface chemistry

The surface chemistries of the photocured metal chelating copolymer coatings were characterized using ATR-FTIR spectroscopy (Figure A2.4). GBB coated films (GBB(1), GBB(2), GBB(3)) exhibited absorption bands at 3000-2800 cm^{-1} (C-H stretch), a strong absorption band at 1710 cm^{-1} (C=O stretch), and absorption bands at 1260-1160 cm^{-1} (C-O-C stretch). These absorption bands are characteristic for poly(BA) and poly(GMA) based materials.[6, 40] FTIR was unable to distinguish the chemical bonds in GMA and BA. The FTIR spectra of GBB(1), GBB(2) and GBB(3) coated surfaces had similar wavenumbers and intensities indicating key chemical bonds despite having different copolymer compositions. The GBB coated films were further subjected to XPS analysis at the Carbon 1s region (Figure A2.5). Each C1s spectrum showed three

different oxidation states indicating C=O (288.2 eV), C-O (286.0 eV) and C-C/C-H (283.9 eV) carbons. The percentage of C-O carbons in GBB(1), GBB(2) and GBB(3) was 16.3 ± 2.7 %, 24.6 ± 0.9 %, and 35.1 ± 3.9 %, respectively, and corresponds to the difference in epoxide content related to GMA content. These results are in agreement with those of the NMR analysis (Figure A2.2) which rank the epoxide content in the copolymers in the order GBB(3) > GBB(2) > GBB(1). The XPS results suggested that the GBB coated materials had different contents of surface epoxide groups that were contributed by the GBB copolymers.

The GBB coated materials were subjected to subsequent reaction in IDA solutions to prepare IDA functionalized materials (GBB(1)-IDA, GBB(2)-IDA and GBB(3)-IDA) (Figure A2.4). Surface immobilized IDA presented characteristic FTIR absorption bands at 3600-3200 cm^{-1} (O-H stretch), 1620 cm^{-1} (C=O stretch of the deprotonated carboxylic acid), and 1260-1160 cm^{-1} (stretching vibrations related to C-O bonds).[29, 33-34] In comparison to GBB(1), the FTIR spectra of GBB(1)-IDA presented no noticeable difference, suggesting a low amount of IDA tethered on the surface. In contrast, GBB(2)-IDA presented an increase in absorption at 3600-3200 cm^{-1}, 1620 cm^{-1}, and 1260-1160 cm^{-1}, corresponding to immobilized IDA ligand). GBB(3)-IDA had the more significant increase in the aforementioned absorption regions than GBB(2)-IDA, suggesting more IDA was immobilized on GBB(3)-IDA. The increase in the surface immobilized IDA corresponded to the greater epoxide content on the GBB coated surfaces. The results confirmed the presence of epoxide groups on the GBB coatings, and suggested the surface pendent epoxide groups were capable of reacting

with the nucleophilic IDA ligands. The surface immobilized IDA content of the materials were quantified using a TBO dye assay (Figure A2.6). TBO dye is a cationic dye that is hypothesized to bind to the carboxylic acid groups at 1:1 binding ratio[37], and has been used to characterize surface immobilized IDA ligand.[33] Native PP films and GBB coated materials did not bind to the TBO dye, indicating clean materials without IDA or other carboxylic acid containing functional groups on the surface. The IDA functionalized GBB coatings had higher IDA content than the corresponding GBB coatings, and the IDA content increased as the epoxide content increased GBB(1)-IDA, GBB(2)-IDA, GBB(3)-IDA had a survey IDA content of 1.47 ± 0.08 nmol/cm^2, 18.67 ± 1.46 nmol/cm^2, and 49.05 ± 2.88 nmol/cm^2, respectively. These results are in agreement with the ATR-FTIR results and suggest that the epoxide groups on the GBB coated materials were able to react with IDA via ring opening reactions, and that the amount of IDA immobilization was correlated to the amount of surface epoxide groups.

Surface morphology and wettability

The surface morphology of the materials were analyzed using SEM (Figure A2.5). GBB(1) had a smooth surface, while GBB(2) and GBB(3) had porous surfaces with pores of approximately 1-2 μm in diameter. Epoxy content GBB(1)-IDA presented a similar surface morphology as GBB(1), in agreement with results of other surface analyses which suggested a lack of epoxy or IDA groups on coatings prepared with the lowest epoxide content copolymer. GBB(2)-IDA and GBB(3)-IDA retained the porous surface morphology, yet exhibited a change in morphology compared to their corresponding GBB coatings resulting from IDA functionalization reactions, with

evidence of coating degradation at the highest epoxy/IDA content. It was worthwhile to note that GBB(1)-IDA contained 1.47 ± 0.08 nmol/cm^2 of IDA, and increased to 18.67 ± 1.46 nmol/cm^2, and 49.05 ± 2.88 nmol/cm^2 for GBB(2)-IDA and GBB(3)-IDA, respectively (Figure A2.6). However, the epoxide content in GBB(1), GBB(2) and GBB(3) copolymers was determined to be 22 mol %, 64 mol % and 91 mol %, respectively. It is possible that the high surface porosity of the GBB(2) and GBB(3) coatings provided additional surface areas for IDA immobilization, leading to an increased in IDA content beyond what is proportional to the theoretical epoxide content.

The surface wettabilities of the coatings were analyzed using dynamic water contact angle analysis (Table A2.2). GBB(2) and GBB(3) presented advancing water contact angles of 115.1 ^{o} ± 4.0 and 126.9 ^{o} ± 7.6, respectively, higher than native PP and GBB(1). All three GBB coated materials had lower receding water contact angles comparing to native PP, suggesting high interaction between the water and the GBB coated surfaces, likely a result of the introduction of functional epoxy groups. The high porosity of GBB(2) and GBB(3) might contributed to the increase in advancing water contact angles, as it has long been reported that porosity can hinder surface wetting.[41] After immobilization of IDA ligands, GBB(1)-IDA, GBB(2)-IDA, GBB(3)-IDA presented advancing water contact angles of 83.4^o ± 1.3, 97.1^o ± 9.5, and 64.8^o ± 5.0, respectively. As expected, the IDA functionalized GBB coatings had lower advancing water contact angles than the corresponding GBB coatings. The receding water contact angles of the IDA functionalized GBB coating were also lower than corresponding GBB coatings. Immobilization of the IDA ligands increased the hydrophilicity of the

acrylate/methacrylate based GBB coatings, and similar results had been reported in previous studies.[33-34] The surface wettability analysis again suggested successful immobilization of IDA ligands onto the epoxide functionalized surfaces.

Metal chelation

The chelating activity of the IDA functionalized GBB coatings towards Fe^{3+} and Cu^{2+} were analyzed at pH 4.0 (Figure A2.8A and A2.8B). Native PP does not chelate transition metals and was used a negative control. Similarly, none of the GBB coatings chelated Fe^{3+} or Cu^{2+}, suggesting that the observed chelating capacity of the IDA functionalized surfaces was due to successful immobilization of the IDA ligand and not due to non-specific interactions with the epoxy group. In agreement with the TBO dye assay results, GBB(1)-IDA did not have chelating activity towards either Fe^{3+} or Cu^{2+} at pH 4.0. Both GBB(2)-IDA and GBB(3)-IDA showed positive metal chelating activity, with GBB(2)-IDA chelating 31.2 ± 2.2 nmol/cm^2 of Fe^{3+} and 36.5 ± 2.5 nmol/cm^2 of Cu^{2+}, and GBB(3)-IDA chelating 65.0 ± 5.2 nmol/cm^2 of Fe^{3+} and 76.5 nmol/cm^2 of Cu^{2+}. The metal chelating results were in agreement with the surface IDA content (Figure A2.6), with the chelating capacity of each material corresponded to the IDA content. The metal chelating results again confirmed the immobilization of IDA ligands on the GBB coated materials.

Conclusions

Photocurable epoxide functionalized copolymers, poly(glycidyl methacrylate-*co*-butyl acrylate-*co*-4-benzoylphenyl methacrylate) (GBB) were synthesized via single electron transfer-living radical polymerization (SET-LRP). The reactions produced

copolymers with tunable epoxide content and controllable molecular weight. The GBB copolymer were photocurable and were coated on plastic substrates (e.g. PP) as functional copolymer coatings. The photocured GBB coatings had pendent epoxide groups, the contents of which were correlated to epoxide content of copolymers. The epoxide functionalized surfaces were available for further chemical functionalization, which was successfully demonstrated via immobilization of a metal chelating ligand, iminodiacetic acid (IDA). The IDA functionalized GBB coatings showed metal chelating capability towards transition metals (e.g. iron and copper) and can potentially be used chelating applications, such as water purification, protein binding, and active food packaging. The photocurable epoxide functionalized copolymer coating technology represents a facile coat/cure preparation of epoxide functionalized materials, with extended applications in scalable manufacturing of functional coatings, such as roll-to-roll.

Tables and Figures

Table A2.1. Molar composition of the polymerization feeds and the copolymers, and weight average molecular weight (Mw) and polydispersity index (PDI) of the copolymers.

	Feed composition (mol %)			**Copolymer composition (mol %)**			**Mw (kDa)**	**PDI**
	GMA	BA	BPM	GMA	BA	BPM		
GBB(1)	85	0	15	91	0	9	18.1 ± 0.1	1.17 ± 0.01
GBB(2)	55	35	15	64	27	9	16.0 ± 0.2	1.27 ± 0.00
GBB(3)	25	65	15	22	70	8	17.0 ± 0.3	1.21 ± 0.01

Table A2.2. Water contact angle measurements of modified and unmodified copolymer coatings. Means are significantly different (Tukey, $p<0.05$) if they share different letters in the same column.

	Adv. Angle (º)	**Rec. angle (º)**
PP	105.2 ± 2.7 ^{e}	85.7 ± 3.4 ^{d}
GBB(1)	93.2 ± 3.5 ^{e}	60.0 ± 3.3 ^{c}
GBB(2)	115.1 ± 4.0 ^{f}	32.5 ± 4.2 ^{b}
GBB(3)	126.9 ± 7.6 ^{f}	28.8 ± 1.7 ^{b}
GBB(1)-IDA	83.4 ± 1.3 ^{bc}	18.9 ± 1.3 ^{a}
GBB(2)-IDA	97.1 ± 9.5 ^{cde}	16.6 ± 0.4 ^{a}
GBB(3)-IDA	64.8 ± 5.0 ^{ab}	16.9 ± 1.0 ^{a}

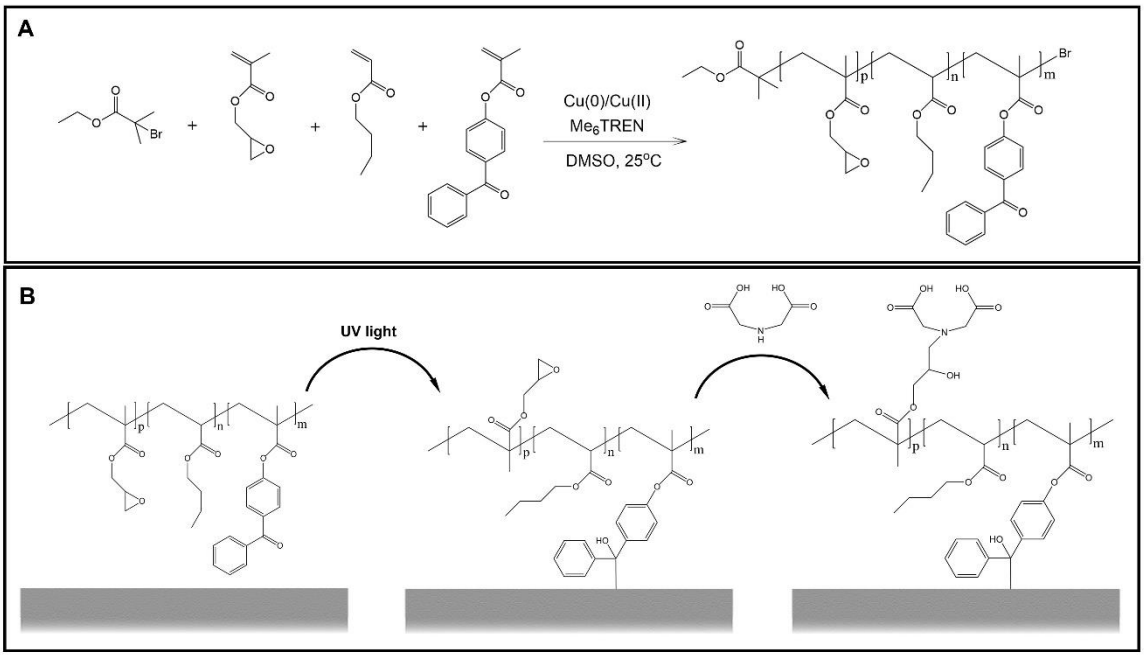

Figure A2.1. Synthesis of poly(glycidyl methacrylate-co-butyl acrylate-co-4-benzoylphenyl methacrylate) (GBB) copolymer via single electron transfer- living radical polymerization (SET-LRP) (A), and schematic preparation of IDA functionalized surface (B).

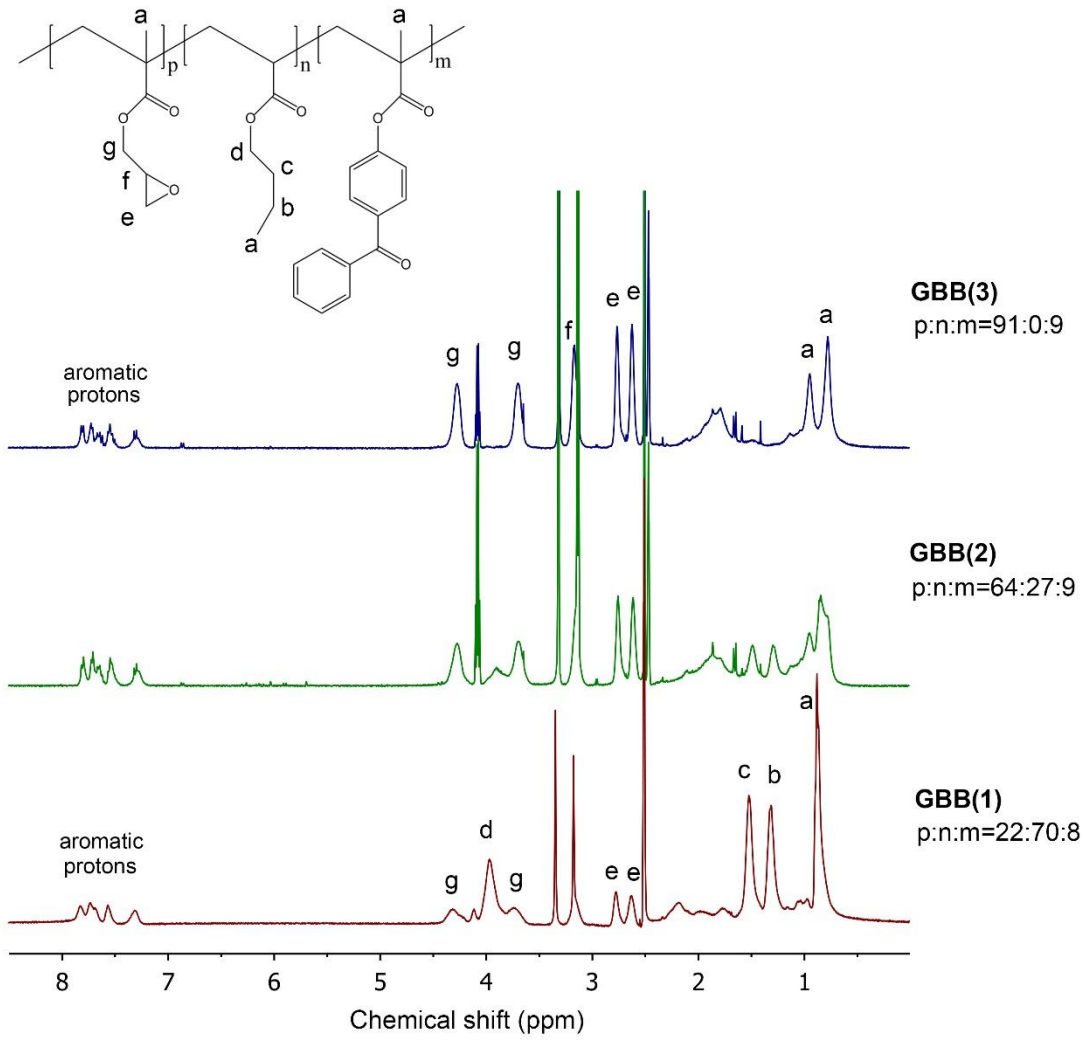

Figure A2.2. Proton NMR spectra of GBB copolymers with varying glycidyl methcrylate: butyl acrylate ratios collected in DMSO-d6 (400 MHz).

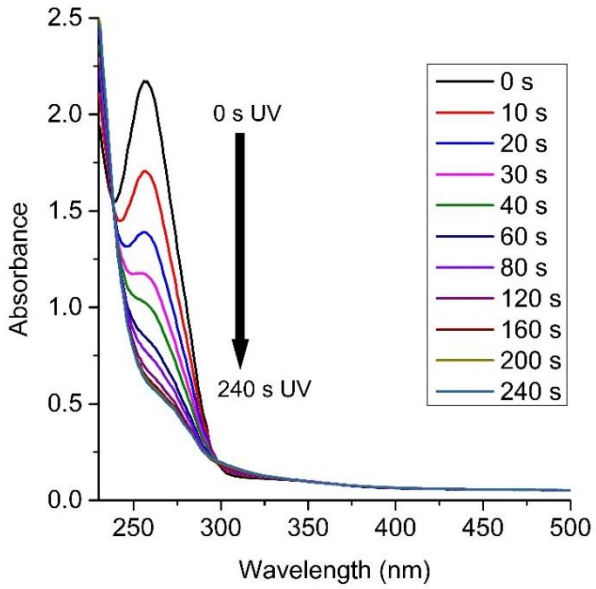

Figure A2.3. Representative benzophenone absorption spectra of a copolymer coating during UV curing process (collected using GBB(1) copolymer coating).

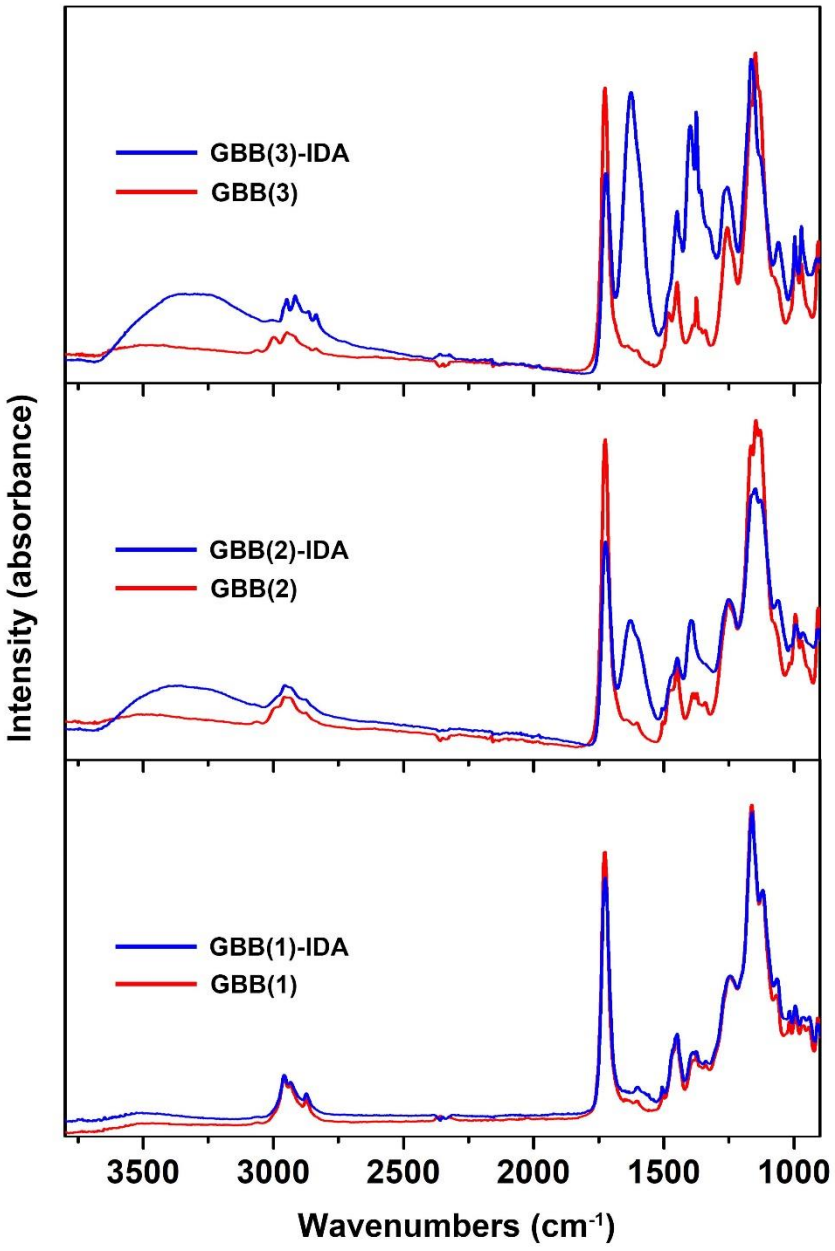

Figure A2.4. Representative FTIR spectra of GBB coatings on PP films and IDA functionalized GBB coatings.

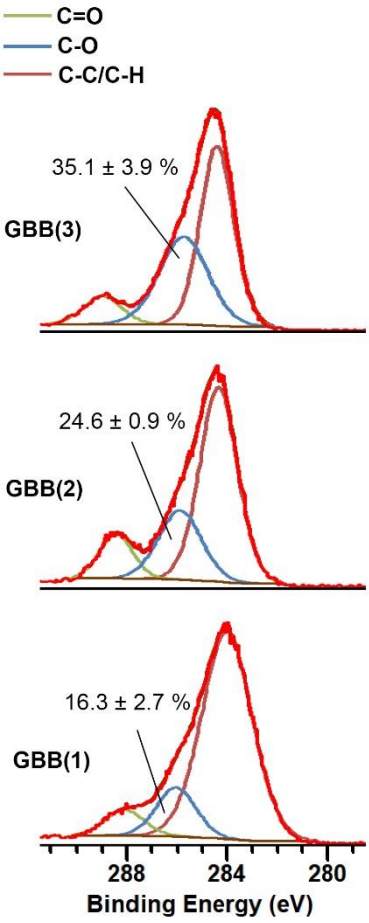

Figure A2.5. Representative C1s XPS spectra of GBB copolymer coatings cured on polypropylene.

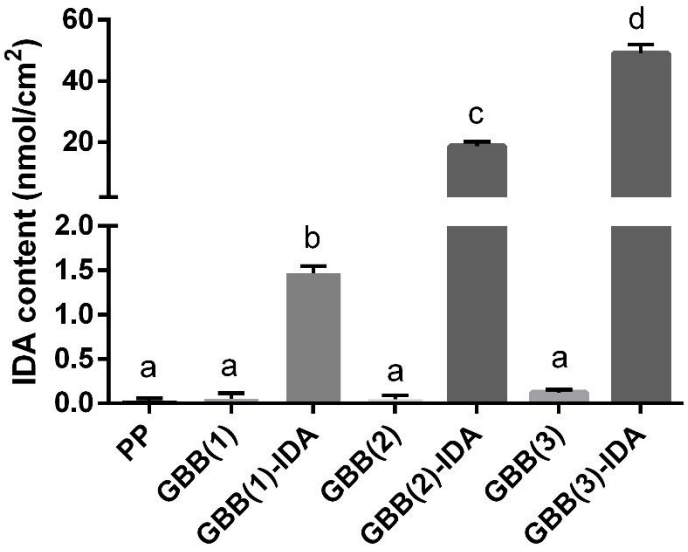

Figure A2.6. IDA content of modified and unmodified copolymer coatings. Means are significantly different (Tukey, $p<0.05$) if they share different letters in the same graph.

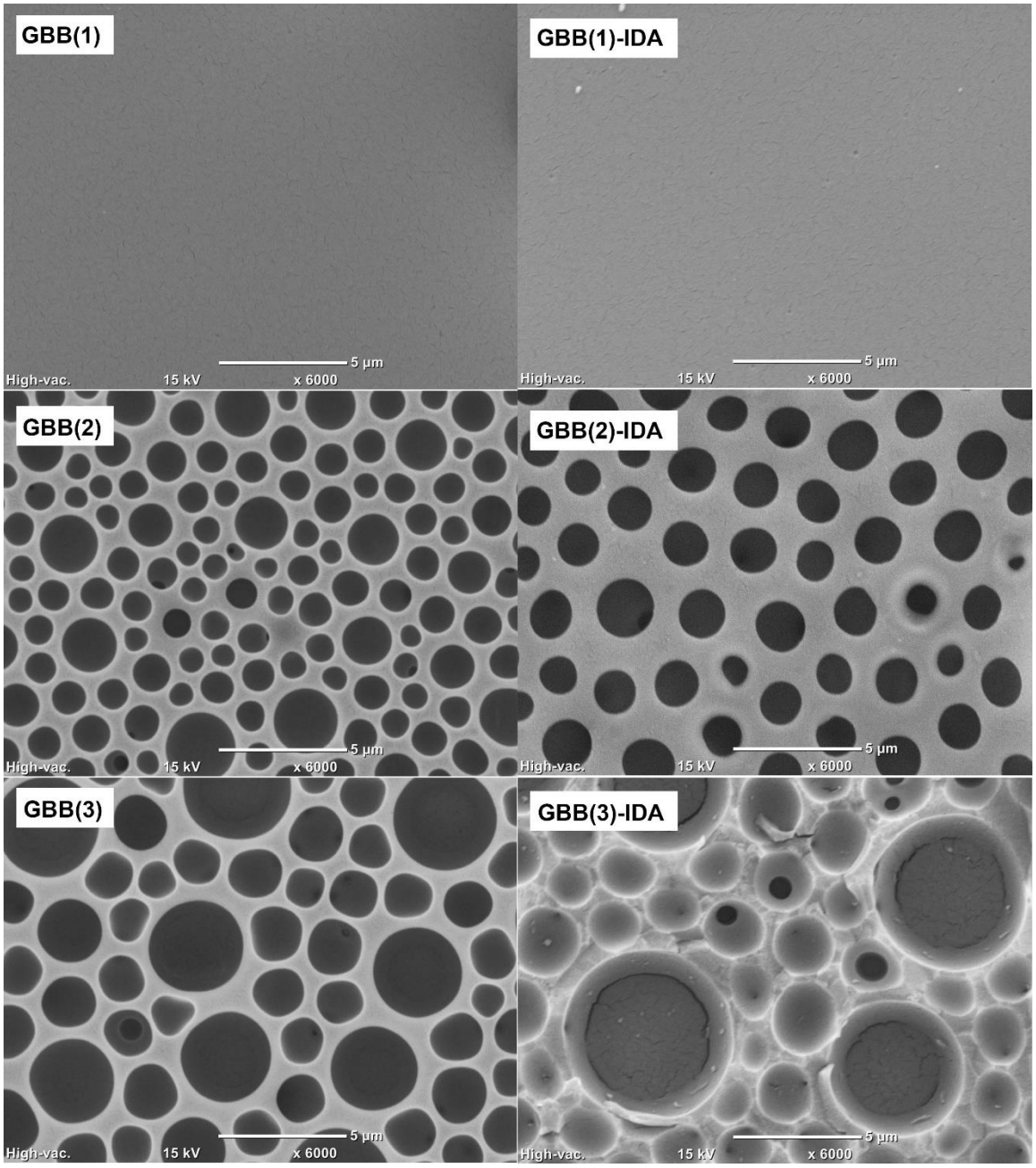

Figure A2.7. Representative SEM micrographs of GBB copolymer coatings and IDA functionalized GBB copolymer coatings.

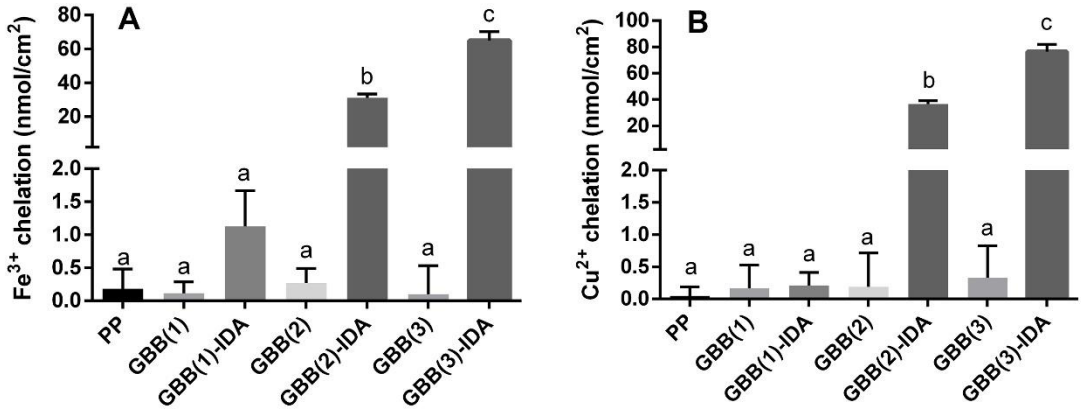

Figure A2.8. Fe^{3+} chelating activity (A) and Cu^{2+} chelating activity (B) at pH 4.0 of modified and unmodified copolymer coatings. Means are significantly different (Tukey, $p<0.05$) if they share different letters in the same graph.

References

1. Yamada, K.; Nagano, R.; Hirata, M., Adsorption and desorption properties of the chelating membranes prepared from the PE films. *J. Appl. Polym. Sci.* **2006,** *99* (4), 1895-1902.

2. Donia, A. M.; Atia, A. A.; Moussa, E. M.; El-Sherif, A. M.; El-Magied, M. O. A., Removal of uranium (VI) from aqueous solutions using glycidyl methacrylate chelating resins. *Hydrometallurgy* **2009,** *95* (3-4), 183-189.

3. Kim, M.; Kiyohara, S.; Konishi, S.; Tsuneda, S.; Saito, K.; Sugo, T., Ring-opening reaction of poly-GMA chain grafted onto a porous membrane. *Journal of Membrane Science* **1996,** *117* (1-2), 33-38.

4. Benaglia, M.; Alberti, A.; Giorgini, L.; Magnoni, F.; Tozzi, S., Poly(glycidyl methacrylate): a highly versatile polymeric building block for post-polymerization modifications. *Polymer Chemistry* **2013,** *4* (1), 124-132.

5. Xie, W.; Weng, L.-T.; Chan, C.-K.; Yeung, K. L.; Chan, C.-M., Reactions of SO 2 and NH 3 with epoxy groups on the surface of graphite oxide powder. *Physical Chemistry Chemical Physics* **2018,** *20* (9), 6431-6439.

6. Liu, R.; Zheng, J.; Guo, R.; Luo, J.; Yuan, Y.; Liu, X., Synthesis of New Biobased Antibacterial Methacrylates Derived from Tannic Acid and Their Application in UV-Cured Coatings. *Industrial & Engineering Chemistry Research* **2014,** *53* (27), 10835-10840.

7. Nanjundan, S.; Selvamalar, C. S. J.; Jayakumar, R., Synthesis and characterization of poly(3-acetyl-4-hydroxyphenyl acrylate) and its Cu(II) and Ni(II) complexes. *European Polymer Journal* **2004,** *40* (10), 2313-2321.

8. Oh, J.-S.; Kim, M. P.; Kim, J.-H.; Son, H.; Kim, K.-H.; Kim, S.-H.; Yoo, J.-B.; Lee, Y.; Yi, G.-R.; Nam, J.-D., Diffusion-assisted post-crosslinking of polymer microspheres containing epoxy functional groups. *Polymer* **2017,** *133*, 110-118.

9. Larson, B.; Helgren, J.; Manolache, S.; Lau, A.; Lagally, M.; Denes, F., Cold-plasma modification of oxide surfaces for covalent biomolecule attachment. *Biosensors and Bioelectronics* **2005,** *21* (5), 796-801.

10. Zhao, Y.-G.; Shen, H.-Y.; Pan, S.-D.; Hu, M.-Q., Synthesis, characterization and properties of ethylenediamine-functionalized Fe3O4 magnetic polymers for removal of Cr (VI) in wastewater. *Journal of Hazardous Materials* **2010,** *182* (1-3), 295-302.

11. Deng, Y.; Gao, Z.; Liu, B.; Hu, X.; Wei, Z.; Sun, C., Selective removal of lead from aqueous solutions by ethylenediamine-modified attapulgite. *Chemical engineering journal* **2013,** *223*, 91-98.

12. Lee, W.; Furusaki, S.; Saito, K.; Sugo, T., Tailoring a brush-type interface favorable for capturing microbial cells. *Journal of colloid and interface science* **1998,** *200* (1), 66-73.

13. Yu, W.; Kang, E.; Neoh, K., Controlled grafting of well-defined epoxide polymers on hydrogen-terminated silicon substrates by surface-initiated ATRP at ambient temperature. *Langmuir* **2004,** *20* (19), 8294-8300.

14. Edmondson, S.; Huck, W. T., Controlled growth and subsequent chemical modification of poly (glycidyl methacrylate) brushes on silicon wafers. *Journal of Materials Chemistry* **2004,** *14* (4), 730-734.

15. Bastarrachea, L.; Wong, D.; Roman, M.; Lin, Z.; Goddard, J., Active Packaging Coatings. *Coatings* **2015,** *5* (4), 771.

16. Tarducci, C.; Kinmond, E.; Badyal, J.; Brewer, S.; Willis, C., Epoxide-functionalized solid surfaces. *Chem. Mater.* **2000,** *12* (7), 1884-1889.

17. Dhende, V. P.; Samanta, S.; Jones, D. M.; Hardin, I. R.; Locklin, J., One-step photochemical synthesis of permanent, nonleaching, ultrathin antimicrobial coatings for textiles and plastics. *ACS applied materials & interfaces* **2011,** *3* (8), 2830-7.

18. Hsu, B. B.; Klibanov, A. M., Light-Activated Covalent Coating of Cotton with Bactericidal Hydrophobic Polycations. *Biomacromolecules* **2011,** *12* (1), 6-9.

19. Liu, Q.; Singha, P.; Handa, H.; Locklin, J., Covalent Grafting of Antifouling Phosphorylcholine-Based Copolymers with Antimicrobial Nitric Oxide Releasing Polymers to Enhance Infection-Resistant Properties of Medical Device Coatings. *Langmuir* **2017,** *33* (45), 13105-13113.

20. Baek, N. S.; Kim, Y. H.; Han, Y. H.; Offenhausser, A.; Chung, M. A.; Jung, S. D., Fine neurite patterns from photocrosslinking of cell-repellent benzophenone copolymer. *J Neurosci Methods* **2012,** *210* (2), 161-8.

21. Li, K.; Pandiyarajan, C. K.; Prucker, O.; Rühe, J., On the Lubrication Mechanism of Surfaces Covered with Surface-Attached Hydrogels. *Macromolecular Chemistry and Physics* **2016,** *217* (4), 526-536.

22. Lin, Z.; Goddard, J., Photocurable coatings prepared by emulsion polymerization present chelating properties. *Colloids and Surfaces B: Biointerfaces* **2018,** *Submitted*.

23. Nanjundan, S.; Unnithan, C. S.; Selvamalar, C. S. J.; Penlidis, A., Homopolymer of 4-benzoylphenyl methacrylate and its copolymers with glycidyl methacrylate: synthesis, characterization, monomer reactivity ratios and application as adhesives. *Reactive and Functional Polymers* **2005,** *62* (1), 11-24.

24. Schlemmer, C.; Betz, W.; Berchtold, B.; Ruhe, J.; Santer, S., The design of thin polymer membranes filled with magnetic particles on a microstructured silicon surface. *Nanotechnology* **2009,** *20* (25), 255301.

25. Janko, M.; Jocher, M.; Boehm, A.; Babel, L.; Bump, S.; Biesalski, M.; Meckel, T.; Stark, R. W., Cross-Linking Cellulosic Fibers with Photoreactive Polymers: Visualization with Confocal Raman and Fluorescence Microscopy. *Biomacromolecules* **2015,** *16* (7), 2179-87.

26. Dorman, G.; Prestwich, G. D., Benzophenone Photophores in Biochemistry. *Biochemistry* **1994,** *33* (19), 5661-5673.

27. Li, T.; Chen, S.; Li, H.; Li, Q.; Wu, L., Preparation of an ion-imprinted fiber for the selective removal of Cu2+. *Langmuir* **2011,** *27* (11), 6753-8.

28. Kavaklı, P. A.; Kavaklı, C.; Güven, O., Preparation and characterization of Fe(III)-loaded iminodiacetic acid modified GMA grafted nonwoven fabric adsorbent for anion adsorption. *Radiation Physics and Chemistry* **2014,** *94*, 105-110.

29. Zhu, J.; Sun, G., Facile fabrication of hydrophilic nanofibrous membranes with an immobilized metal-chelate affinity complex for selective protein separation. *ACS applied materials & interfaces* **2014,** *6* (2), 925-32.

30. Sun, L.; Dai, J.; Baker, G. L.; Bruening, M. L., High-Capacity, Protein-Binding Membranes Based on Polymer Brushes Grown in Porous Substrates. *Chem. Mater.* **2006,** *18* (17), 4033-4039.

31. Wijeratne, S.; Liu, W.; Dong, J.; Ning, W.; Ratnayake, N. D.; Walker, K. D.; Bruening, M. L., Layer-by-Layer Deposition with Polymers Containing Nitrilotriacetate, A Convenient Route to Fabricate Metal-and Protein-Binding Films. *ACS applied materials & interfaces* **2016,** *8* (16), 10164-10173.

32. Ning, W.; Wijeratne, S.; Dong, J.; Bruening, M. L., Immobilization of carboxymethylated polyethylenimine-metal-ion complexes in porous membranes to selectively capture his-tagged protein. *ACS applied materials & interfaces* **2015,** *7* (4), 2575-84.

33. Lin, Z.; Goddard, J., Photo-Curable Metal-Chelating Coatings Offer a Scalable Approach to Production of Antioxidant Active Packaging. *Journal of food science* **2018**.

34. Lin, Z.; Roman, M. J.; Decker, E. A.; Goddard, J. M., Synthesis of Iminodiacetate Functionalized Polypropylene Films and Their Efficacy as Antioxidant Active-Packaging Materials. *J. Agric. Food. Chem.* **2016,** *64* (22), 4606-4617.

35. Lin, Z.; Decker, E. A.; Goddard, J. M., Preparation of metal chelating active packaging materials by laminated photografting. *Journal of Coatings Technology and Research* **2016,** *13* (2), 395-404.

36. Korhonen, J. T.; Huhtamaki, T.; Ikkala, O.; Ras, R. H., Reliable measurement of the receding contact angle. *Langmuir* **2013,** *29* (12), 3858-63.

37. Kang, E. T.; Tan, K. L.; Kato, K.; Uyama, Y.; Ikada, Y., Surface Modification and Functionalization of Polytetrafluoroethylene Films. *Macromolecules* **1996,** *29* (21), 6872-6879.

38. Rush, R. M.; Yoe, J. H., Colorimetric Determination of Zinc and Copper with 2-Carboxy-2-hydroxy-5-sulfoformazylbenzene. *Analytical Chemistry* **1954,** *26* (8), 1345-1347.

39. Dawson, M. V.; Lyle, S. J., Spectrophotometric determination of iron and cobalt with Ferrozine and dithizone. *Talanta* **1990,** *37* (12), 1189-1191.

40. Taenghom, T.; Pan, Q.; Rempel, G. L.; Kiatkamjornwong, S., Synthesis and characterization of nano-sized poly[(butyl acrylate)-co-(methyl methacrylate)-co-(methacrylic acid)] latex via differential microemulsion polymerization. *Colloid and Polymer Science* **2013,** *291* (6), 1365-1374.

41. Cassie, A.; Baxter, S., Wettability of porous surfaces. *Transactions of the Faraday society* **1944,** *40*, 546-551.